

HIERARCHICAL APPROACH TO SEMI-DISTRIBUTED HYDROLOGICAL
MODEL CALIBRATION

A THESIS SUBMITTED TO
THE GRADUATE SCHOOL OF NATURAL AND APPLIED SCIENCES
OF
MIDDLE EAST TECHNICAL UNIVERSITY

BY

AYFER ÖZDEMİR

IN PARTIAL FULFILLMENT OF THE REQUIREMENTS
FOR
THE DEGREE OF DOCTOR OF PHILOSOPHY
IN
GEODETIC AND GEOGRAPHICAL INFORMATION TECHNOLOGIES

MARCH 2016

Approval of thesis:

**HIERARCHICAL APPROACH TO SEMI-DISTRIBUTED
HYDROLOGICAL MODEL CALIBRATION**

submitted by **AYFER ÖZDEMİR** in partial fulfillment of the requirements for the degree of **Doctor of Philosophy in Geodetic and Geographical Information Technologies Department, Middle East Technical University** by,

Prof. Dr. Gülbin Dural Ünver
Dean, **Graduate School of Natural and Applied Sciences** _____

Assoc. Prof. Dr. Uğur Murat Leloğlu
Head of Department, **Geodetic and Geographical Information Tech.** _____

Assoc. Prof. Dr. Uğur Murat Leloğlu
Supervisor, **Geodetic and Geographical Information Tech. Dept., METU** _____

Examining Committee Members:

Prof. Dr. Mahmut Onur Karşlıoğlu
Civil Engineering Dept., METU _____

Assoc. Prof. Dr. Uğur Murat Leloğlu
Geodetic and Geographic Information Tech. Dept., METU _____

Assoc. Prof. Dr. Emre Alp
Environmental Engineering Dept., METU _____

Assoc. Prof. Dr. Ali Ertürk
Faculty of Fisheries, Freshwater Biology Dept., IU _____

Assoc. Prof. Dr. Alpaslan Ekdal
Environmental Engineering Dept., ITU _____

Date: 29/03/2016

I hereby declare that all information in this document has been obtained and presented in accordance with academic rules and ethical conduct. I also declare that, as required by these rules and conduct, I have fully cited and referenced all material and results that are not original to this work.

Name, Last name : Ayfer ÖZDEMİR

Signature :

ABSTRACT

HIERARCHICAL APPROACH TO SEMI-DISTRIBUTED HYDROLOGICAL MODEL CALIBRATION

Özdemir, Ayfer

PhD, Department of Geodetic and Geographic Information Technologies

Supervisor: Assoc. Prof. Dr. Uğur Murat Leloğlu

Co-Supervisor: Dr. Karim Abbaspour

March 2016, 164 pages

In recent years, water resources were negatively affected from uncontrolled agricultural, industrial activities and settlements on river basins. Hydrologists and water resource managers have widely used hydrologic models as tools for water resources development, water environment preservation, water resources allocation and understanding utilization. In order to apply hydrological models successfully in practical water resources investigations, careful calibration and uncertainty analysis are needed. Hydrological models are validated by comparing the outputs of the models to measurements. The deviations of the outputs from the ground truth, the error, can be the result of uncertainties of the inputs, uncertainties of the parameters of the model and the model itself. When a hydrologic model is calibrated, the parameters of the model are fine-tuned within a predefined range to minimize an error metric created from error terms. One such hydrological transport model is the Soil and Water Assessment Tool (SWAT) which is also integrated into a Geographic Information System (GIS) that supports the input of topography, land use, soil type, and other digital data. SWAT is a semi-distributed hydrological model that simulates hydrological processes at subbasin level by deriving Hydrologic Response Units (HRU) by thresholding areas of soil type, land use and management combinations. Currently, there are automated calibration methods for SWAT using nonlinear optimization such as Levenberg-Macquart or global optimization methods like Genetic

Algorithms. These optimization approaches that try to calibrate very complex models have some drawbacks: 1) Since the search space is large and the model is complicated, the convergence takes very long time, 2) for the same reasons, probability of finding a local optimum is large, 3) final result is too sensitive to the initial estimates of the parameters, 4) the sizes of the HRUs, which are the areas over which the parameters are assumed to be constant, are left to the user and their relation to the performance of calibration/validation is unknown. In this thesis, a hierarchical (coarse-to-fine) approach to HRU selection and calibration is investigated. The HRUs are generated automatically by a script and the number of HRUs are increased at each level of the hierarchy. The calibration results at each level are used as initial values for the next level. This way, we obtain not only an increase in the speed and accuracy of the calibration, but we also find out the optimum HRU sizes and HRU generation parameters. The algorithm developed in this thesis is tested on two basins with different properties and the results are promising.

Keywords: SWAT, GIS, semi-distributed hydrological models, calibration, optimization, hydrology, water management

ÖZ

YARI DAĞITIK HİDROLOJİK MODEL KALİBRASYONUNA HİYERARŞİK YAKLAŞIM

ÖZDEMİR, Ayfer

Doktora, Jeodezi ve Coğrafi Bilgi Sistemleri Bölümü

Tez Yöneticisi: Doç. Dr. Uğur Murat Leloğlu

Eş Danışman: Dr. Karim Abbaspour

Mart 2016, 164 Sayfa

Son yıllarda, su kaynakları nehir havzaları üzerindeki kontrolsüz tarımsal, endüstriyel faaliyetler ve yerleşimlerden olumsuz yönde etkilenmektedir. Hidrologlar ve su kaynakları yöneticileri hidrolojik modelleri, su kaynaklarının geliştirilmesi, su kaynaklarının korunması, su kaynaklarının tahsisi ve kullanımının anlaşılması için araç olarak sık sık kullanmaktadır. Hidrolojik modellerin su kaynaklarının araştırılmasında başarılı bir şekilde uygulanması için, dikkatli kalibrasyon ve tahmin belirsizlik analizi gereklidir. Hidrolojik modeller, model sonuçları ölçümlerle karşılaştırılarak doğrulanır. Sonuçların yer gerçeklerinden sapmaları, yani hata, model girdilerindeki, model parametrelerindeki ve modelin kendisindeki belirsizliklerin sonucu olabilir. Bir hidrolojik model kalibre edilirken, hata terimlerinden oluşturulan hata metriğini minimize etmek için, model parametrelerine daha önce tanımlanmış bir aralıkta ince ayar yapılmaktadır. Bu tür bir hidrolojik taşınım modeli, içerisine topoğrafi, arazi kullanımı, toprak türü ve diğer sayısal veri girişini destekleyen Coğrafi Bilgi Sistemi (CBS) ile tümleşik Toprak ve Su Değerlendirme Aracı'dır (The Soil and Water Assessment Tool, SWAT). SWAT, hidrolojik süreçleri, toprak türü, arazi kullanımı ve yönetimi kombinasyonlarının alanlarını eşikleyerek Hidrolojik Cevap Birimleri (Hydrologic Response Units, HRU) üretmek suretiyle alt-havza düzeyinde simüle eden yarı dağıtık bir hidrolojik modeldir. Günümüzde, SWAT için Levenberg-Macquart gibi doğrusal olmayan optimizasyon veya Genetik Algoritmalar gibi global

optimizasyon yöntemleri kullanan otomatik kalibrasyonu yöntemleri vardır. Karmaşık modelleri kalibre etmek için kullanılan bu optimizasyon yaklaşımlarının bazı dezavantajları vardır: 1) Arama uzayı geniş ve model karmaşık olduğu için yakınsama çok uzun zaman alır, 2) aynı nedenle, yerel bir optimum bulma olasılığı yüksektir, 3) nihai sonuç parametrelerin başlangıç tahminlerine fazlasıyla hassastır, 4) içerisinde parametrelerin sabit kabul edildiği HRU'ların büyüklükleri kullanıcıya bırakılmıştır ve bunların kalibrasyon / doğrulama performansı bilinmemektedir. Bu tezde, HRU seçimi ve kalibrasyon için hiyerarşik (kabadan inceye) bir yaklaşım incelenmiştir. HRU'lar bir komut dosyası tarafından otomatik olarak oluşturulmaktadır ve her hiyerarşinin her düzeyinde, HRU'ların sayısı arttırılmaktadır. Her bir düzeyin kalibrasyon sonuçları bir sonraki düzey için başlangıç değeri tahminiolarak kullanılır. Bu şekilde, sadece hızda ve kalibrasyon doğruluğunda bir artış elde etmekle kalmıyoruz, aynı zamanda ve optimum HRU boyutlarını ve HRU oluşturma parametrelerini de buluyoruz. Bu tezde geliştirilen algoritma, farklı özelliklere sahip iki havzada test edilmiştir ve sonuçlar ümit vericidir.

Anahtar kelimeler: SWAT, CBS, yarı-dağıtık hidrolojik modeller, kalibrasyon, optimizasyon, hidroloji, su yönetimi,

to my mother Ayşe ÖZDEMİR and my father Cemil ÖZDEMİR

ACKNOWLEDGEMENTS

I would like to express special thanks to my supervisor Assoc. Prof. Dr. Uğur Murat LELOĞLU for continuous guidance, support, motivation and encouragement during this study. I deeply thank to my co-advisor Dr. Karim ABBASPOUR for his hospitality in Zürich, SWITZERLAND, support, humanity, motivation and encouragement. I sincerely appreciate the time and effort my supervisor and co-advisor have spent to improve my studies during my thesis.

I would like to thank my friends Mine KALKANCI and Bekir YILMAZ for their support, help and friendship during my graduate years. I would like to thank my friends, Gökhan CÜCELOĞLU and John WASIGE for listening to me every time and their support while writing the thesis. I would like to thank my teacher, friend, confidant Hülya TÜRKMENDAĞ since she always supports me and gives me positive energy.

Moreover, I would like to thank General Manager of the Department of Water Management, The Ministry of Forestry and Water Affairs, Prof. Dr. Cumali KINACI for giving permission for my PhD.

I would like to thank TÜBİTAK for supporting my research via 2211 C and 2214 A programs.

Finally, I deeply thank to my mother Ayşe ÖZDEMİR and my father Cemil ÖZDEMİR for their devotion, love and patience they have shown throughout my life. I would like to thank my brothers, Asım, İhsan and Savaş ÖZDEMİR for their support and love.

TABLE OF CONTENTS

ABSTRACT	v
ÖZ	vii
ACKNOWLEDGEMENTS	x
TABLE OF CONTENTS	xi
LIST OF FIGURES	xv
LIST OF TABLES	xx
CHAPTER 1	1
INTRODUCTION	1
1.1. Problem Description	2
1.2. Contribution of the thesis	3
CHAPTER 2	5
LITERATURE REVIEW AND BACKGROUND	5
2.1. Literature Review	5
2.2. Hydrologic Modeling and Calibration	10
2.1.1 Semi-Automated Calibration Methods	12
2.1.1.1 Particle Swarm Optimization (PSO)	13
2.1.1.2 Monte Carlo Marcov Chain (MCMC)	14
2.1.1.3 Generalized Likelihood Uncertainty Technique (GLUE)	15
2.1.1.4 ParaSol	16
2.1.1.5 SUFI-2	17
2.1.1.5.1 SUFI-2 Procedure	19
2.1.1.5.2 Latin Hypercube Sampling	22

2.1.2 Comparison of the GLUE, ParaSol, SUFI-2, MCMC, and PSO Methods for Calibration.....	23
2.2 SWAT Model and SWAT Calibration	27
2.2.1 SWAT Model.....	27
2.2.2 SWAT Calibration	30
CHAPTER 3.....	33
HIERARCHICAL APPROACH TO SEMI-DISTRIBUTED HYDROLOGICAL MODEL CALIBRATION	33
3.1 Full Automatic Version of SUFI-2	36
3.1.1 File Structure of SUFI-2	37
3.1.2 SUFI-2 Running Procedures in SWAT-CUP	38
3.1.3 Developed SUFI-2 Algorithm on MATLAB.....	40
3.2 Soil Database for SWAT	42
3.2.1 Soil Texture Classification through the Watershed	44
3.2.2 Definition of USLE_K FACTOR	46
3.2.3 Definition of SOL_BD (Soil Bulk Density)	47
3.2.4 Definition of SOL_AWC (Soil Available Water Capacity)	47
3.2.5 Definition of SOL_K (Soil Hydraulic Conductivity)	48
CHAPTER 4.....	51
RESULTS	51
4.1. Case Study: Sarısu-Eylıklar River, Konya, Turkey.....	51
4.1.1. SWAT Input Layers.....	53
4.1.1.1 Delineation of Watershed.....	53

4.1.1.2 Soil Class Layer	56
4.1.1.3 Land use/Land cover Layer.....	59
4.1.1.4 Slope Layer	61
4.2 The SWAT Model Results of Sarisu-Eylikler Basin by Using The Current Method for HRU Creation.....	63
4.3 HRU Division based on CN2 parameter	63
4.4 HRU Creation based on SOL_K	74
4.5 HRU Creation based on CN2+SOL_K+Slope Classification Parameters	86
4.5.1 Two-HRU Types which were Created BAsed on Slope, CN2 and SOL_K parameters results	88
4.5.2 Four-HRU Types which were created with respect to Slope, CN2 and SOL_K parameters results	91
4.5.3 Eight-HRU Types which were created with respect to Slope, CN2 and SOL_K parameters results	98
4.6 2. Case Study: Namazgah Dam Basin, Kocaeli, TURKEY	102
4.6.1. SWAT Input Layers.....	104
4.6.1.1 Delineation of Watershed.....	104
4.6.1.2 Soil Class Layer	108
4.6.1.3 Land use/Land cover Layer.....	110
4.6.1.4 Slope Layer	113
4.6.1.5 Meteorological Data.....	114

4.6.2 SWAT Model Results of Namazgah Dam Basin by using the current methodology for HRU division SWAT	115
4.6.3 HRUs division depending on CN2 parameter	115
4.6.3.1 Two-HRU Types which were created with respect to CN2 parameter results	119
4.6.3.2 Four-HRU types which were created with respect to CN2 parameter results	121
4.6.3.2 Eight-HRU types which were created with respect to CN2 parameter results	124
CHAPTER 5.....	127
SUMMARY AND DISCUSSION	127
CHAPTER 6.....	133
CONCLUSION	133
REFERENCES.....	135
APPENDICES.....	145
A: Full Automatic version of SUFI 2.....	145
B: 4-HRU TYPES based on combinations of SOL_K, CN2 and Slope classification	155
C: 4-HRU TYPES based on combinations of SOL_K, CN2 and Slope classification	157
CURRICULUM VITAE.....	163

LIST OF FIGURES

Figure 1 SWAT-CUP program structure (Abbaspour et al., 2007)	13
Figure 2 The relation between parameter uncertainty and prediction uncertainty (Abbaspour et al., 2007).....	18
Figure 3 The hydrologic cycle as represented in SWAT	28
Figure 4 Representation of sub-basins and streams	28
Figure 5 Distribution of HRUs in a subbasin.....	29
Figure 6 The water management pathways in SWAT (Neitsch et., al., 2011).....	29
Figure 7 Example flowchart of manual calibration in SWAT (Engel et al., 2007; Santhi et al., 2001).....	31
Figure 8 General concept of hierarchical methodology.....	36
Figure 9 Sequence of program execution of SUFI-2 in SWAT-CUP (Abbaspour et al., 2007)	39
Figure 10 Developed SUFI-2 algorithm on MATLAB.....	41
Figure 11 Soil triangle (Ley et al., 1994).....	45
Figure 12 Study Area	52
Figure 13 Digital Elevation Model of Sarısu-Eylikler Basin.....	54
Figure 14 Sub-basins of Sarısu-Eylikler Stream.....	55
Figure 15 Soil map of the Sarısu-Eylikler stream basin.	57
Figure 16 Soil type histogram representation of the study area.....	57
Figure 17 Land use map of the Sarısu-Eylikler Stream.....	59
Figure 18 Land use/land cover type histogram representation of the study area.....	61
Figure 19 Land slope in the Sarısu-Eylikler basin.	62

Figure 20 Relation between runoff and rainfall in SCS curve number method (SCS 1986).....	64
Figure 21 Distribution of HRU types according to CN2 in the basin at each level ...	66
Figure 22 Model results of two-HRU types based on CN2 parameter	68
Figure 23 Model results of four-HRU types based on CN2 parameter.....	68
Figure 24 Model results of eight-HRU types based on CN2 parameter	69
Figure 25 Model results of eighteen-HRU types based on CN2 parameter.....	69
Figure 26 Calibration results of two-HRU types	71
Figure 27 Calibration results of four-HRU types.....	72
Figure 28 Calibration results of eight-HRU types	72
Figure 29 Calibration results of eighteen-HRU types.....	73
Figure 30 HRU types based on SOL_K parameter division	77
Figure 31 Model results of two-HRU types based on SOL_K parameter	80
Figure 32 Model results of four-HRU types based on SOL_K parameter.....	80
Figure 33 Model results of all HRU types based on SOL_K parameter.....	81
Figure 34 Calibration results of two-HRU types model.	81
Figure 35 Calibration steps of two-HRU based on SOL_K parameter.....	82
Figure 36 Calibration results of four-HRU types model (based on SOL_K).....	82
Figure 37 Calibration steps of four-HRU types based on SOL_K parameter.....	83
Figure 38 All HRU types model calibration results (based on SOL_K).....	83
Figure 39 Model results of four-HRU types (calibrated parameters values of two-HRU types used as an initials for four-HRUs)	84
Figure 40 Calibration results of 4-HRU types model (initial value of 4 HRUs obtained from calibrated 2-HRU types model parameters)	85

Figure 41 Calibration steps of four-HRU types model (initial value of 4 HRUs obtained from calibrated two-HRU types model parameters)	85
Figure 42 Calibration result of all soil HRU types model based on SOL_K classification (initial value of four HRUs obtained from calibrated two HRU types model parameters).....	86
Figure 43 HRU division methodology for Sarisu-Eylikler Stream Basin	87
Figure 44 Two-HRU types division based on SOL_K, CN2 and slope parameters ..	88
Figure 45 The flowchart of two-HRU types generation.	89
Figure 46 The slope classification of the study area	89
Figure 47 Model results of two-HRU types (based on soil hydraulic conductivity, CN2 and slope classification)	90
Figure 48 Two-HRU types model calibration results (SM=250), which are generated by CN2+SOL_K+Slope.	91
Figure 49 Four-HRU types division depending on SOL_K, CN2 and Slope	92
Figure 50 The flowchart of four-HRU types generation.....	93
Figure 51 Four-HRU types model results without including initial values which are calibrated model parameters of two HRU types	93
Figure 52 Four-HRU types calibration model results (simulation count =500)	94
Figure 53 Four-HRU types model results by using calibrated parameters values of two-HRUs as initial values.....	95
Figure 54 Four-HRUs calibration model results (simulation count =500) calibrated two HRU types model parameters used as an initials for four HRUs.....	96
Figure 55 Calibration performance of the model between 1998 and 2010 years	97
Figure 56 Four-HRU types model performance after verification.....	97

Figure 57 Eight-HRU types division depending on SOL_K, CN2 and slope classification.....	98
Figure 58 Model results eight-HRU types which are produced by combining CN2, SOL_K and slope classification.	99
Figure 59 Calibration results of 8 HRU types model that are produced by combining CN2, SOL_K and slope classification.....	100
Figure 60 Model results of 8 HRU types which are produced by combining CN2, Sol_K and slope classification (calibrated parameters values of 4 HRU types model as initials for 8 HRUs).....	100
Figure 61 Calibration results of 8 HRU types model which are produced by combining CN2, SOL_K and slope classification (calibrated parameters values of 4 HRUs type model as initials for 8 HRUs).....	101
Figure 62 2. Case Study Area.....	103
Figure 63 Digital Elevation Model of Namazgah Dam Basin	105
Figure 64 Sub-basins of Namazgah Dam Basin.....	107
Figure 65 Soil Map of Namazgah Dam Basin.	109
Figure 66 Soil type histogram representation of the study area.	110
Figure 67 Land use/Land cover Map of Namazgah Dam Basin	111
Figure 68 Land use/land cover type histogram representation of Namazgah Dam Basin.	112
Figure 69 Slope Map of Namazgah Dam Basin.....	113
Figure 70 HRU division methodology for Namazgah Dam Basin	117
Figure 71 HRU type division based on CN2 on Namazgah Dam Basin.....	118
Figure 72 Model results of two-HRU types of Namazgah Dam Basin.....	119

Figure 73 Model calibration results of two-HRU types which were divided according to CN2 values.....	121
Figure 74 Model results of four-HRU types on Namazgah Dam Basin	122
Figure 75 Calibration results of four-HRU types model on Namazgah Dam Basin (SM=500).....	123
Figure 76 Model calibration results of four-HRU types (include initials).....	123
Figure 77 Model results of eight-HRU types on Namazgah Dam Basin.....	125
Figure 78 Calibration results of eight-HRU types model which are produced by division of CN2 (calibrated parameter values of 4 HRUs type model as initials for 8 HRUs).	125

LIST OF TABLES

Table 1 Comparison of uncertainty analysis techniques for a SWAT application to the Chaohe Basin in China (Yang et al., 2008).....	26
Table 2 Example of land use for current HRU division.....	34
Table 3 Depth of Class Reference Ranges	44
Table 4 The relationship between texture class and ranges of clay, sand and silt	45
Table 5 USLE_K Values with respect to soil texture. Source: Rosewell, 1993.	46
Table 6 SOL_BD Values with respect soil textures (Mg/m ³) Source: Guidelines for Soil Description, 2005.....	47
Table 7 SOL_AWC Values with respect to soil textures (mm H ₂ O/mm soil) Source: Guidelines for Soil Description, 2005.....	48
Table 8 SOL_K values depending on soil textures (mm/h) (Guidelines for Soil Description, 2005).....	49
Table 9 DEM Properties.....	54
Table 10 Major Soils Group in the area	56
Table 11 User soil database in SWAT for the study area	58
Table 12 Land use/ land cover distribution in the study area.....	60
Table 13 Slope class distribution in the Sarisu-Eylikler basin.....	61
Table 14 HRU division according to CN2	65
Table 15 Calibration parameters and their ranges.....	71
Table 16 Calibration results of HRU levels that are created based on the CN2 parameter.....	73
Table 17 HRU division based on SOL_K parameter	76

Table 18 Calibration results of HRU types which are divided according to SOL_K parameter.....	79
Table 19 Two-HRU types model calibration results depending on simulation count	91
Table 20 Four-HRU types model calibration results depending on simulation count	92
Table 21 Four-HRU types model calibration results depending on simulation count	95
Table 22 8 HRU types model calibration results depending on simulation count.....	99
Table 23 8 HRU types model calibration results which include calibrated parameter values of 4 HRUs depending on simulation count.....	101
Table 24 DEM Characteristics of Namazgah Dam Basin.....	106
Table 25 Major Soils Group in Namazgah Dam Basin.....	108
Table 26 User soil database in SWAT for Namazgah Dam Basin	110
Table 27 Land use/ land cover distribution in Namazgah Dam Basin.....	112
Table 28 Statistical Values of Meteorological Data	115
Table 29 HRUs division based on CN2 parameter on Namazgah Dam basin.....	116
Table 30 Calibration parameters and their range	120
Table 31 Calibration results of 2 HRU types depending on simulation counts.	121
Table 32 Calibration results of four-HRU types depending on simulation counts..	122
Table 33 Calibration results of eight-HRU types model depending on simulation counts.	124
Table 34 Summary of results for Sarısu-Eylikler Basin.	130
Table 35 Summary of results for Namazgah Dam Basin.....	131

CHAPTER 1

INTRODUCTION

The water framework directive (WFD, 2000/60/EC), created by the European Union, indicates new approaches on water management and protection of aquatic environment since uncontrolled agricultural, industrial activities and settlements on river basins threaten water quality and quantity. The directive points out that integrated water resources planning and management at the river basin is important for sustainable water management. The suitable management and protection of valuable water resources can be succeed by understanding temporal and spatial distribution of water on river basins, which includes groundwater recharge and contaminant loadings. Thus, to develop and apply mathematical simulation models, which are representations of all the important hydrological processes at the suitable scale, may play a major role in anticipating short and long-term effects on the aquatic for a successful river basin management plan.

Hydrologists and water resource managers have widely applied hydrologic models as tools for understanding and reliably estimating human activities that impact on river basin systems. Uncertainty analysis and accurate calibration processes are needed for successful application of hydrological models in water resources management (Duan et al., 1992; Beven and Binley, 1992; Vrugt et al., 2003; Van Griensven et al., 2008; Yang et al., 2008). In recent years, many researchers have studied and developed many calibration and uncertainty analysis methods in order to improve reliability of model prediction and estimation of prediction uncertainty (van Griensven and Meixner, 2006; Abbaspour et al., 2007). However, calibration of models is not an easy task because there are many uncertainties, namely: input, model structure, parameter and output uncertainties (Arnold et al., 2010). If there are too many parameters to be optimized in the calibration, the task can become labour-intensive and time-consuming (Balascio et al., 1998). Moreover, with increasing complexity of hydrologic models, the complexity of calibration also increases (Gupta et al., 1998).

In this study, “The Soil and Water Assessment Tool (SWAT) (Arnold et al., 1998)”, which is a physical hydrologic model and has been popular worldwide for evaluating water resources, is used. In accordance with the semi-distributed approach, the smallest spatial component of water balance simulation in SWAT is the Hydrological Response Unit (HRU). HRU generation in SWAT is based on user defined thresholds to be applied to areas of soil, land use and management combinations at subbasin level.

Since the current approach of HRU creation may ignore some combinations important for hydrological processes, the model performance may decline. If the number of HRUs are increased to avoid that problem, then the computational complexity of the calibration will increase. In this study, we present a hierarchical (coarse-to-fine) approach to HRU definition that increases model performance and reduces computational overhead simultaneously. The performance of the hierarchical methodology is demonstrated on two basins with different characteristics: Sarısu-Eylıklar sub-basin and Namazgah Dam Lake in Turkey.

1.1. Problem Description

Hydrologists and water resource managers use watershed models to realize and control negative effects on the river basins, either natural or anthropogenic. SWAT model (Arnold et al., 1998) has been applied as hydrologic and water quality model worldwide. However, the hydrologic models include parameters the values of which cannot be determined directly since the parameters cannot be measured or there can be scaling problems. The time consumed for running the hydrologic model is still a problem for hydrologic modelers. Calibration of hydrologic models takes a long time, especially when they are complicated and large scale.

Until now, many automated calibration methods for SWAT were developed and used, which are based on nonlinear optimization algorithms like Levenberg-Macquart (Macquart, 1963) or global optimization methods like Genetic Algorithms (Holland, 1970), in order to increase calibration performance. However, these optimization

approaches that try to calibrate very complex models have some drawbacks: 1) Since the search space is large and model is complicated, the convergence takes very long time, 2) for the same reasons, probability of getting stuck into a local optimum is large, 3) final result is too dependent on the initial estimates of the parameters, and 4) the sizes of the HRUs, which are the areas over which the parameters are assumed to be constant, are left to the user and their relation to the performance of calibration/validation is unknown. Furthermore, to evaluate the optimization algorithms for the complex models is nearly impossible because running hydrologic models is time-intensive. So as to enhance model performance and reduce the computational complexity for calibration, a different calibration approach should be developed.

1.2. Contribution of the thesis

The success of a hydrologic model relates to model calibration accuracy (Duan et al., 1992). The model parameters are adjusted so that the difference between the predictions of the model and actual measurements are as small as possible. In this study, we used SWAT (Arnold et al., 1998), which is a semi-physically based hydrologic model and is very popular. The smallest spatial unit of water balance calculation in SWAT is the HRU. HRUs are created in SWAT by applying user defined threshold area of soil, land use and management combinations at sub-basin level.

Since the sizes of the HRUs are left to the user and their relation to the performance of calibration/ validation is unknown, a hierarchical approach to HRU definition was developed in order to increase model performance and reduce computational overhead simultaneously. Thus, the prediction reliabilities and uncertainty estimations of SWAT simulations are improved by developing a tool, which works under MATLAB in order to run the SWAT model efficiently and effectively. Input layers for SWAT, which are topography, land use, soil type, and other digital data, are supported by Geographic Information Systems (GIS). In this study, MATLAB is used to control SWAT

remotely in order to apply hierarchical approach for hydrological model calibration. By using MATLAB, we can create the HRUs ourselves and hence we can control their number and type. Thus, the HRUs are generated automatically by a computer program implemented as MATLAB scripts and at each level, the number of HRUs are increased systematically. In order to evaluate our hierarchical approach, SUFI-2 optimization method is used due to its ability to combine optimization with uncertainty analysis in high-dimensional space. Furthermore, SUFI-2 can reach acceptable model calibration performance with relatively small iteration number and hence shorter calibration time. The HRUs are generated automatically by a script and the number of HRU types are doubled at each level. The calibration results at each level will be used for estimating initial values for the next level. This way, not only an increase in the speed and success of the calibration, but also the optimum HRU sizes and HRU generation parameters are reached. The effectiveness of the method is demonstrated on two basins with different characteristics.

CHAPTER 2

LITERATURE REVIEW AND BACKGROUND

2.1. Literature Review

Although the computers' speed and capacity have improved substantially in the recent years, computational complexity for running hydrologic models is a still major problem for the modelers especially when the complicated physically based distributed hydrologic models are applied. Several studies evaluated the performance of the calibration process by applying various algorithms in order to enhance the model performance and/or reduce the computational time. For example, Duan et al. (1992) developed the shuffled complex evolution algorithm (SCE-UA). The method is a consistent and effective method for searching global optimum parameter values of hydrologic models. Some researchers have studied effects of input data on the model accuracy. For instance, Brown et al. (1993) indicated that the degree of spatial dependence within the input variables had effect in the outcomes. DEM grid size importantly affects topographic parameters according to study of Zhang and Montgomery (1994). The finest resolution DEM (10 m) resulted in better outcomes than 30 m and 90 m data. The SCE-UA was compared with other methods, GA and SA, for optimization of the tank model by Cooper et al., (1997). The comparison between SCE-UA, GA, and multiple random starts using either simplex or quasi-Newton local searches for parameter optimization of catchment models were studied by Kuczera (1997). The differences between multi-start Powell and SCE-UA methods for calibrating the Tank model were assessed by Chen et al. (2005). The model accuracy and calibration performance have been effected by uncertainties which are input, model structure, parameter and output uncertainty. Uncertainties originating from model structure were evaluated by choosing distinct reasonable model structures within a general hydrological modeling tool by Butts et al. (2004a). They indicated that the model constructions are important for modeling approach. In order to

determine optimum input parameters based on the global objective criteria, an SCE module was directly integrated into the SWAT code by Van Griensven and Bauwens (2003, 2005). The effect of DEM mesh size and soil map scale on SWAT runoff, sediment, and NO₃ predictions were assessed by Chaplot (2005). In that study, various map scales (1/25,000; 1/250,000, and 1/500,000 scale) within the SWAT were used for simulating runoff, sediment and NO₃ load. Although the map scales had few differences in runoff, nitrogen as well as sediment loads were greatly affected by the scale of the soil. The finest soil information improved the forecast quality for runoff, nitrogen and sediment loads for all DEM mesh sizes were improved. Food and Agricultural Organization (FAO) soils with the State Soil Geographic Dataset (STATSGO) and the Soil Survey Geographic Database (SSURGO) were compared by Levick et al. (2004). The comparison was made by using the Kinematic Runoff and Erosion Model (KINEROS2). At the end of this study, when the STATSGO soils used, runoff were generally higher than with the SSURGO. Furthermore, FAO soils generated less runoff than the STATSGO soils in most cases. The difference in data resolution caused the variations in runoff and soil properties.

GA and GLUE methods for conducting parameter calibration and uncertainty analysis of SWAT were combined by Muleta and Nicklow (2005). Parameter Estimation method (PEST) was applied in order to calibrate important hydrologic parameters for SWAT applications in South Africa and Northwest Minnesota, respectively, by Govender and Everson (2005) and Wang and Melesse (2005). When PEST approach was compared between its automatic and manual versions, the automated PEST approach leads to less accurate predictions than manual calibration according to Wang and Melesse (2005). For easy implementation of calibration algorithms, SWAT-CUP, which is a semi-automated calibration and uncertainty software for the SWAT, was developed by Abbaspour et al. (2007). It includes a multi-site, semi-automated inverse modeling routine (SUFI-2) for calibration and uncertainty analysis. The model accuracy and calibration performance have been evaluated by using many different methods. According to Moriasi, D. N. et al., 2007, Nash-Sutcliffe efficiency (NSE), percent bias (PBIAS), and ratio of the root mean square error to the standard deviation of measured data (RSR) are most suitable methods for assessing model accuracy by comparing simulated and measured data with graphical techniques. Before calibration

process, sensitivity analysis should be performed to find key parameters that have great effect on hydrologic cycle. The process is needed for understanding the main processes for the element of interest. Most sensitive parameters for hydrology and water quality are the physical soil properties such as bulk density, available water capacity or hydraulic conductivity, plant specific parameters similar to maximum stomatal conductance or maximum leaf area index as well as slope length, slope steepness, and curve number (Lenhart et al., and T., 2008). Yang et al. (2008) compared GLUE, ParaSol, SUFI-2, and a Bayesian framework implemented using Markov Chain Monte Carlo (MCMC) and Importance Sampling (IS) techniques on a SWAT model of the Chaohe Basin in China, based on the posterior parameter distributions, performances of their best estimates, prediction uncertainty, conceptual bases, computational efficiency, and difficulty of implementation. At the end of the study, Bayesian-based approaches were found to be the most acceptable since the approach contains parameter correlation. However, construction and test of the likelihood function needs essential notice. The GA and Bayesian Model Averaging (BMA) were employed for calibration and uncertainty analysis at the same time for SWAT by Zhang et al., (2008). After several SWAT models were examined with various snow, potential evaporation and flow routing methods, the specific model elements of SWAT were selected. The GA was applied to calibrate each model using observed stream flow data. At the end of the study, BMA was applied in order to combine union prediction and supply uncertainty interval estimation. When a single-objective optimization method (GA) and a multi-objective optimization algorithm (SPEA2) were used on three observing areas within the Reynolds Creek Experimental Watershed to calibrate the parameters of SWAT by using observed stream flow data (Zhang et al., 2008), GA method had better identification of parameter solutions in the calibration process, while the SPEA2 method performance in the calibration stage was better than the GA. The SUFI-2 algorithm accounting for prediction uncertainty was used for the calibration of a hydrologic model of Iran by Faramarzi et al. (2009).

Advantages and disadvantages of the PEST against the GLUE method for calibrating SWAT were studied by Ng et al. (2010b). Arnold et al. (2011) mentioned a semi-automated approach (SUFI-2) comprising sensitivity and uncertainty analysis. It provides a decision-making framework. Schuol et al. (2008) applied SWAT on 18

countries in West Africa in order to estimate freshwater validity in the West African sub-continent. While generating HRUs, dominant land use and soil type within each sub-basin were applied due to very large surface area and hence elongated computational time required. In that study, SUFI-2 was applied for calibration and validation procedure of the model since calibration and uncertainty analysis performance of SUFI-2 is good at such computationally extensive models. This is because calibration and uncertainty analysis can be executed with relatively small number of simulations by SUFI-2. The SWAT model with Variable Source of Area (VSA) Hydrology was re-conceptualized (Easton et al., 2008) in order to measure overland flow by changing the curve number (CN2) and available water content. This approach was named as SWAT-VSA. The SWAT and the SWAT-VSA were employed on a sub-watershed in the Cannonsville basin in upstate New York in order to see differences between model predictions of incorporated and dispersed effects, including surface runoff, shallowly perched water table depth, and stream phosphorus loads versus straight estimations. Although the SWAT-VSA and the SWAT predicted runoff similarly well, the SWAT-VSA forecasted the dissemination of shallowly perched water table depth and dissolved phosphorus export from the watershed better.

Different model structures in hydrologic models, which are lumped, hydrologic response unit (HRUs) or hydrotope, catena, and grid, were used by Arnold et al. (2010) in order evaluate differences between these model structures. The lumped models can be calibrated like complicated structures, but the effect of upslope management on downslope landscape situations cannot be shown. If sub-basins are adequately small, the lumped method is efficient. Although soil, land use, and slope heterogeneity are preserved by the HRU method, it does not have spatial position. The effect of spatial position on management such as plant growth, crop yields and runoff can be simulated by the grid representation. Nevertheless, using a small grid size is not feasible for large scale river basin modeling. A catena approach simulates the models as discrete units while preserving landscape position and allowing riparian and flood plain areas. If HRUs are preferred to simulate within each landscape unit, the catena approach may be more suitable choice for large scale modeling studies. Lumped, semi-lumped and semi-distributed structures of the Sacramento Soil Moisture Accounting model (SAC-SMA) were compared by Ajami et al. (2004). The calibration results showed that the

simulation results were improved from a lumped model structure to a semi-distributed model construction when each sub-basins used averaged data which were identical for all sub-basins. However, the simulation results at the outlet and an interior testing point were not further improved by using various parameters between sub-basins.

The effects of land use variations in the SWAT were assessed by Baker and Miller (2013). They found that there was relationship between surface runoff and groundwater recharge. With increases in surface runoff, groundwater recharge decreases.

The SWAT model for Europe was calibrated by Abbaspour et al. (2015). They used SUFI-2 in SWAT-CUP package for uncertainty analysis, sensitivity and calibration process. Large-scale model development includes many difficulties and limitations because of restricted and unequally dispersed nitrate data and discharge stations within time series lengths, limited knowledge of attributes and management of the reservoirs and lack of information about agricultural management operations, and lack of soil and groundwater data. As a result, calibration results were affected negatively on some places in this large-scale model.

Faramarzi et al. (2015) indicated that proper calibration and uncertainty analysis of large scale hydrological model depends correctly setup. While building a hydrological model of Alberta, they used different source of data (e.g., MODIS land cover, GlobCorine, National Climate Data Center, European Climate Assessment Dataset., etc.) of data and evaluated the results. They mention that data discrimination analyses prior to calibration is an important step in order to reach better results.

A grid-based form of the SWAT landscape model was developed to improve the spatial representation of hydrological and transportation procedure by Rathjens et al., 2014. As a result of the model construction, the impact of the landscape position on surface runoff, subsurface runoff and evapotranspiration could be simulated reasonably. Fenicia et al. (2016) studied the distributed hydrological models in order to understand discretizing the landscape used for model structures. According to their

results, the model results of geology-based HRUs are better than topography-based HRUs in capturing the spatial variability of stream flow time series.

2.2. Hydrologic Modeling and Calibration

Many hydrologic models, which are hydrological transport models, distributed hydrological models, composite models etc., have been used in order to understand hydrological processes in the world.

Distributed hydrologic models take spatial dependence of meteorological input, soils, vegetation and land use into account. Since the distributed hydrological models combine spatial variability of these inputs while simulating hydrologic process in the watershed basin, the models are frequently applied to produce water management strategies. Advantages of these models are that they can better streamflow prediction at the basin outlet and predict streamflow at the interior locations where streamflow measurements may not be applicable (Koren et al., 2004). Semi-distributed models are based on lumped models, which treat the complete basins as a homogeneous whole. They model hydrological processes at sub-basins or sub-areas of the basin that are considered as homogeneous within themselves. The semi-distributed models can estimate the stream flow at the basin outlet and at the interior points more accurately than distributed models (Khakbaz et al., 2012). Since semi-distributed models are easier to setup and require relatively shorter running times, the semi-distributed SWAT model was chosen for this study.

Careful calibration and uncertainty analysis are important for these models so that they can be used for guiding water management policies. Calibration of watershed models is not an easy process because the models include many uncertainty types, which are input, model structure, and parameter and output uncertainties. Input uncertainties are caused by imprecise or spatially interpolated measurements of model input like elevation data, land use data, rainfall intensity, temperature or initial conditions like initial groundwater levels. Some unknown activities and oversimplification of the

processes regarded in the model cause uncertainties. Moreover, unknown parameters and errors in the data that are utilized for parameter calibration lead to uncertainties in the models (Arnold et al., 2010).

Uncertainty analyses of the models can be divided into three main categories:

(i) All uncertainties can be represented by an enhanced parameter uncertainty without rigorous statistical assumptions. “Generalized Likelihood Uncertainty Estimation (GLUE) (Beven and Binley, 1992)” and “Sequential Uncertainty Fitting (SUFI-2) (Abbaspour et al., 2004, 2007)” are some examples.

(ii) An additive error model introducing temporal correlation of the residuals shows the impact of input and model structural errors on the output. Autoregressive error models can be given as an example for this kind of analyses.

(iii) Input errors and/or model structure errors are represented by developing likelihood functions such as a Bayesian framework implemented using Markov Chain Monte Carlo (MCMC).

When comparing these methods, the most acceptable ones are the techniques in category (iii) due to their ability to handle parameter correlation. However, these techniques require more computation time when applied to hydrological models. For this reason, practical applications of the first and the second techniques to complex hydrological models are important (Yang and et al., 2008). Because of this, in this study, a second type method, “Sequential Uncertainty Fitting (SUFI-2)”, was preferred. Since one of the aims of this study is to reduce calibration computational time, an automatic calibration method was needed. SWAT-CUP is a semi-automated computer program for calibration of SWAT models. The program includes GLUE, ParaSol, SUFI-2, MCMC, and PSO, which provides sensitivity analysis, calibration, validation, and uncertainty analysis of a SWAT model. In order to implement hierarchical approach to hydrological model calibration/validation, we selected one of the methods. When selecting calibration techniques in hydrological modeling, we confront various difficulties. Philosophies and subjective choices of most techniques are different with regard to prior parameter distribution. This results in various

objective functions for various techniques that are used in hydrological applications. Thus, their intercomparison is difficult. Calibration techniques were chosen according to ease of application, computational efficiency, accuracy of uncertainty range estimation and the model prediction performance.

2.1.1 Semi-Automated Calibration Methods

To fulfil the requirements of an automatic calibration tool, SWAT-CUP was developed for SWAT as an interface. The primary function of the interface is to manage the flow of information between the model and a calibration program. The data exchange is realized through text files. The interface provides the ability that any calibration/uncertainty or sensitivity program can simply be integrated into SWAT. The model parameters to be optimized are systematically modified, the model is simulated and the needed results (relating to simulated data) are obtained from the model output files in the automated model calibration. Particle Swarm Optimization (PSO), Sequential Uncertainty Fitting Algorithm (SUFI2), Monte Carlo Markov Chain (MCMC), Generalized Likelihood Uncertainty Technique (GLUE) and Parameter Solution (ParaSol) are connected to SWAT by the program (Figure 1). Sensitivity analysis, calibration, validation, and uncertainty analysis of a SWAT model are provided.

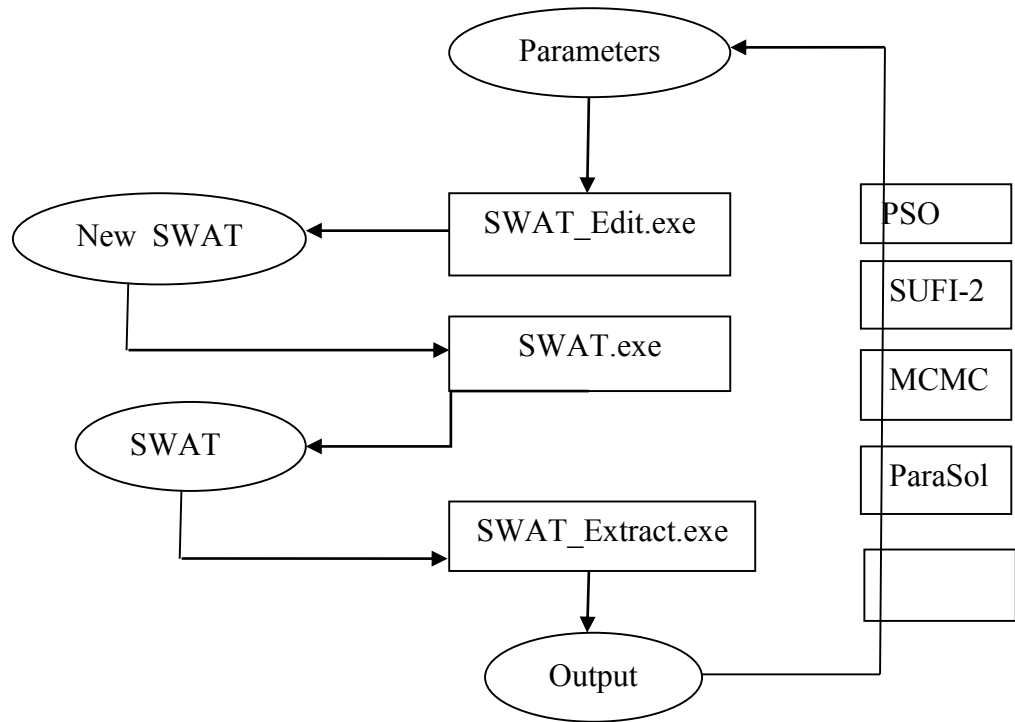


Figure 1 SWAT-CUP program structure (Abbaspour et al., 2007)

2.1.1.1 Particle Swarm Optimization (PSO)

Particle swarm optimization (PSO), which is known as a population based on stochastic optimization technique, was developed by Eberhart and Kennedy (1995). PSO solves a problem by having a population of candidate solutions (called particles). These particles are moved in the multi-dimensional search-space depending on a few simple formulae. Its local best-known position space effects each particle's movement. Other particles try to find better positions while the best-known positions in the search-space are updated. This is anticipated to move the swarm toward the best solutions. Since the particles have memory, they keep part of their previous state. Although the same point in the belief space can be shared by particles, their identities are protected. Particles' movement depend on both an initial random velocity and two randomly weighted influences which are individuality, the inclination to come back to the particle's best previous position, and sociality, the inclination to displace towards the neighborhood's best prior position. However, optimization performance depends on the choice of PSO parameters.

2.1.1.2 Monte Carlo Markov Chain (MCMC)

Samples from a random walk that suits to the posterior distribution (Kuczera and Parent, 1998) are produced by MCMC. Parameter sets representing the posterior distribution in a sequence (Markov Chain) is built as below:

- 1) In order to determine a first beginning point in the parameter space, a point is determined randomly.
- 2) By using a symmetrical jump distribution (*jump f*) in order to add a random realization, a candidate for deciding the next point is suggested. The next point of the sequence has coordinates:

$$\theta_{k+1\varphi}^* = \theta_k + rand(f_{jump})$$

- 3) The candidate points are determined based on the ratio *r*:

$$r = \frac{f_{\theta post|Y}(\theta_{k+1}^* | y_{means})}{f_{\theta post\varphi|Y}(\theta_k | y_{means})}$$

$$f_{y^m|\theta}(y|\theta) =$$

$$\frac{1}{\sqrt{2\pi}} \frac{1}{\sigma} \exp\left(-\frac{1}{2} \frac{[g(y_{t_0}) - g(y_{t_0}^m(\theta))]^2}{\sigma^2}\right) \cdot \left| \frac{dg}{dx} \right|_{y=y_{t_0}}$$

$$\prod_{i=1}^n \left(\frac{1}{\sqrt{2\pi}} \frac{1}{\sigma \sqrt{1 - \exp\left(-2\frac{t_i - t_{i-1}}{t}\right)}} \exp\left(-\frac{1}{2} \frac{[g(y_{t_i}) - g(y_{t_i}^m(\theta)) - [g(y_{t_{i-1}})] \exp\left(-\frac{t_i - t_{i-1}}{t}\right)]]^2}{\sigma^2 \left(1 - \exp\left(-2\frac{t_i - t_{i-1}}{t}\right)\right)}\right) \cdot \left| \frac{dg}{dy} \right|_{y=y_{t_i}} \right)$$

The asymptotic standard deviation of the errors is *r*, the characteristic correlation time is *s*, the vector of model parameters is θ , the observation and model simulation are y_{t_i} and $y_{t_i}^M(\theta)$ at time t_i , and *g*, respectively.

If $r \geq 1$, then a new point with probability *r* is used as a candidate. If the point is unaccepted, the following point of the sequence is used for deciding. The shuffled complex global optimization algorithm supports to calculate the posterior distribution. If the chain is initiated at a numerical estimation of the maximum of the posterior

distribution, long burn-in periods or even lack of convergence to the posterior distribution are avoided (Duan et al., 1992).

2.1.2.3 Generalized Likelihood Uncertainty Technique (GLUE)

GLUE is “an Importance sampling and regional sensitivity analysis (RSA)” are executed by GLUE, which is an uncertainty analysis technique (Hornberger and Spear, 1981). The technique can handle input uncertainty, structural uncertainty, parameter uncertainty and response uncertainty, since it is connected with parameters and illustrates all uncertainties and impact of the co-variation of parameter values on model performance indirectly (Beven and Freer, 2001). When the model is non-linear and there are various sources of error that affect each other to generate the measure bias (Gupta et al., 2005), GLUE can be used.

A GLUE analysis is comprised of three steps:

(1) In order to measure generalized likelihood measure, the previous distribution is used for determining parameter sets, each parameter set is assessed as “behavioral” or “non-behavioral” using the “likelihood measure” with a chosen threshold value.

(2) “Likelihood weight” is calculated from each behavioral parameter

$$W_i = \frac{L(\theta_j)}{\sum_{k=1}^N L(\theta_k)}$$

The number of behavioral parameter sets is N.

(3) Quantiles of the cumulative distribution obtained from the weighted behavioral parameter sets defines prediction uncertainty. GLUE has used widely the Nash–Sutcliffe coefficient (NS) as likelihood measure for (e.g., Beven and Freer, 2001; Freer et al., 1996).

$$NS = \frac{\sum_{ti=1}^n (y_{ti=1}^m(\theta) - y_{ti})^2}{\sum_{ti=1}^n (y_{ti} - \bar{y})^2}$$

The number of the observed data points is shown as n , the observation and model simulation with parameters θ at time t_i are represented by y_{ti} and $y_{ti=1}^m(\theta)$, respectively and the average value of the observations is \bar{y} .

2.1.1.4 ParaSol

When the global optimization algorithm SCE-UA was modified, It was called as ParaSol (Duan et al., 1992) algorithm. The procedure of ParaSol is as below:

(1) The coverage of the parameter space is first improved using the modified SCE-UA algorithm. “good” and “not good” simulations in GLUE are determined according to a threshold value of the objective function. As a result, good simulations’ parameter set is defined as “good” parameter set and vice visa.

(2) Equally weighting all “good” simulations construct prediction uncertainty.

The sum of the squares of the residuals (SSQ) is used by the objective function in ParaSol:

$$SSQ = \sum_{ti=1}^n (y_{ti}^m(\theta) - y_{ti})^2$$

$$NS = 1 = \frac{1}{\sum_{ti=1}^n (y_{ti} - \bar{y})^2}$$

A fixed value for given observations is $\sum_{ti=1}^n (y_{ti} - \bar{y})^2$. In order to enhance the comparability with GLUE, NS were used as an objective function in ParaSol.

The χ^2 statistics is used for determining the threshold of the objective function.

2.1.1.5 SUFI-2

SUFI-2 can calculate all sources of uncertainties, which are input, conceptual model, parameter and measured data uncertainty. The degree of uncertainty can be accounted by a P factor, which is the percentage of measured data bracketed by the 95% prediction uncertainty (95PPU). Although the model, which includes all important hydrological processes, is constructed very well and input parameters such as precipitation and temperature distributions are rightly modeled, the model still includes error since its prediction contains uncertainty. The assessment of the strength of the uncertainty analysis is made by the percentage of data bracketed by the prediction uncertainty. By using Latin hypercube sampling, the 95PPU, which is calculated at the 2.5% and 97.5% levels of the cumulative distribution of an output variable, is obtained. Five percent of the very bad simulations are disallowed. Parameter uncertainty can be calculated by the 95PPU, if the measured variables include all forms of uncertainties (e.g., discharge). The R factor is another representative measurement for a calibration/uncertainty analysis. It is calculated by the average thickness of the 95PPU band divided by the standard deviation of the measured data. Hence, SUFI-2 searches the smallest possible uncertainty band. In Figure 2, the concept of the SUFI-2 algorithm is illustrated graphically. When a single parameter value causes a single model response, the relationship between parameter uncertainty and prediction uncertainty is like in Figure 2a. The shaded region in Figure 2b is observed when the 95PPU causes the uncertainty to spread in a parameter (represented by a line). Increase of parameter uncertainty causes an increase in the output uncertainty (Figure 2c). As a result of this, at the first step of SUFI-2, it begins by presuming a physically meaningful large parameter uncertainty, then the uncertainty is reduced by SUFI-2 in steps while the P-factor and the R-factor are observed. In each step, while accounting the sensitivity matrix (equivalent to the Jacobian), an equivalent of a Hessian matrix, followed by the calculation of covariance matrix, 95% confidence intervals of the parameters, and the correlation matrix, antecedent parameter ranges are updated (Abbaspour, 2007). Updated parameter ranges shrink at each calibration step of SUFI2 (Abbaspour et al., 2004, 2007). The model is assessed according to ranges of P-factor and R-factor in SUFI2. The P factor

ranges are between 0% and 100%, whereas the R-factor ranges are between zero and infinity. If the P-factor is close to unity and the R-factor is close to zero in a simulation, then the simulated data match the measured data. These values provide the assessment of the strength of our calibration. There is a balance between the P-factor and the R-factor: if a larger P-factor is obtained, a larger R-factor can be achieved. If acceptable values of R factor and P-factor are obtained, the desired parameter ranges are reached. The goodness of fit between the measured and observed data is calculated by the R^2 and/or NSE. If parameter ranges are set equal to the maximum physically meaningful ranges are set and a 95PPU still cannot be found, calibration of the parameter and the model construction must be reviewed (Figure 2d).

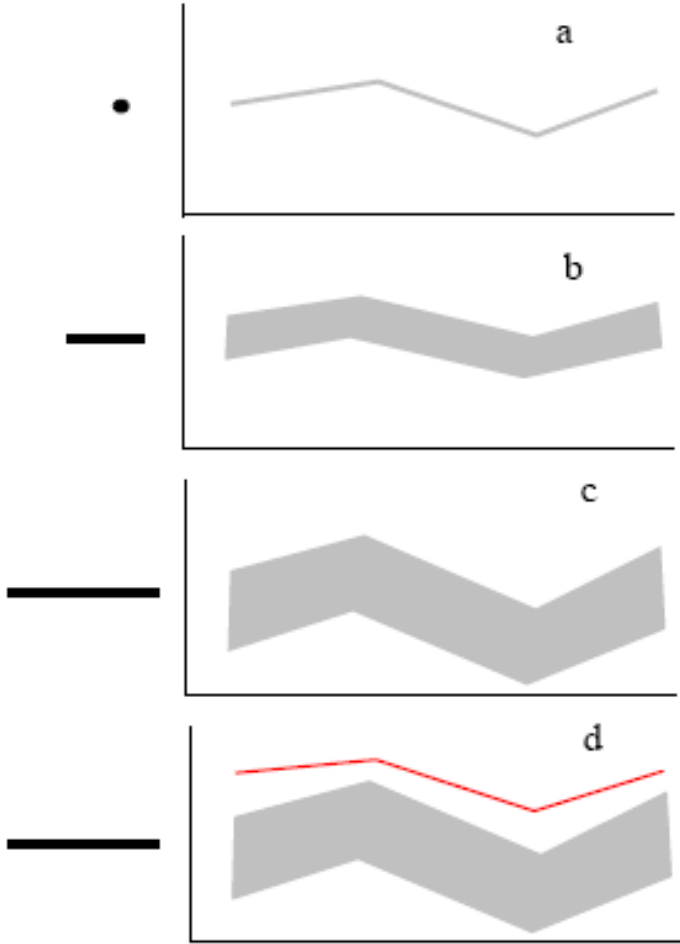


Figure 2 The relation between parameter uncertainty and prediction uncertainty (Abbaspour et al., 2007)

2.1.1.5.1 SUFI-2 Procedure

SUFI-2 includes all uncertainties, which are the input data (e.g., rainfall), the conceptual model, the parameters, and the measured data. SUFI2 uses Latin hypercube sampling for producing an independent parameter set (Abbaspour et al., 2007). A multivariate uniform distribution in a parameter hypercube defines the parameter uncertainty. When the measured variables (e.g. discharge) include all forms of uncertainties, the 95PPU, which is produced by the parameter uncertainties, describes all uncertainties. The 95PPU is accounted at the 2.5% and 97.5% levels of cumulative distribution of an output variable by using the cumulative distribution of an output variable that is got from Latin hypercube sampling (Abbaspour et al., 2007).

SUFI-2 is described as below:

Step 1. An objective function is determined. Since an objective function can be formulated in different ways (Legates and McCabe, 1999; Gupta et al., 1998), each expression may cause a distinct outcome. The last parameter extents are always adopted depending on the type of the objective function. This problem is got over by combining different types of functions (e.g., Yapo et al., 1998) like root mean square error, absolute difference, logarithm of differences, R^2 , Chi square, Nash-Sutcliffe to provide a “multi-criteria” formulation. Moreover, when a “multi-objective” formulation (Duan et al. 2003; Gupta et al., 1998) is used, the non-uniqueness problem is reduced since various variables are comprised in the objective function.

Step 2. Minimum and maximum ranges of parameters are determined so as to define boundary at the parameter range. These ranges should be physically meaningful. The probability density function of all parameters are modelled as uniform distribution within the extreme values. Certain parameter ranges should be as large as possible since they play a constraining role:

$$b_j: b_j, \text{abs_min} \leq b_j \leq b_j, \text{abs_max} \quad j = 1 \dots m, \quad (1)$$

The j-th parameter is represented by b_j and the number of parameters to be estimated is shown as m .

Step 3. Sensitivity analysis should be made in order to realize the physical system and to obtain knowledge about the impacts of parameters on the system response.

Step 4. To initiate the first iteration of Latin hypercube sampling, initial ranges are assigned to the parameters:

$$b_j: [b_{j,\min} \leq b_j \leq b_{j,\max}] \quad j = 1, m \quad (2)$$

The parameter range selection is based on experience and it is subjective. The sensitivity analysis can help to decide selection of suitable ranges.

Step 5. Subsequently, Latin hypercube sampling is implemented with respect to n combinations of parameters (McKay et al., 1979). Simulation count should be as large as possible (approximately 500-1000) in order to adjust to fine parameter combinations.

Step 6. The objective function, g , is evaluated as a first stage in iterating the simulations,

$$J_{ij} = \frac{\Delta g_i}{\Delta b_j} \quad i=1, \dots, C_2^n, \quad j = 1, \dots, m \quad (3)$$

C_2^n represents the number of rows in the sensitivity matrix. In that matrix, whole possible combinations of two simulations are shown. The number of columns, number of parameters, are shown as j . Then, \mathbf{H} , a Hessian matrix, is obtained using the Gauss-Newton method and ignoring the higher-order derivatives as:

$$\mathbf{H} = \mathbf{J}^T \mathbf{J} \quad (4)$$

An estimate of the lower bound of the parameter covariance matrix, \mathbf{C} , is calculated according to the Cramer-Rao theorem (Press et al., 1992):

$$\mathbf{C} = \mathbf{S}_g^{-2} (\mathbf{J}^T \mathbf{J})^{-1} \quad (5)$$

Step 7. At the end of n runs, the variance of the objective function values, \mathbf{S}_g^2 , is found. Diagonal elements of \mathbf{C} is used for calculating standard deviation and 95% confidence interval of a parameter b_j (Press et al., 1992):

$$S_j = \sqrt{C_{jj}} \quad (6)$$

$$B_{j, \text{ lower}} = b_j^* - t_{v, 0.0025} S_j \quad (7)$$

$$B_{j, \text{ upper}} = b_j^* + t_{v, 0.0025} S_j \quad (8)$$

One of the most suitable choice such as parameters which generate the smallest value of the objective function is shown as the parameter b , and the degrees of freedom ($n - m$) is represented by v . The evaluation of parameter is provided by the diagonal and off-diagonal variables of the covariance matrix:

$$r_{ij} = \frac{C_{ij}}{\sqrt{C_{ii}} \sqrt{C_{jj}}} \quad (9)$$

The correlation matrix is represented by r which is quantified based on the change in the objective function as a result of a change in parameter i relative to changes in other parameter j . The correlation between any two parameters is anticipated to be very insignificant since in SUFI-2 sets of parameters hold all parameters constant while only one is changed. Averaging the columns of the Jacobian matrix provides parameter sensitivities, S as seen as in Step 3. The sensitivities,

$$S_j = b_j \frac{1}{C_2^n} \sum_{i=1}^{C_2^n} \left| \frac{\Delta g_i}{\Delta b_j} \right| \quad j=1, \dots, m, \quad (10)$$

The mean differences in the objective function that is resulting from differences in each parameter is estimated while all other parameters are changing. As a result, relative sensitivities based on linear approximations are given by [10]. Thus, the sensitivity of the objective function to model parameters is quantified. The absolute sensitivity of a parameter is described in Step 3. When output variable(s) of interest is/are taken by other parameters, the absolute sensitivity of a parameter can change in relation to the other parameters that assume different optimized values.

Step 8. The uncertainties are computed. The 2.5th (XL) and 97.5th (XU) percentiles of the cumulative distribution of every simulated point shows the 95% prediction uncertainties (95PPU) for all the variable(s) in the objective function. The uncertainty measures which is calculated from the percentage of measured data bracketed by the

95PPU band evaluates the goodness of fit. The average distances d between the upper and the lower 95PPU (or the degree of uncertainty) are obtained as below:

$$d_x = \frac{1}{k} \sum_{i=1}^k (X_{u1} - d)l, \quad (11)$$

The number of observed data points are shown as k . Although the best result is that 100% of the measurements are bracketed by the 95PPU, and d is close to zero, the ideal values will generally not be obtained due to measurement errors and model uncertainties. An acceptable measure for d is calculated by the R-factor:

$$\text{R-factor} = \frac{dx}{\vartheta_x} \quad (12)$$

The standard deviation of the measured variable X is indicated as ϑ_x . If a value of less than 1, it is a valuable estimation for the R-factor.

Step 9: Since at the first step, there is too big parameter uncertainties, the value of d is expected to incline to be large during the first step of SUFI2. As a result, further step of the optimization is made with updated parameter ranges computed from:

$$b'_{j,\min} = b'_{j,\text{lower}} - \text{Max}\left(\frac{(b_{j,\text{lower}} - b_{j,\min})}{2}, \frac{(b_{j,\max} - b_{j,\text{upper}})}{2}\right)$$

$$b'_{j,\max} = b'_{j,\text{upper}} - \text{Max}\left(\frac{(b_{j,\text{lower}} - b_{j,\min})}{2}, \frac{(b_{j,\max} - b_{j,\text{upper}})}{2}\right)$$

The updated value is indicated by b' . Parameters of the best simulation are used to calculate $b_{j,\text{lower}}$ and $b_{j,\text{upper}}$. With new iterations, parameter ranges get narrower and the parameters are updated as the center of the range.

2.1.1.5.2 Latin Hypercube Sampling

Latin hypercube sampling (LHS) was described by McKay in 1979. It is a statistical technique used for reducing the number of samples from multidimensional distributions. While sampling a function of K variables, the range of each variable is separated into evenly feasible intervals (Liebetrau and Doctor, 1987). Secondly, N

sample points are located to provide for Latin hypercube requirements. The number of divisions must be equal for each variable. The sampling schema does not need more samples for more dimensions. There are two important points in Latin Hypercube: number of sample points to use and which row and column of the sample point is taken. Accept that each of the k components X_j of the vector X is divided into N intervals. Indicate these intervals as $I_{1j}, I_{2j} \dots I_{Nj}$ for $j=1, 2 \dots k$ (k is the number of parameters). For each parameter X_j the interval is separated so that

1. It divides the range of X in N intervals and
2. $P_{ij} = \text{Prob}\{X_j \in I_{ij}\} = 1/N \quad i=1,2,\dots,N.$

The set of all Cartesian products generated from the intervals is:

$$\{I_{n_1} * I_{n_2} * \dots * I_{n_k} : n_j = 1, 2 \dots N; j=1,2,\dots,k\}$$

A separation P of the parameter-input space into N^k cells is obtained by these maps. The coordinate vector $n = (n_1, n_2, \dots, n_k)$ defines the “location” of each cell in P . A LHS design of size N includes N cells randomly chosen from P by getting randomly one of the $N!$ permutations of the integers $\{1, 2, \dots, N\}$ which is written in the first column of the n_k “design” matrix D . Then, a second permutation is produced and written in the second column, etc. The vector of integers in each row of the “design” matrix D defines a cell in P . The N cells that are specified by D are the LHS design.

2.1.2 Comparison of the GLUE, ParaSol, SUFI-2, MCMC, and PSO Methods for Calibration

The GLUE, ParaSol, SUFI-2, MCMC, and PSO methods have been studied for calibration by many researcher. These methods were compared in Table 1 (Yang and et al., 2008). If GLUE is calibrated by using the Nash–Sutcliffe coefficient as objective function, the broadest marginal parameter uncertainty intervals of the model parameters are observed. Although, GLUE supplies good prediction uncertainty with regard to coverage of measurements by the uncertainty bands, it is inefficient to find location of the maximum or maxima of the objective due to the global sampling procedure. A good estimation to the global maximum of NS can be found by ParaSol

optimization technique. However, it results in too narrow prediction uncertainty bands since independent and normal distributed errors assumption is not satisfied in reality. The prediction uncertainty bands in smallest number of model simulations provides that SUFI-2 could reach good prediction uncertainty ranges with regard to a suitable coverage of data points. It is significant for models that are computationally difficult. Although SUFI-2 has these advantages, the decision of a small sample size clearly reduces the parameter space and causes the poorly defined convergence criterion. However, since it does not consider parameter correlations, it reduces the ability of finding a unique posterior. The MCMC is applied according to “a continuous-time autoregressive error model”. Since the global optimization is executed before initiating the Markov chain, a good estimation to the maximum of the posterior is achieved by the MCMC. There are many advantages in MCMC methodology: the statistical assumptions of the error model can be tested, and they can adapt to empirical evidence. Moreover, the method provides the user some independence in determination of the effect of input and model structure error by additional parameters of the error. The construction of the likelihood function and coverage of multi-model distributions are difficult since the great number of simulations are needed to obtain a good estimation to the posterior.

Permitting for arbitrary likelihood measures/objective functions make GLUE and SUFI-2 very flexible. However, the decision of the objective function affects the ability of searching the parameter space. The MCMC, whose likelihood function is based on testable statistical basis, has no violation of the assumption in the test result. The impact of input, model structure and output uncertainty on model output (e.g., autoregressive error model) are delineated by the likelihood function, and analyses the different sources of uncertainty. However, while using complex hydrological models, the computation still takes a long time.

Although GLUE, SUFI-2 and MCMC have different concepts and performance, they result in not very different uncertainty bands (Yang and et al., 2008). SUFI-2 is chosen for testing our methodology since SUFI-2 associates optimization with uncertainty analysis and can handle a large number of parameters. Applying gradient methods can end up in local minimum since these methods are very sensitive to the initial values of the parameters to be optimized. Furthermore, a reliable estimate of parameter

uncertainty is not supplied by gradient methods. Global methods for calibration have required too many iterations. SUFI-2 has been developed to get over these problems. The beginning (large) uncertainty in the model parameters is gradually decreased until certain calibration criteria for prediction uncertainty are met in SUFI-2 method.

Table 1 Comparison of uncertainty analysis techniques for a SWAT application to the Chaohe Basin in China (Yang et al., 2008).

Criterion	GLUE	ParaSol	SUFI-2	MCMC
	Yes	Yes	Yes	yes
Parameter correlation				
Parameter uncertainty describes uncertainty	All sources of uncertainty	Parameter uncertainty only	All sources of uncertainty	Parameter uncertainty only
Source of prediction uncertainty	Parameter uncertainty	Parameter uncertainty	Parameter uncertainty	the autoregressive error model describes Parameter uncertainty + all other uncertainties
Theoretical basis	a. Normalization of generalized likelihood measure b. Primitive random sampling strategy	a. Least squares (probability theory) b. SCE-UA based sampling strategy	a. Generalized objective function b. Latin hypercube sampling; limited by sampling intervals	a. Likelihood function (Probability theory) b. MCMC beginning from optimal parameter set based on SCE-UA
Difficulty of implement	Very easy	Easy	Easy	More complicated
R2 for calibration	0.80	0.82	0.81	0.78
R2 for validation	0.84	0.85	0.81	0.81
Number of runs	10,000	7500	1500 + 1500	5000 + 20,000 + 20,000

2.2 SWAT Model and SWAT Calibration

2.2.1 SWAT Model

SWAT has been used for hydrological transport modeling (Figure 3). The main model elements are weather, hydrology, soil temperature and properties, plant growth, nutrients, pesticides, bacteria and pathogens and land management. The watershed is separated into a number of sub-watersheds based on the topography (Figure 4). Each sub-watershed is further separated into hydrologic response units (HRUs), which comprise similar land use and soil type combinations within the sub-watershed (Figure 5). Hydrologic process at the sub-catchment level are simulated by SWAT by obtaining from hydrological response units (HRUs). The smallest element of SWAT is the HRU. Many inputs such as digital elevation model, soil type, land use, and slopes effects the size of an HRU. The HRU distribution is defined by user-defined thresholds in the current implementation of SWAT. Although, the size of an HRU changes based on user requirements, the typical area of an HRU in SWAT ranges from about 50 to 500 ha. SWAT simulates hydrological process in two steps: (1) upland flow and loadings of sediment, nutrients, bacteria, and pesticides from each HRU are calculated, and then HRU-level loadings to the sub-watershed level are combined proportionally; and (2) The upland loadings from each sub-watershed through the channel/stream network are routed by the model as seen in Figure 6 (Gassman, 2007).

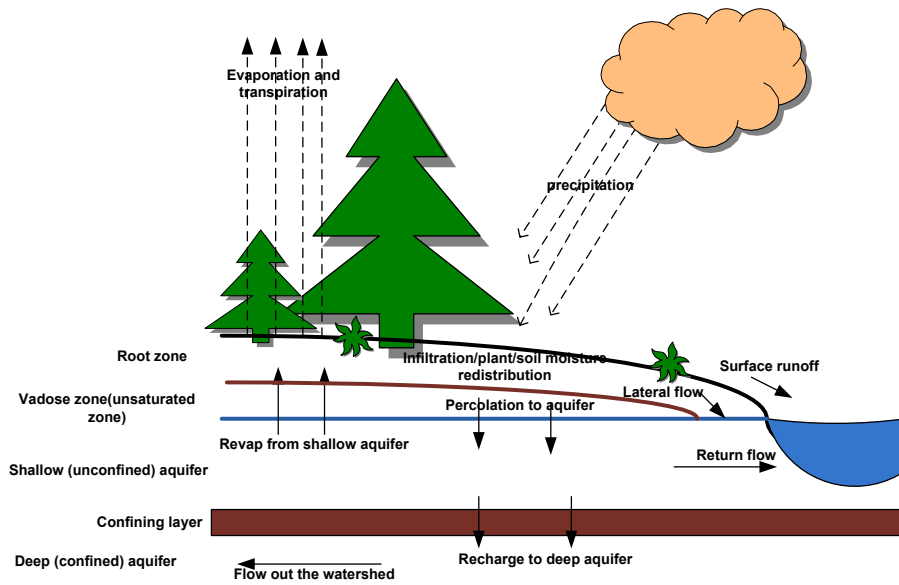


Figure 3 The hydrologic cycle as represented in SWAT

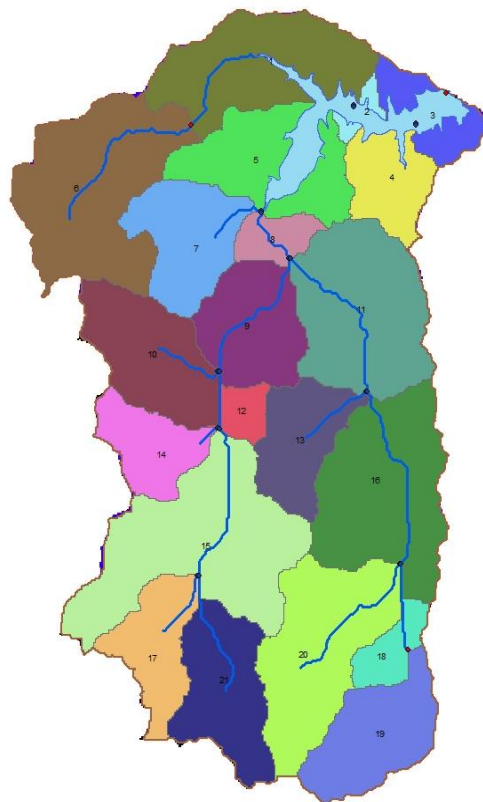


Figure 4 Representation of sub-basins and streams

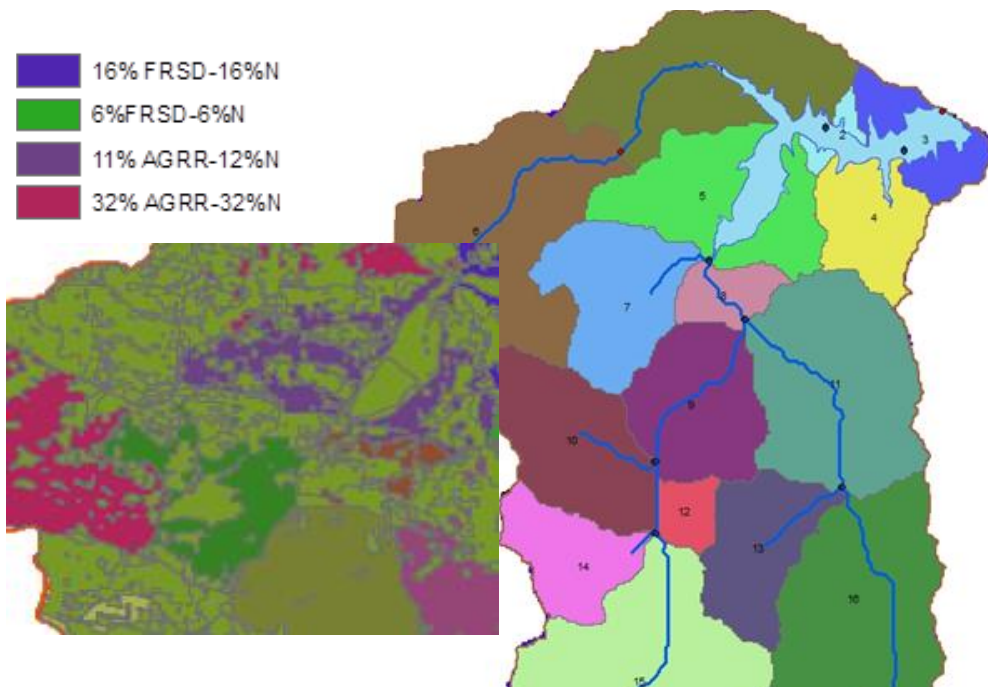


Figure 5 Distribution of HRUs in a subbasin

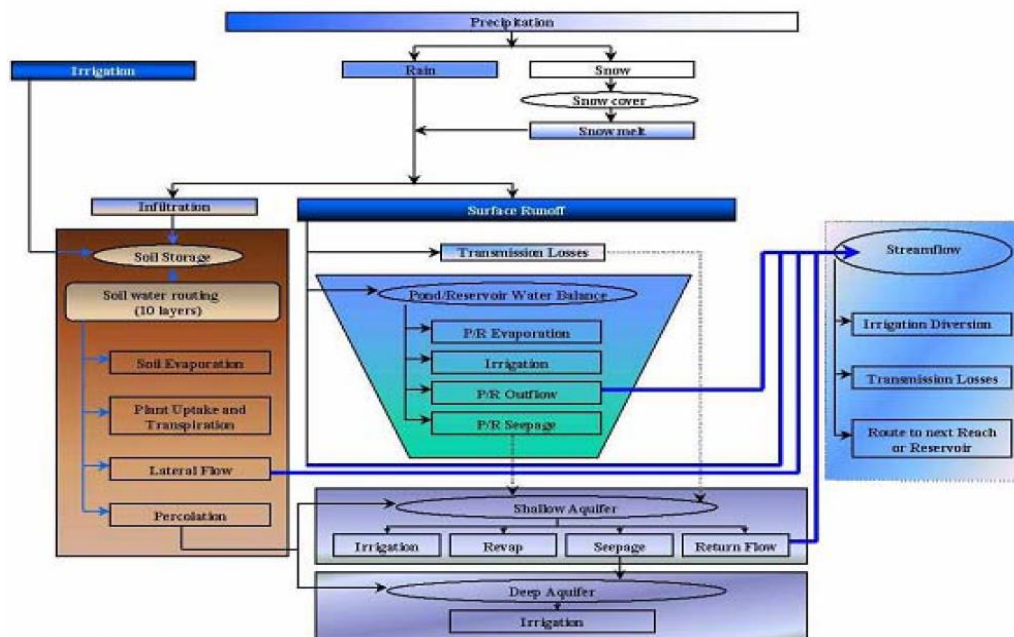


Figure 6 The water management pathways in SWAT (Neitsch et., al., 2011)

2.2.2 SWAT Calibration

Major components of SWAT input parameters, which are weather, hydrology, soil temperature and characteristics, plant growth, nutrients, pesticides, bacteria and pathogens, and land management (consumptive use through pumping, return flow, and recharge by seepage from surface water bodies, ponds, and tributary channels), must be within reasonable uncertainty range. Firstly, the most delicate parameters for hydrologic process in the watershed or sub-watershed under question should be found out for the calibration and validation process in SWAT. Sensitivity analysis, which is the procedure of the deciding the rate of difference in model output with regard to differences in parameters, should be applied in order to find key parameters which has great impact on the hydrologic process. This step is required for understanding the main processes for the element of interest. The calibration process is the second step. The prediction uncertainty is reduced by elaborating on finding a better parametric model according to local conditions in the calibration step. Model calibration is carried out as model prediction are compared with the observed data. The process is continued to find acceptable prediction model output according to measured data while changing model input parameter values. The flowchart of general calibration for flow, sediment, and nutrients is represented in Figure 7 as formulated by Engel et al., 2007. The manual calibration steps are as follows:

- (1) The simulation is performed,
- (2) Measured and simulated values are compared,
- (3) It is evaluated whether acceptable outcomes have been achieved,
- (4) If there is no reasonable result, input parameters are adjusted within acceptable parameter value ranges depending on expert opinion and
- (5) The process is repeated until it is thought that the best outcomes have been obtained.

The hydrologic process parameters (evaporation, evapotranspiration, surface/base flow ratios, tile flow proportions, plant yield, and biomass) should be controlled during the calibration process so as to ensure that the predictions are acceptable for the watershed. Transportation processes such as stream flow, sediment and nutrient transport should be fine-tuned consecutively since there are relationships between components due to shared transport processes (Santhi et al., 2001; Engel et al., 2007).

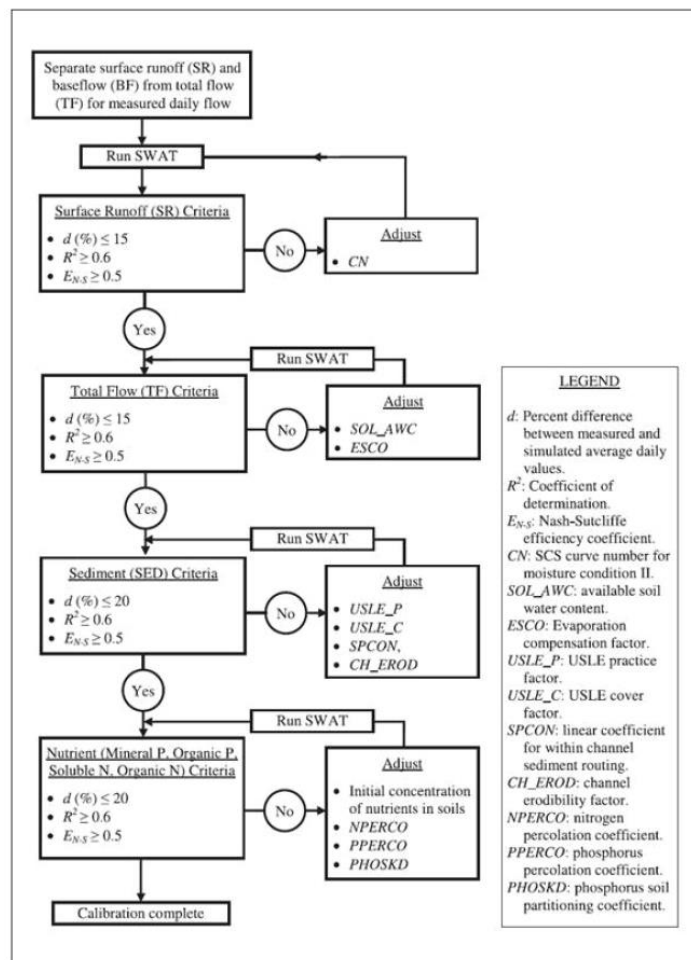


Figure 7 Example flowchart of manual calibration in SWAT (Engel et al., 2007; Santhi et al., 2001).

When there are many uncertainties in the model and complicated hydrologic models are generated, manual calibration can take a long time (Balascio et al., 1998). Many semi-automated or automated calibration methods were developed to attack that problem. Semi-automatic calibration and uncertainty analysis have been integrated in

SWAT2009 (Gassman et al., 2010) through the SWAT-CUP software developed by Eawag (2009). SWAT-CUP is an interface that was developed for SWAT. Although many semi-automated calibration methods have been developed for SWAT such as “generalized likelihood uncertainty estimation (GLUE), shuffled complex evolution (SCE), and the Parameter Estimation (PEST)” methods, calibration processes have still computational inefficiency since comparison between calibration parameters and measured data requires several thousand SWAT simulation for completion.

CHAPTER 3

HIERARCHICAL APPROACH TO SEMI-DISTRIBUTED HYDROLOGICAL MODEL CALIBRATION

There are at least five different discretization methods which are: “lumped approach (Chiew et al., 1993), hydrologic response unit (HRU; Arnold et al., 1998) or hydrotope approach (Krysanova et al., 1998), catena approach (Kirby et al., 1998; Lane and Nearing, 1989), topographic index approach (Beven and Kirkby, 1979), and complex fully distributed approach (Abbott et al., 1986; Bronstert and Plate, 1997)” in hydrologic models. The dominant soil, dominant land use and average land slope generate HRU in one of the lumped methods. In HRU methodology, firstly, a watershed is divided into a number of sub-basins depending on topography. Each sub-basin is further divided into HRUs. Similar land use and soil type combinations within the sub-basin generates HRUs. There is no spatial reference for HRU, and there is no flow between HRUs in hydrotope method. Water yield at the watershed outlet is calculated while streaming from each HRU is summarized at each sub-basin. The watershed is separated into the divide, hillslope, and valley bottom in the catena method. The catena approach struggles to force a systematized upscaling from topographic location to watershed scale. More detailed downslope routing of surface runoff, lateral flow and groundwater can be achieved, and the effect of upslope direction on downslope landscape situations can be evaluated within the catena. Although catena method has many advantages, the problem of catena is that it is not easy to find representative catenas for different regimes. Moreover, in contrast to permitting routing, the catena approach assumes one rather simple slope configuration for the whole sub-watershed. Watershed is divided into a grid that has unique soil, land use, and slope with watershed-weighted precipitation. The DEM determines stream pathway, all water flowing from a cell flows into another cell, from Although the grid representation delivers substantially more spatial detail than the catena delineation, it requires too much computational time and memory (Brien, et al., 2013). Differences

in hydrologic conditions for various land covers/crops and soils in the model are provided by HRUs. Runoff is anticipated independently for each HRU and routed to get the total runoff for the watershed. Thus, the accuracy of load predictions is increased and physical definition of the water balance gets much better. The HRU distribution is divided into two options which are, a single HRU is assigned to each sub-watershed or a multiple HRUs are assigned to each sub-watershed. When a single HRU per sub-basin is chosen, the dominant land use, soil and slope within each watershed determines the HRU, soil type, and slope class. If multiple HRUs are preferred, sensitivities are defined for the land use, soil, and slope data that will be employed to decide the number and variety of HRUs in each sub-basins. In order to eliminate minor land uses in each su-basin, threshold values are used. After the thresholds are defined, the remaining area is reallocated proportionately so that 100% of the land area in the sub-basin is modeled. For instance, let us suppose we have a sub-basin that has landuse types and areas given in (Table 2).

Table 2 Example of land use for current HRU division

Landuse	Area %
Barren	4.3%
Slender Wheatgrass	6.6%
Forest-Deciduous	11.57%
Forest-Evergreen	0.35%
Residential-High Density	0.44%
Agricultural Land-Generic	39%
Residential	0.26%
Residential-Low Density	0.09%
Agricultural Land-Row Crops	0.39%
Garrigue	26 %
Pasture	11 %

If 25% is defined for the threshold level for land use, HRUs would be generated for agricultural land-generic and garrigue. The areas of modeled land uses would be changed as below:

agricultural land generic: $(39 \% \div 65\%) \times 100\% = 60\%$

Garrigue: $(26\% \div 65\%) \times 100\% = 40\%$

Creation of HRUs depending on threshold area of soil and land use separation leads to ignoring some important combinations that may have great impact on hydrological process in watershed such as surface runoff. As a result, the model performance declines and the calibration takes a long time. In contrast, a large number of HRUs can handle a variety of land covers. Using small and comparatively homogeneous HRUs decreases the error caused by lumping effects (Geza and McCray, 2008). However, it results in a complicated cost function, hence increased probability of sticking into local minima. Moreover, the required computation time increases with HRUs non-linearly. In this work, we adopt a hierarchic approach, similar to many other optimization problems, in order to increase performance and reduce computational complexity simultaneously. For hierarchical optimization, we divide each sub-basin into two-HRUs and optimize with respect to some important parameters that may have important effect on hydrological processes in the watershed. Then, each HRU is further divided into two. Each child HRU inherits the optimum parameters of the parent HRU as its initial values. Thus, we expect to decrease the total calibration time and a solution closer to the global minimum of the cost function. To be able to do that, we have created a totally different HRU generation algorithm based on some important parameters which have great impact in water cycle such as the curve number, the available water capacity or the bulk density. By combining default curve number default soil hydraulic conductivity and soil classification, HRU types are generated by using MATLAB scripts. In order to understand HRU type model performance, SUFI-2 was chosen as calibration process since SUFI-2 simulation iterations are less than other methods while similar NSE and r^2 values are produced (Yang et al., 2008). According to Nash-Sutcliffe objective function, the model performance is controlled. Depending on assessment of NS and r^2 values, HRU types are increased until reaching acceptable results or the steady state (Figure 8).

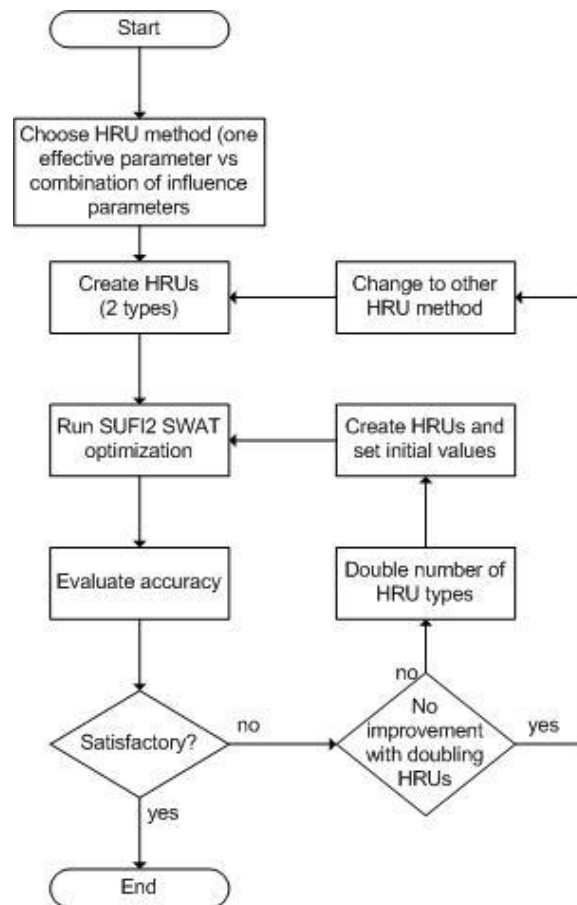


Figure 8 General concept of hierarchical methodology

3.1 Full Automatic Version of SUFI-2

In order to reduce calibration computational time and to provide easy usage of calibration methods, Semi-automatic calibration with uncertainty analysis tools was developed by Eawag (2009) and integrated into the SWAT-CUP software program. To provide a connection between input/output of calibration programs and the model is the primary role of the interface. The file exchange is through formatted text files in the interface. The uncertain model parameters are consistently transferred in the automated model calibration, the model is run and the needed outcomes (relating to measured data) are derived from the model output files. Any calibration/uncertainty or sensitivity program can simply be connected to SWAT by using the interface. It provides computational efficiency. SUFI-2 in SWAT-CUP uses Latin hypercube with

a global search algorithm that describes the behavior an objective function by analyzing the Jacobian and Hessian matrices. By using Latin Hypercube, parameters cube is generated depending on given parameters range and simulation count. Depending on SUFI-2 in SWATCUP working principle, the beginning (large) uncertainty in the model parameters is gradually decreased at each iteration until constant calibration values for prediction uncertainty are obtained in SUFI-2 procedure. While comparing SWAT model results by using each parameter range in Latin Hypercube, best range of parameters is found at each iteration. If found parameter range at the end of the iteration is reasonable, calibration process is finished. If the assessment of calibration value does not give satisfactory results, another calibration process is initiated by using new parameter range at the end of the last iteration. To continue further calibration by using new parameter range at the end of iteration is decided by user. Moreover, semi-automatic SUFI-2 is inefficient for updating SWAT parameter values. In order to solve these problems, reduce time for calibration, minimize user interaction and increase performance of the calibration procedure, a software package was produced by developing full automatic calibration model in MATLAB. Calibration procedure of SUFI-2 can be performed full automatically by this method.

3.1.1 File Structure of SUFI-2

The uncertain model parameters are gradually changed in SUFI-2 semi-automated model calibration. In the semi-automatic calibration method, the file exchange is through text file formats. At the first step of the calibration, input files, namely, *Par_inf.txt*, *trk.txt*, *SUFI-2_swEdit.def*, *observed_rch.txt*, *observed.txt* and *var_file_name.txt* should be prepared. **Par_inf.txt** file includes parameters which will be optimized the maximum and minimum values of these parameters and also number of the parameters and number of simulation counts. **trk.txt** file behaves as a counter. Simulation count number is written in this file. The start which does not contain the warm up period and the termination simulation years are located in **SUFI-2_swEdit.def** file. **observed_rch.txt** file includes the name of the variable and the sub-basin number to be contained in the objective function. There are the number of data

points for this variable, first column is a sequential number from beginning and second column is variable name and date (format arbitrary), third column is variable value. **Objective Function** is defined in the observed file. All the information for the calculation of objective function is in **observed_rch.txt**. Likewise, the variables, which should be contained in the objective function, are listed by the **Var_file_name.txt**.

3.1.2 SUFI-2 Running Procedures in SWAT-CUP

SUFI-2 calibration methodology has been applied in SWAT-CUP by using many system files (exe) in order to easy implementation. First step is that Latin Hypercube sampling (LHS) which is a statistical method is applied in SUFI-2 for reduce the number of samples from multidimensional distributions. SUFI-2_LH_sample.exe provides to run Latin Hypercube sampling. SUFI-2_LH_sample.exe is used for producing the parameter cube which is written in par_val.txt file. Each parameter set in par_val.txt is placed sequentially into the model by using SUFI-2_make_input.exe. While the program uses trk.txt, par_inf.txt, par_val.txt, it generates echo_make_par.txt and model_in that is used for finding the best model. By using model_in and BACKUP file, which is SWAT model input files in order to update SWAT output files, SWAT_Edit.exe program creates new parameter files for running SWAT model. While using parameters in model.in, SWAT.exe runs the model so as to produce output files of the model. According to results of output files of the model, SUFI-2_extract_rch.exe creates stream flow values with respect to simulation number written in trk.txt. The input files, namely, par_inf.txt, observed.txt, par_val.txt, var_file_name.txt, are used for reaching the best simulation. Best parameters and best simulation number are found by running SUFI-2_goal_fn.exe.

Finally, SUFI-2_95ppu.exe finds objective functions values by using par_inf.txt, observed.txt and var_file_rch.txt. Summary_stat.txt file includes some statistical values that are uncertainty values, p-factor and r-factor, and R2, NS, bR2, MSE, and SSQR representing the best simulation of the current iteration. The file contains the objective function type, best simulation number of the present iteration, and the best

value of the objective function for the present run. The best parameters of the current iteration and the best simulated values are represented respectively in **best_par.txt** and **best_sim.txt**. The value of all parameter sets and the objective function are represented in the **Goal.txt**. By using **SUFI2_new_pars.exe**, new parameters are generated. They are showed in **New_Pars.txt** file. New parameter ranges in the file can be used for the next iteration (Figure 9).

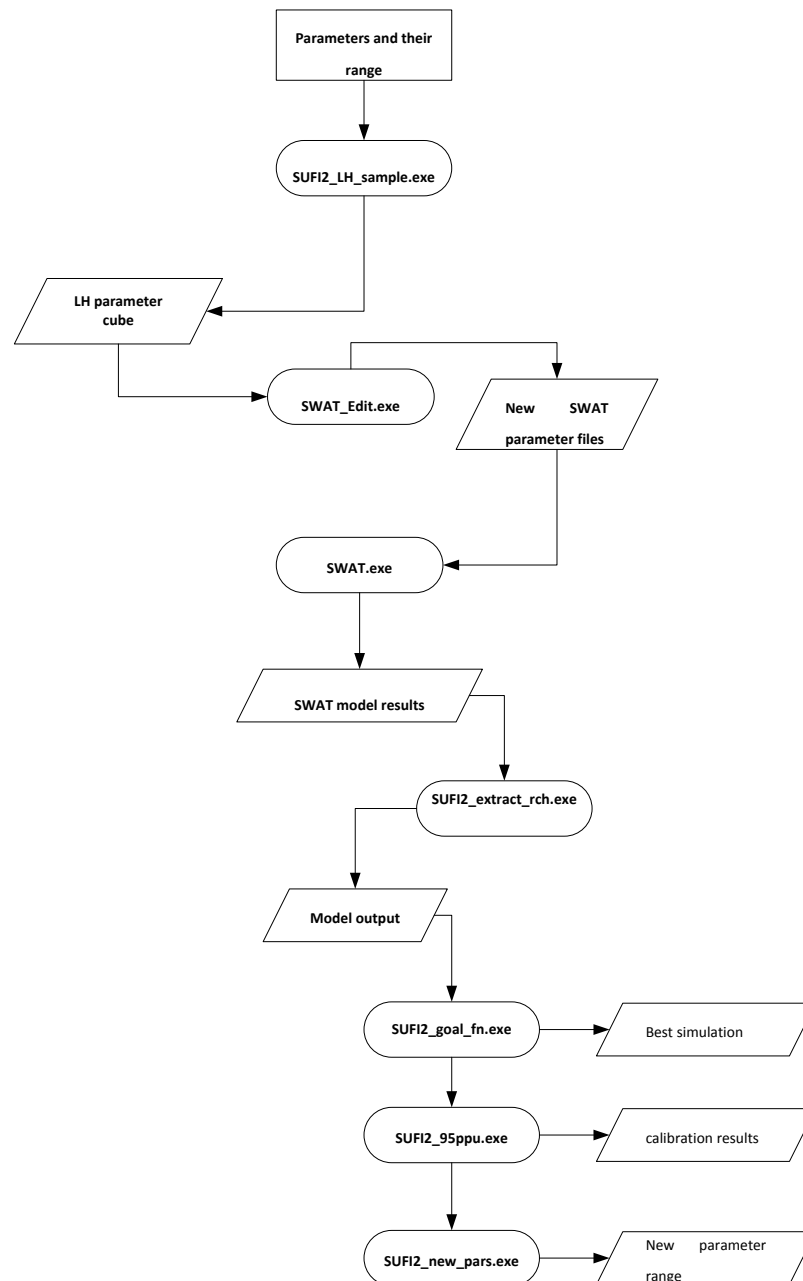


Figure 9 Sequence of program execution of SUFI-2 in SWAT-CUP (Abbaspour et al., 2007)

3.1.3 Developed SUFI-2 Algorithm on MATLAB

At the first step, in order to start calibration process, parameters and parameter ranges should be defined. Parameters that are expected to have great impact on hydrological processes in the watershed and their ranges were determined by using a script. Although the user can change these, calibration process can be completed in one step by defining simulation count in our system. With respect to simulation count, SUFI-2 is run once. So as to assess calibration result, Nash-Sutcliffe coefficient of effectiveness (NSE) (Nash and Sutcliffe, 1970) was selected to be objective function since NSE function represents not only the relationship between simulated and observed discharge but also the evaluation of amount of water. In each iteration, objective function value is evaluated automatically and according to the value, calibration procedures is performed automatically. At the end of each iteration, new parameter ranges are obtained and the ranges are used in SUFI-2 automatically. Until the largest NSE value is reached, SUFI-2 calibration process is repeated without any user interaction. Using graphical interface, calibration process can be monitored. When the best calibration value is obtained, calibration process is finished automatically, and backup file, which includes SWAT model results used for calibration process, is updated without any user interaction. Thus, depending on the user demand, the backup file can be used for further calibration process (Figure 10).

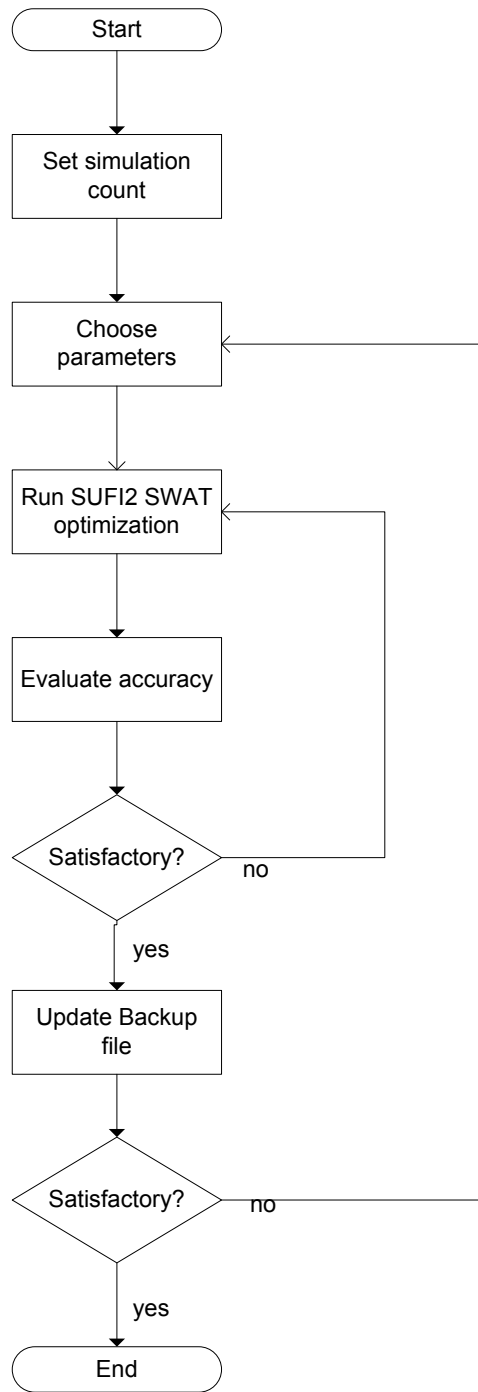


Figure 10 Developed SUFI-2 algorithm on MATLAB

3.2 Soil Database for SWAT

Physical and chemical properties of soil can be represented in SWAT as a soil database. Physical characteristics of the soil are texture, length of soil layer from surface to bottom, moist bulk density, available water capacity of the soil layer, saturated hydraulic conductivity, soil erodibility (K) factor etc. Chemical characteristics of soil are used to establish primary values of chemicals present in the soil. Physical properties for each soil type is an important because the displacement water and air via the profile are governed by these properties. Furthermore, they have great effect on the hydrological processes within the HRU.

SWAT soil data type is different from Turkey so many properties of soil class in the area were obtained from (Ardas, S., and Creutberg, D., 1997). Required data for SWAT are listed as follow containing interpretations (Neitsch et al., 2002a):

SNAM	: Name of soil
HYDGRP	: Hydrologic class of soil (A, B, C or D)
A	: A high transmission water capability of the soils even when completely moistened. It includes mainly sands or gravel, they are deep and unconscionable drained.
B	: Moderate transmission water capability when the soils are from end to end moistened. It includes partially coarse textures.
C	: Slow infiltration capability (high runoff potential) when completely moistened.
D	: Very slow transmission water capabilities (high runoff potential) when completely moistened. It includes mainly clay soils that have high swelling potential. There can be a high persistent water table.

SOL_ZMX	: The maximum root depth of soil profile (mm). If no value is assigned, the model presumes the roots can enhance from the beginning to the end of the complete depth of the soil profile.
ANION_EXCL	: Fraction of porosity (void space) from which anions are left out. When soil minerals are negatively loaded at normal pH and the net interaction with anions like sulfate is resilience from particle surfaces. This recoil is called as negative adsorption or anion exclusion. The model set ANION_EXCL = 0.50 is given when there is no data for ANION_EXCL.
SOL_CRK	: A fraction of the total soil volume which means probable or maximum crack volume of the soil profile (if there is no data about SOL_CRK, no value can be entered in the database).
TEXTURE	: Texture of soil layer.
SOL_Z (layer number (layer #))	: Soil layer extent from surface to bottom (mm).
SOL_BD (layer #)	: moist bulk density (Mg/m^3 or g/cm^3). The ratio of the mass of solid particles to the total volume of the soil is showed by the soil bulk density. Mean values for distinct soil types were assigned in the model based on literature.
SOL_AWC (layer #)	: Available water capacity of the soil layer ($\text{mm H}_2\text{O/mm soil}$). It is measured from taking out the fraction of water store at persistent wilting point from that store at field capacity. It is also known as the plant available water. Mean values for distinct soil types were assigned in the model by using literature.
SOL_K (layer #)	: Saturated hydraulic conductivity (mm/hr). According to soil texture, mean values for distinct soil types were assigned in the model by using Guidelines for Soil Description, 2005.
SOL_CBN (layer #)	: Organic carbon content (% soil weight).

- CLAY (layer #) : Clay content (% soil weight).
- SILT (layer #) : Silt content (% soil weight).
- SAND (layer #) : Sand content (% soil weight).
- ROCK (layer #) : Rock fragment content (% total weight).
- USLE_K (layer #) : USLE equation soil erodibility (K) factor

3.2.1 Soil Texture Classification through the Watershed

The Ministry of Food, Agriculture and Livestock has classified soils in Turkey based on depth, salinity, slope and drainage properties of them. According to Ardas, S., and Creutberg, D., 1997, soils textures are determined by using depth and slope information of the soils (Table 3).

Table 3 Depth of Class Reference Ranges

Depth Classification	Depth (cm)
Lithosol	< 5
Very shallow	0 – 20
shallow	20 – 50
Moderately deep	50 – 90
deeper	90 – 150

Compositions of sand, silt and clay contents as a percentage for various soil textures in literature are shown in Figure 11. The compositions of % Clay, %Sand and % Silt, are given in (Table 4)

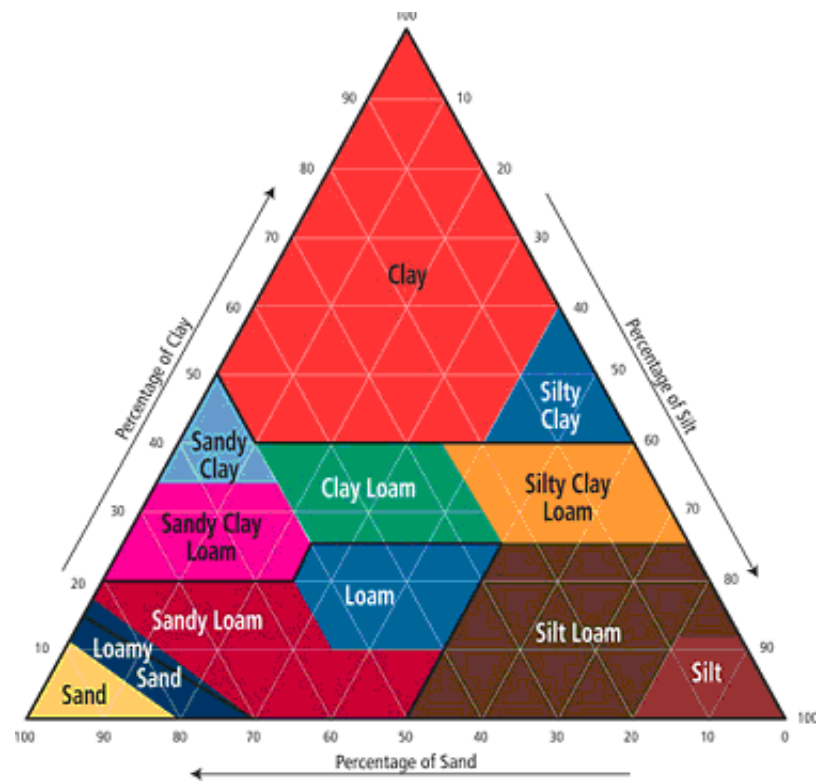


Figure 11 Soil triangle (Ley et al., 1994)

Table 4 The relationship between texture class and ranges of clay, sand and silt

Texture	Sand (%)	Clay (%)	Silt (%)
coarse	80	10	10
Moderately coarse	60	20	20
moderately	40	30	30
fine	20	40	40

3.2.2 Definition of USLE_K FACTOR

Rainfall and runoff frequently cause erosion. It is accounted with the Modified Universal Soil Loss Equation (MUSLE) (Williams, 1975). Wischmeier and Smith (1965, 1978) developed MUSLE, which is a revised form of the Universal Soil Loss Equation (USLE). Average annual gross erosion as a function of rainfall energy is anticipated by USLE. Soil erodibility depends on soil properties (Neitsch et al., 2002b). USLE_K factors used in SWAT were established with respect to the soil textures (Table 5). The value of USLE_K is between 0.1 and 0. A value of < 0.02 shows a soil of low erodibility; $0.02 - 0.04$ shows moderate erodibility; and > 0.04 shows high erodibility. When silt content of soil type increases, it can become more erodible regardless of whether there is a comparable reduction in the sand or clay fraction (Rosewell, 1993).

Table 5 USLE_K Values with respect to soil texture. Source: Rosewell, 1993.

Texture	Symbol	Suggested K factor	Texture	Symbol	Suggested K factor
Sand	S	0.015	Clay Loam	CL	0.030
Clayey Sand	CLS	0.025	Silty Clay Loam	SCL	0.040
Loamy Sand	LS	0.020	Fine Sandy Clay	FSC	0.025
Sandy Loam	SL	0.030	Sandy Clay	SC	0.017
Fine Sandy Loam	FSL	0.035	Silty Clay	SiC	0.025
Sandy Clay Loam	SCL	0.025	Light Clay	LC	0.025
Loam	L	0.040	Light Medium Clay	LMC	0.018
Loam, Fine Sandy	LFS	0.050	Medium Clay	MC	0.015
Silt Loam	SL	0.055	Heavy Clay	HC	0.012

3.2.3 Definition of SOL_BD (Soil Bulk Density)

SOL_BD values utilized in SWAT were got from Guides for Editing Soil Properties, (2005) due to inadequacy data. According to soil textures, SOL_BD values are shown in Table 6. SOL_BD values were assigned in the model based on fine (C-SC-SiC), medium (SiL-CL-SCL-SiCL) and coarse (L-SL-LS-S) texture groups.

Table 6 SOL_BD Values with respect soil textures (Mg/m³) Source: Guidelines for Soil Description, 2005.

Texture	Symbol	Suggested SOL_BD		Texture	Symbol	Suggested SOL_BD	
		Range	Avg.			Range	Avg.
Sand	S	1.60 - 1.70	1.65	Clayey Loam	CL	1.40 - 1.50	1.45
Loamy Sand	LS	1.55 - 1.65	1.60	Silty Clay Loam	SiCL	1.45 - 1.55	1.50
Sandy Loam	SL	1.50 - 1.60	1.55	Sandy Clay	SC	1.35 - 1.45	1.40
Silty Loam	SiL	1.45 - 1.55	1.50	Silty Clay	SiC	1.40 - 1.50	1.45
Sandy Clay Loam	SCL	1.45 - 1.55	1.50	Clay	C	1.25 - 1.45	1.35
Loam	L	1.45 - 1.55	1.50				

3.2.4 Definition of SOL_AWC (Soil Available Water Capacity)

Available soil capacity values utilized in SWAT were got from Ley et al., 1994 since there is no data. SOL_AWC values are given in Table 7 with respect to soil texture. SOL_AWC values were assigned in the model with respect to fine (C-SC-SiC), medium (SiL-CL-SCL-SiCL) and coarse (L-SL-LS-S) texture groups. While setting the SOL_AWC in the model, average values of them were used.

Table 7 SOL_AWC Values with respect to soil textures (mm H₂O/mm soil) Source: Guidelines for Soil Description, 2005.

Texture	Symbol	Suggested SOL_AWC		Texture	Symbol	Suggested SOL_AWC	
		Range	Avg.			Range	Avg.
Sand	S	0.06-0.08	0.07	Clayey Loam	CL	0.15-0.19	0.17
Loamy Sand	LS	0.09-0.11	0.10	Silty Clay Loam	SiCL	0.18-0.20	0.19
Sandy Loam	SL	0.12-0.14	0.13	Sandy Clay	SC	0.16-0.21	0.19
Silty Loam	SiL	0.20-0.22	0.21	Silty Clay	SiC	0.11-0.13	0.12
Sandy Clay Loam	SCL	0.16-0.18	0.17	Clay	C	0.09-0.11	0.10
Loam	L	0.17-0.19	0.18				

3.2.5 Definition of SOL_K (Soil Hydraulic Conductivity)

Saturated hydraulic conductivity values utilized in SWAT were taken from Guidelines for Soil Description, 2005 (Table 8). SOL_K values were decided in the model based on fine (C-SC-SiC), medium (SiL-CL-SCL-SiCL) and coarse (L-SL-LS-S) texture groups.

Table 8 SOL_K values depending on soil textures (mm/h) (Guidelines for Soil Description, 2005)

Texture	Symbol	Suggested SOL_K		Texture	Symbol	Suggested SOL_K	
		Range	Avg.			Range	Avg.
Sand	S	152.40-508.10	330.25	Clayey Loam	CL	5.10-15.20	10.15
Loamy Sand	LS	152.40-508.10	330.25	Silty Clay Loam	SiCL	5.10-15.20	10.15
Sandy Loam	SL	50.80-152.40	101.60	Sandy Clay	SC	1.50-5.10	3.3
Silty Loam	SiL	15.20-50.80	33.00	Silty Clay	SiC	1.50-5.10	3.3
Sandy Clay Loam	SCL	5.10-15.20	10.15	Clay	C	1.50-5.10	3.3
Loam	L	15.20-50.80	33.00				

CHAPTER 4

RESULTS

4.1. Case Study: Sarısu-Eylikler River, Konya, Turkey

Sarısu-Eylikler stream basin is located between 37.47°-38.15° latitudes and 31.73°-32.47° longitudes in Konya Closed Basin, Turkey. The area of the Sarısu-Eylikler basin is 1040 km² and the average total annual flow of Sarısu-Eylikler Stream was 68 million m³ between 1992 and 2010 (Figure 12).

The drinking water to Beyşehir district and around is supplied by Beyşehir Lake Basin. Industrialization, agricultural activities and irrigation, fishing, erosion, waste disposal, tourism, soil and sand extraction, storage affect the basin negatively. Since the most significant river to recharge Beyşehir Lake is Sarısu, the proposed methodology applied on this basin.

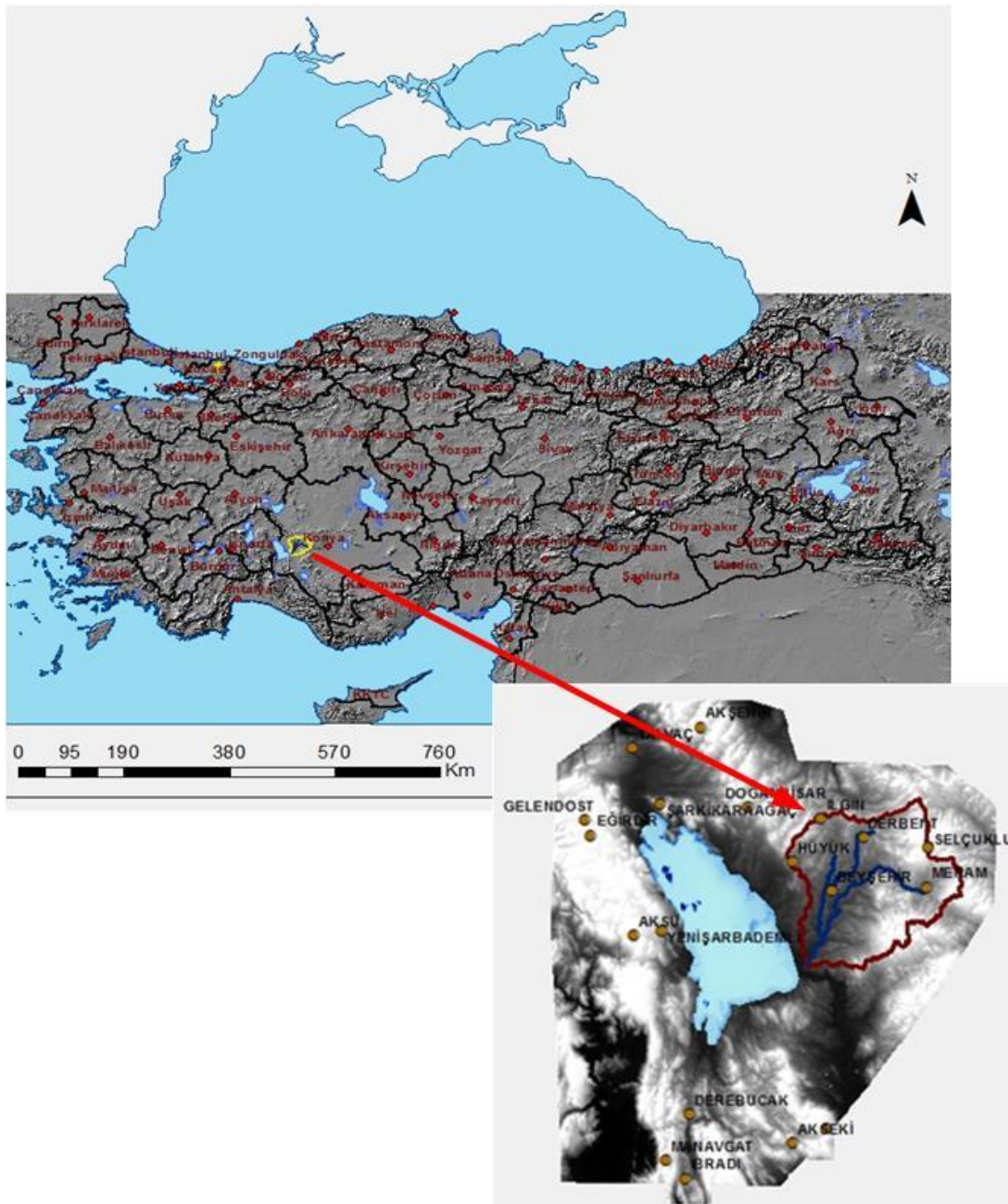


Figure 12 Study Area

4.1.1. SWAT Input Layers

The SWAT elements are weather, hydrology, soil temperature and properties, plant growth, nutrients, pesticides, bacteria and pathogens and land management. The input layers are digital elevation model, soils, land use, and slopes.

4.1.1.1 Delineation of Watershed

The Digital Elevation Model (DEM) was used to define sub-basins by Automatic Delineation Tool of SWAT. Thus, watersheds were segmented into several "hydrologically" related to sub-basins for use in watershed modeling with SWAT (Winchell et al., 2013). The Automatic Delineation Tool creates watershed by using ArcGIS and Spatial Analyst extension function.

The DEM was generated from 1:25 000 scale topographic maps (Figure 13). The DEM properties are given in Table 9.

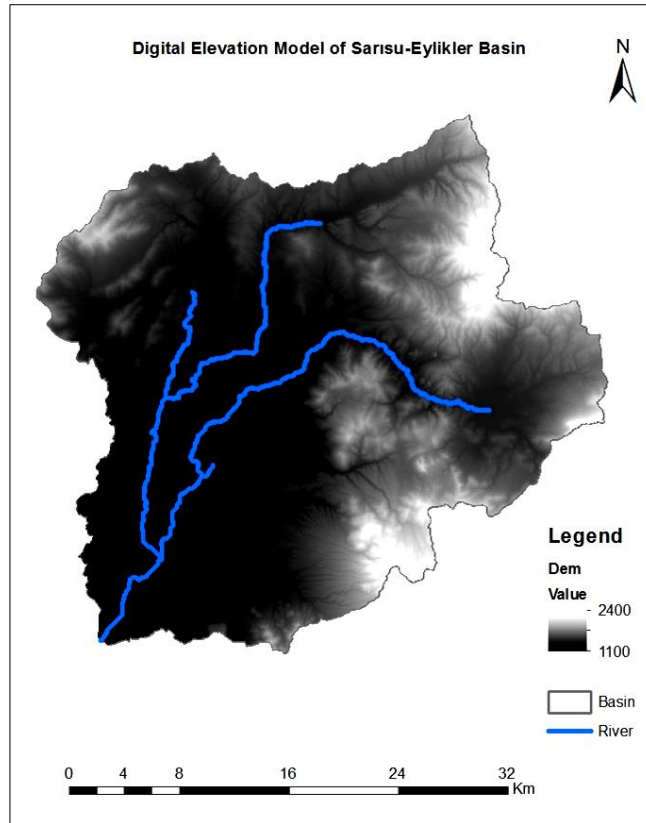


Figure 13 Digital Elevation Model of Sarsu-Eylikler Basin

Table 9 DEM Properties

Metadata parameter	Value
Projection	Universal Transverse Mercator (UTM)
False Northing	500000
False Easting	0.000000
Central Meridian	33
Scale Factor	0.9996
Reference Latitude	0.000000
Geographic Coordination System	WGS_1984_36 N
Column/Row count	4156/3915
Cell size (X/Y) (m/m)	10/10
Bits per pixel	32

In order to produce sub-basins of the watershed from the DEM, many operations were applied on the DEM by using ArcSWAT software program. Firstly, when the preprocessing of the DEM was completed; minimum, maximum, and suggested sub-watershed areas were calculated in hectares as 2.771, 554.232 and 11.085, respectively. Secondly, streams and outlets were defined by SWAT. One outlet was added manually. The outlet was close to Sarısu-Eylikler stream gauging station in the watershed. This choice enables us to compare the results of models and observation data. At the end of watershed delineation, we acquired seven sub-basins (Figure 14) and SWAT calculated minimum, maximum, mean and standard deviation of elevation values, which were 1123 m, 2337 m, 1420 m and 195 m, respectively.

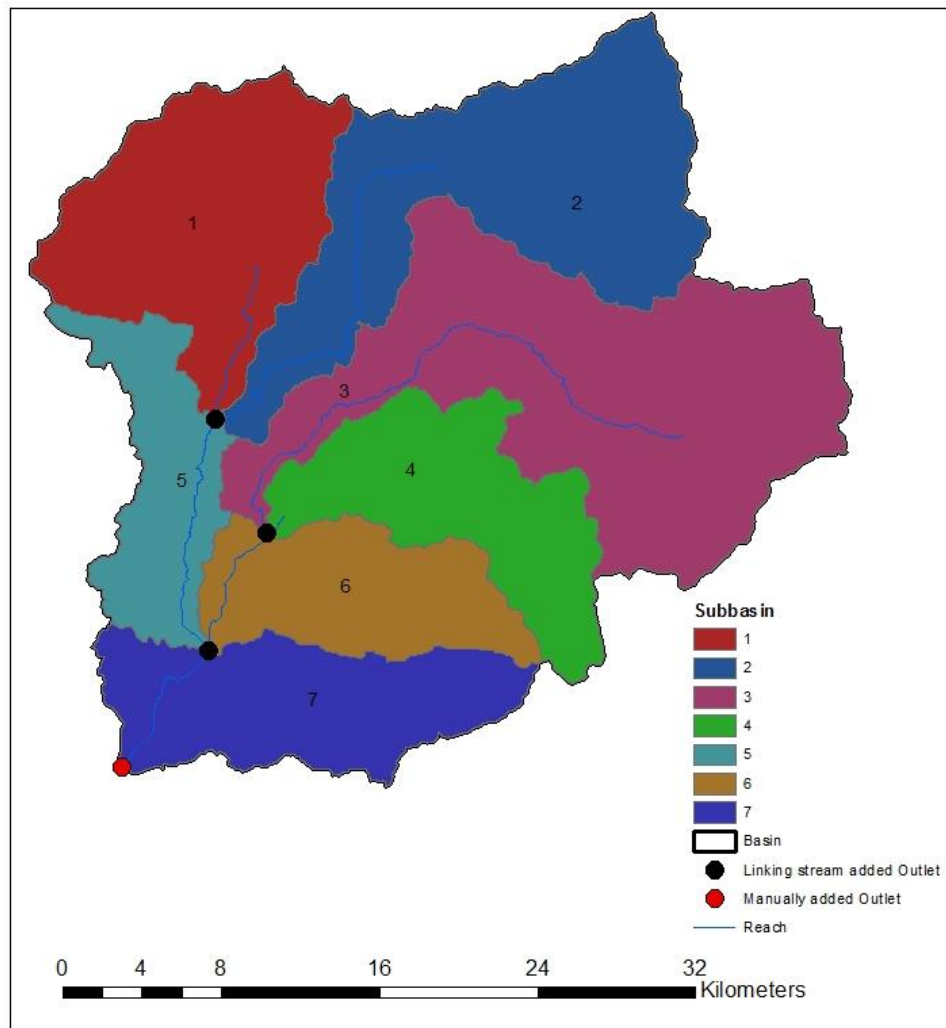


Figure 14 Sub-basins of Sarısu-Eylikler Stream

4.1.1.2 Soil Class Layer

Soil textures in land use map (Scale: 1/25,000) was obtained from the Ministry of Food, Agriculture and Livestock, whose data is classified according to major soils groups (Table 10).

Table 10 Major Soils Group in the area

Soil Classification	Explanation
A	Alluvial
B	Brown Soils
C	Chestnut Soils
D	Reddish-Chestnut soils
F	Reddish-Brown soils
K	Kolluvial
M	Brown Forest Soils
N	Limeless Brown Forest Soils
U	Limeless Brown Soils

The soil map used in SWAT is given in Figure 15. Soil class distribution in the area is observed from Figure 16. There are mostly D and N group of soil, reddish-Chestnut soils and limeless Brown Forest Soils, in the area. Properties of the soils were entered in SWAT soil user database according to Guidelines for Soil Description, 2005; Rosewell, 1993; Ardas, S., and Creutberg, D., 1997 (Table 11).

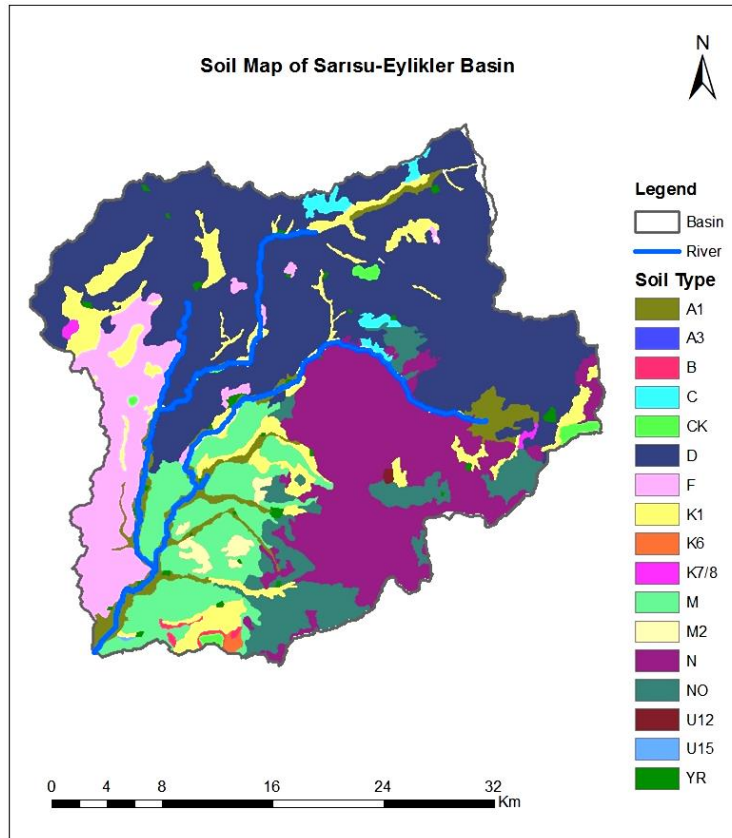


Figure 15 Soil map of the Sarısu-Eylikler stream basin.

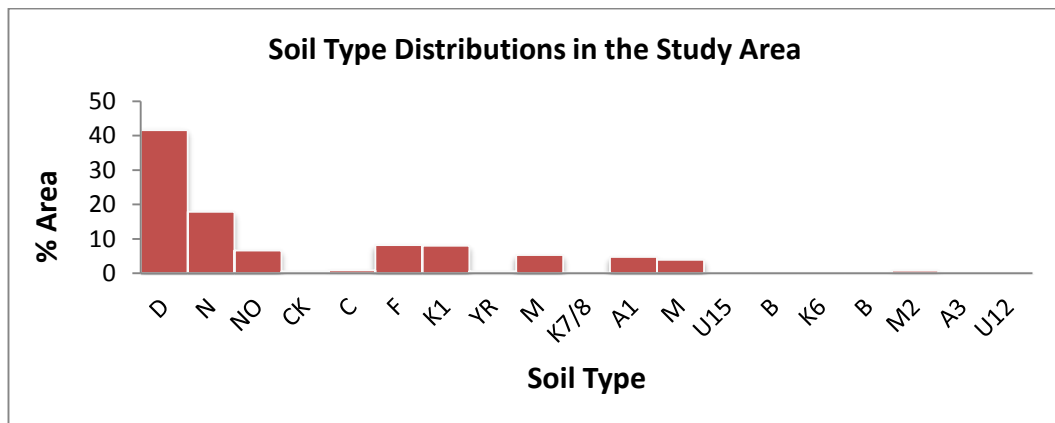


Figure 16 Soil type histogram representation of the study area.

Table 11 User soil database in SWAT for the study area

NAM	LAYERS	HYDGR	SOL_ZMX	ANIO_EXCL	SOL_CRK	TEXTURE	SOL_Z	SOL_BD	SOL_AWC	SOL_K	SOL_CBN	CLAY	SILT	SAND
D	5	D	1200	0.5	0.5	CLAY LOAM-CLAY	50	1.45	0.17	10.15	0.67	40	26	34
N	2	B	200	0.5	0.5	LOAM	50	1.5	0.18	33	0.55	14	38	48
NO	2	D	550	0.5	0.5	CLAY LOAM	200	1.45	0.17	10.15	0.21	31	27	42
CK	1	D	1524	0.5	0.5	UWB	1524	2.5	0.01	180	0	5	25	70
C	3	D	700	0.5	0.5	CLAY	50	1.35	0.1	3.3	1.76	58	19	23
F	4	D	750	0.5	0.5	CLAY LOAM-CLAY	50	1.45	0.17	10.15	0.67	40	26	34
K1	3	D	1200	0.5	0.5	CLAY	350	1.35	0.1	3.3	2.97	40	40	20
YR	1	D	152.4	0.5	0.5	VAR	152.4	1.5	0.1	500	0	15	30	55
M	1	D	150	0.5	0.5	CLAY LOAM	150	1.45	0.17	10.15	1.05	28	32	40
K7/8	2	A	1200	0.5	0.5	SANDY LOAM	750	1.55	0.13	101.6	0.29	20	20	60
A1	1	D	900	0.5	0.5	SILTY CLAY LOAM	900	1.5	0.19	10.15	0.48	40	40	20
M	1	D	150	0.5	0.5	CLAY LOAM	150	1.45	0.17	10.15	1.05	28	32	40
U15	1	D	200	0.5	0.5	CLAY LOAM	200	1.45	0.17	10.15	0.55	31	27	42
B	1	D	550	0.5	0.5	CLAY	50	1.35	0.1	3.3	0.77	44	28	28
K6	1	D	350	0.5	0.5	CLAY LOAM	350	1.45	0.17	10.15	0.86	30	30	40
B	1	D	550	0.5	0.5	CLAY	50	1.35	0.1	3.3	0.77	44	28	28
M2	1	B	750	0.5	0.5	SILTY LOAM	750	1.5	0.21	33	0.43	17	52	31
A3	1	A	900	0.5	0.5	SANDY LOAM	900	1.55	0.13	101.6	0.48	20	20	60
U12	1	B	150	0.5	0.5	LOAM	150	1.5	0.18	33	0.55	14	38	48

4.1.1.3 Land use/Land cover Layer

Soil characteristics and vegetation cover affect water movement. The soil and land use maps are essential for creating the HRUs. Land use layer was created in the framework of a Ministry of Forestry and Water Affairs project, namely, Beysehir Lake Basin Protection Plan and Special Provisions. Land use/land cover data was clipped and reprojected by using the ArcSWAT project database. (Figure 17).

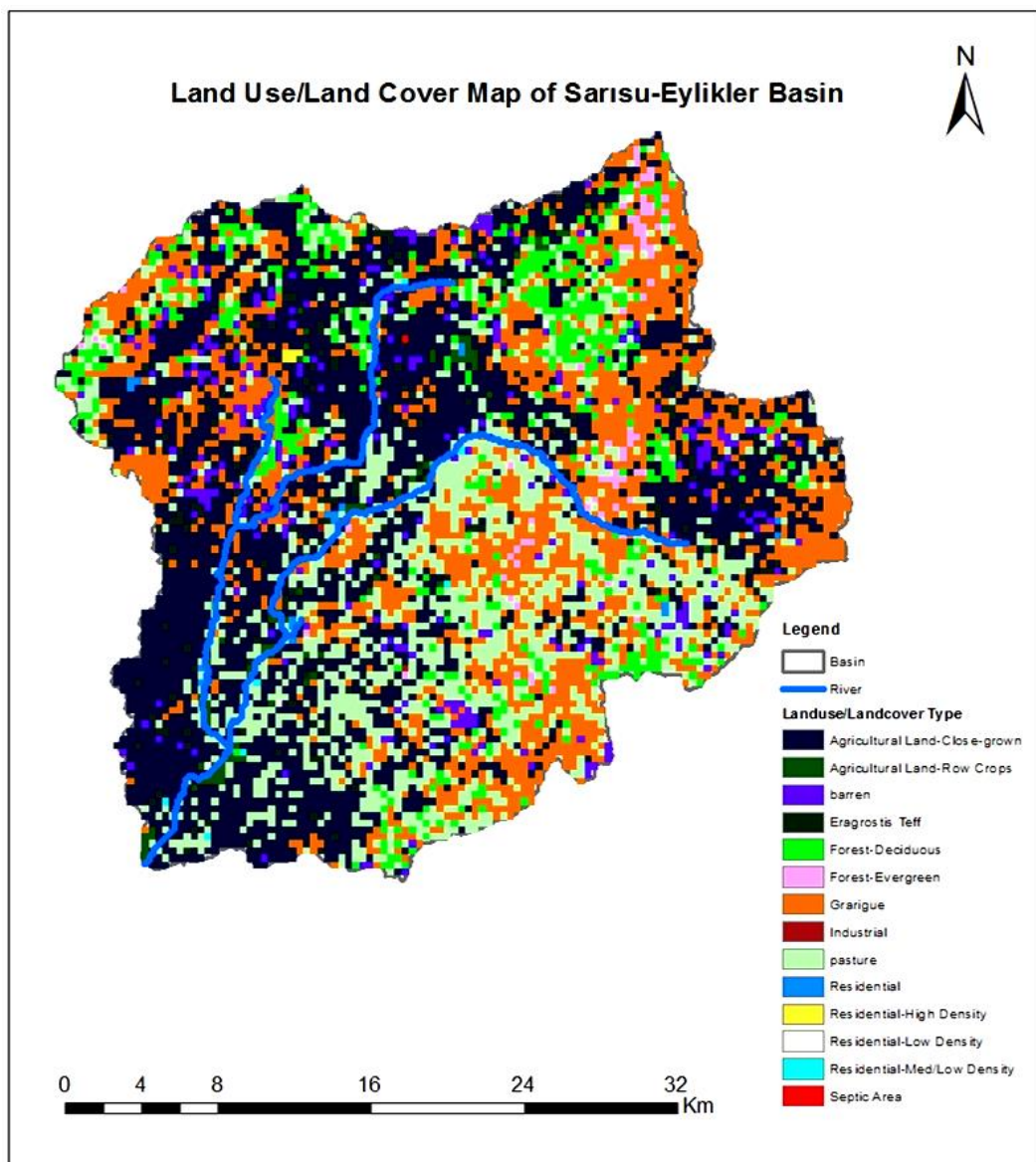


Figure 17 Land use map of the Sarisu-Eylikler Stream

Land use/land cover map resolution is 10x10 m. There are 14 land use/land cover classes in the study area (Table 12). The most dominant type of land use is Agricultural Land-Close Grown, which covers %36.55 of the watershed area (Figure 18). Other dominant land use/land cover areas are garrigue and pasture.

Table 12 Land use/ land cover distribution in the study area

Land use type	Symbol	% Area
Eragrostis Teff	TEFF	2.79
Barren	BARR	4.13
Septic Area	SEPT	0.013
Forest-Deciduous	FRSD	7.03
Forest-Evergreen	FRSE	1.02
Residential-High Density	URHD	0.09
Residential-Med/Low Density	URML	0.092
Agricultural Land-Close-grown	AGRC	36.55
Industrial	UIDU	0.026
Residential	URBN	0.23
Residential-Low Density	URLD	0.039
Agricultural Land-Row Crops	AGRR	1.42
Garrigue	GRAR	25.14
Pasture	PAST	21.42

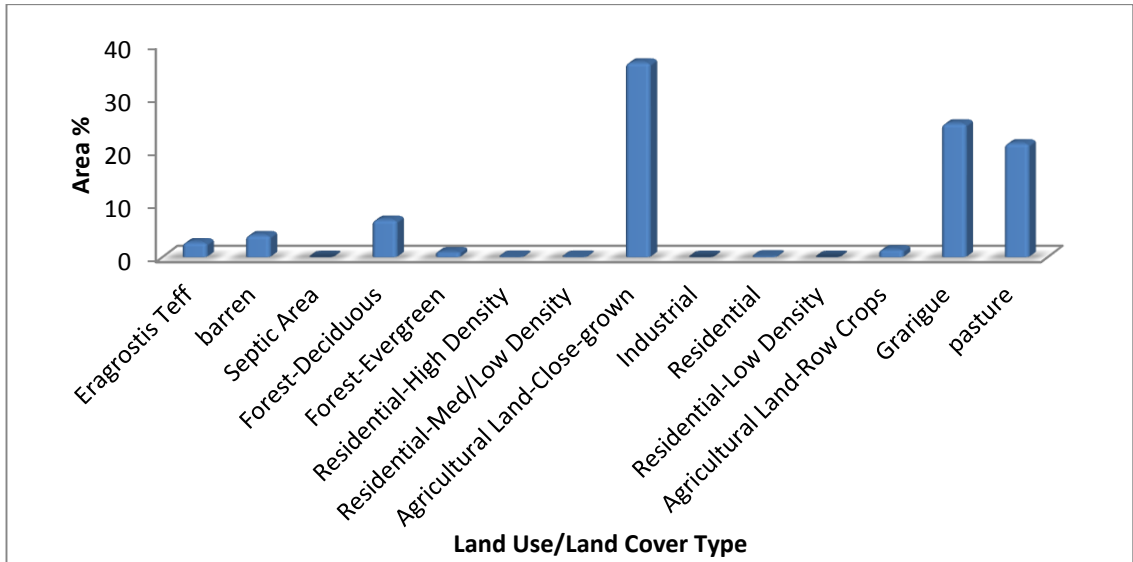


Figure 18 Land use/land cover type histogram representation of the study area.

4.1.1.4 Slope Layer

Slope characterization depends on the DEM specified in the watersheds delineation (Figure 19). Number of slope classes was two and the units for the classes were in percent (%). Slope classes in the area were given in Table 13.

Table 13 Slope class distribution in the Sarisu-Eylikler basin

Slope	Area [ha]	%Watershed Area
0-2	5765.96	5.55
>2	98150.43	94.45

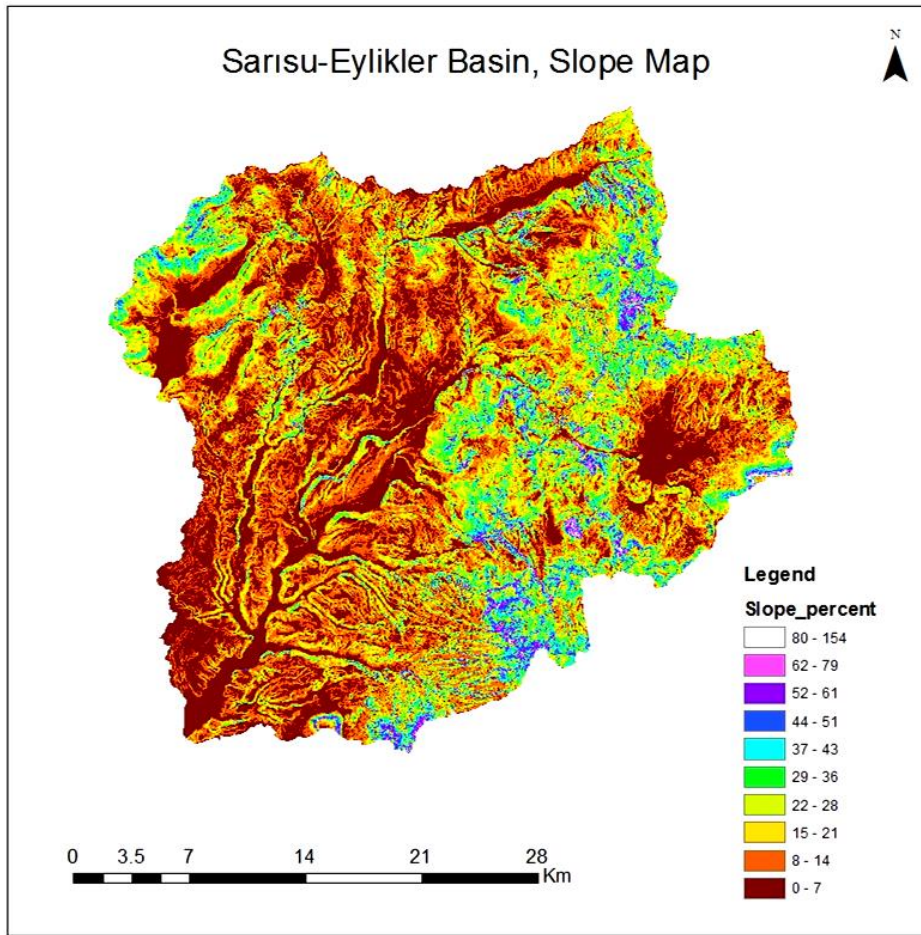


Figure 19 Land slope in the Sarısu-Eylikler basin.

4.2 The SWAT Model Results of Sarisu-Eylikler Basin by Using The Current Method for HRU Creation

Using the current HRU creation method, the model's results were compared depending on total HRU number in seven sub-basins. While using dominant land use/land soil and slope combination approach, we obtained seven HRUs in total. The initial model run had $r^2=0.32$, NS = 0.43 and improved to $r^2 = 0.53$, NS = 0.52 after the calibration. When we increased the total number of HRUs to 14 by using 25%/25%/50% threshold values for land use/soil/slope combination, the initial model run had $r^2=0.34$, NS=-10 and improved to $r^2=0.35$, NS = 0.32 after the calibration. When 20%/20%/60% threshold values for land use/soil/slope combination were used, the total number of HRUs was 21. The initial model run had $r^2=0.34$, NS = -2.69 and improved to $r^2=0.36$, NS = 0.32 after the calibration.

4.3 HRU Division based on CN2 parameter

If the rate of flow of water to the ground surface exceeds the rate of infiltration, surface runoff occurs since the soil is fully saturated with water. If a dry soil begins to be filled with water, the infiltration capability is usually very high. If the soil becomes wetter, infiltration rate will decrease. Surface runoff starts when all surface depression have filled and application rate is higher than the infiltration rate. In order to estimate surface runoff, two methods, which are SCS curve number procedure (SCS, 1972) and the Green & Ampt infiltration method (1911), are provided in SWAT. The amount of runoff is estimated as a function of land use and soil types according to the SCS runoff equation, which is an empirical model (Figure 20).

The SCS curve number equation is (SCS, 1972):

$$Q_{surf} = \frac{(R_{day} - I_a)^2}{(R_{day} - I_a + S)}$$

In this equation, the accumulated runoff or rainfall excess (mm H₂O) is represented by Q_{surf} , the rainfall depth for the day (mm H₂O) is shown as R_{day} , the initial abstractions, which is surface storage, is shown by I_a that contains interception and infiltration prior to runoff (mm H₂O), and the retention parameter (mm H₂O) is indicated by S . The retention parameter diversify spatially because of change in soils, land use, management and slope and temporally due to transfer in soil water content. The retention parameter is defined as:

$$S = 25.4 \left(\frac{1000}{CN} - 10 \right)$$

The curve number for the day is indicated by CN. The initial abstraction, I_a is commonly approximated as $0.2S$

$$Q_{surf} = \frac{(R_{day} - 0.2S)^2}{(R_{day} + 0.8S)}$$

Runoff will only happen when $R_{day} > I_a$.

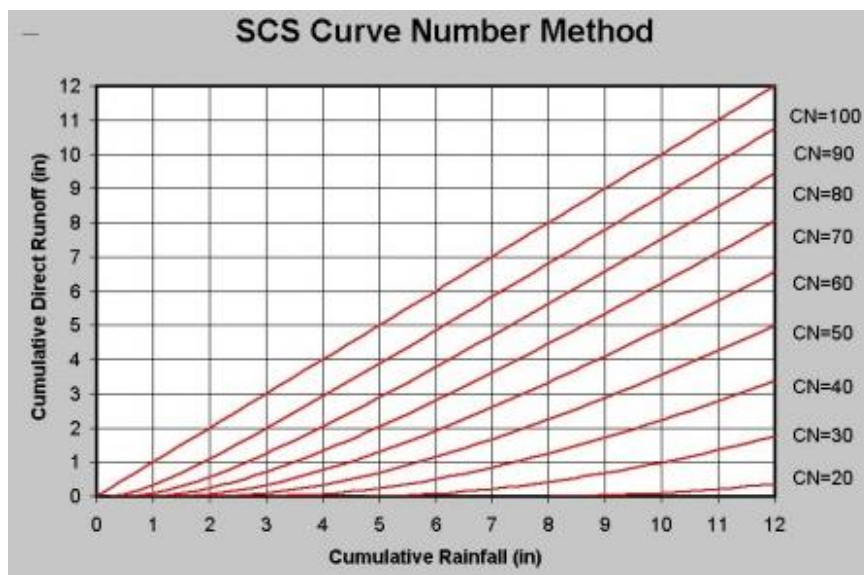


Figure 20 Relation between runoff and rainfall in SCS curve number method (SCS 1986).

Since the SCS curve number is related to the soil's permeability, land use and initial soil water situations, CN2 was chosen for dividing HRU types. A threshold on CN2 found from LU/Soil tables is used to divide a sub-basin into two-HRUs. This guaranties that the two-HRUs are more or less uniform within itself with respect to CN. Then, each HRU is further divided into two-HRUs (Table 14).

Table 14 HRU division according to CN2

Landuse	Symbol	HYRD	CN2	HRU 2	HRU 4	HRU 8	HRU 18
barren	BARR	D	94	>70	80<CN<94	>84	94
Agricultural Land-Row Crops	AGRR	D	89				89
barren	BARR	B	86				86
Agricultural Land-Close-grown	AGRC	D	84			84	
Forest-Deciduous	FRSD	D	83			<84	83
Grarigue	GRAR	D	80				80
Residential	URBN	D	79		73<CN<80	>79	79
Industrial	UIDU	D	79				
Septic Area	SEPT	D	79				
Residential-High Density	URHD	D	79				
Residential-Med/Low Density	URML	D	79			<79	78
Residential-Low Density	URLD	D	79				77
Agricultural Land-Row Crops	AGRR	B	78				73
Forest-Evergreen	FRSE	D	77				
Agricultural Land-Close-grown	AGRC	B	73				
pasture	PAST	B	69	<70	61<CN<70	>66	69
Agricultural Land-Row Crops	AGRR	A	67				67
Forest-Deciduous	FRSD	B	66				66
Eragrostis Teff	TEFF	A	62			<66	61,5
Agricultural Land-Close-grown	AGRC	A	62				
Grarigue	GRAR	B	61				
Grarigue	GRAR	B	61				
Residential-Low Density	URLD	B	59		39<CN<61	>55	59
Residential-High Density	URHD	B	59				
Residential-Med/Low Density	URML	B	59				
Residential-Low Density	URLD	B	59				
Forest-Evergreen	FRSE	B	55			<55	55
pasture	PAST	A	49				49
Grarigue	GRAR	A	39				39

After creating HRU types according to the CN2 parameter, two, four, eight and eighteen HRU types were obtained at different levels (Figure 21). Each level's performance in SWAT were obtained and compared.

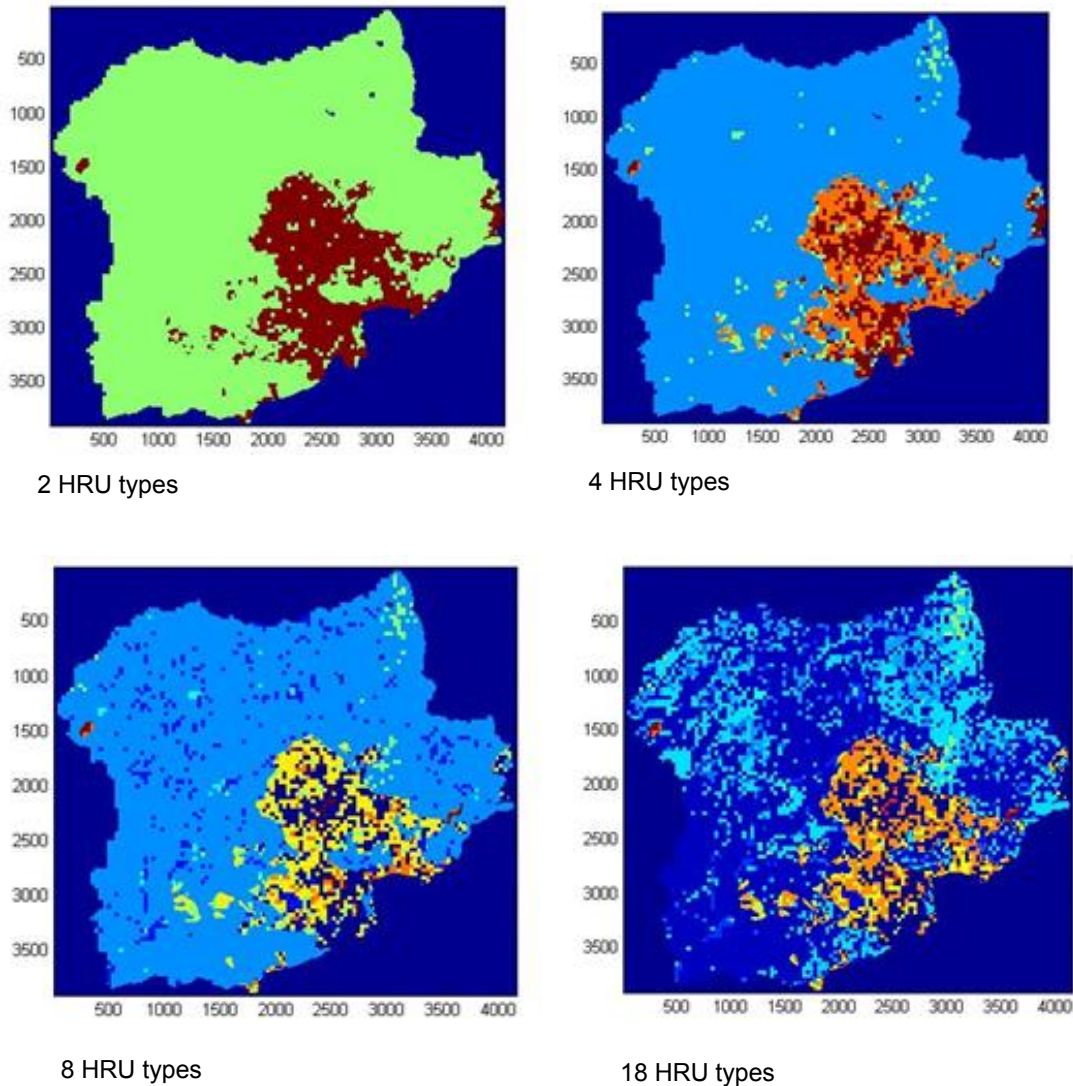


Figure 21 Distribution of HRU types according to CN2 in the basin at each level

Firstly, the model was run with each HRU type set by using MATLAB scripts, then model outputs were compared before calibration. Uncalibrated models is beneficial to assess the variations in model predictions because the variations that may occur during comparison are masked by calibration. Moreover, the uncalibrated model results can represent the performance of each data set that is used for predicting flow. It would point the labor needed for calibration when using each data set. When the results of

the model as a function of the HRU level were compared, it is observed that the model result has improved from two-HRU type to eighteen-HRU type. The r^2 values from two-HRU types to eighteen-HRU types are 0.13, 0.17, 0.18 and 0.20, respectively (Figure 22, Figure 23, Figure 24 and Figure 25).

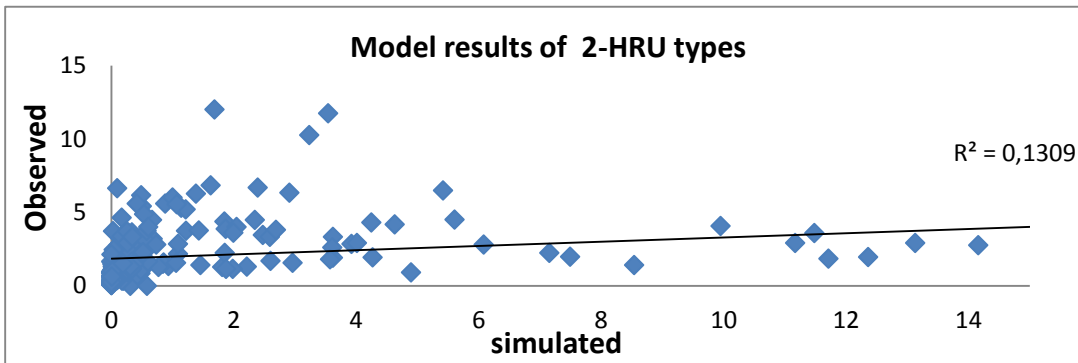
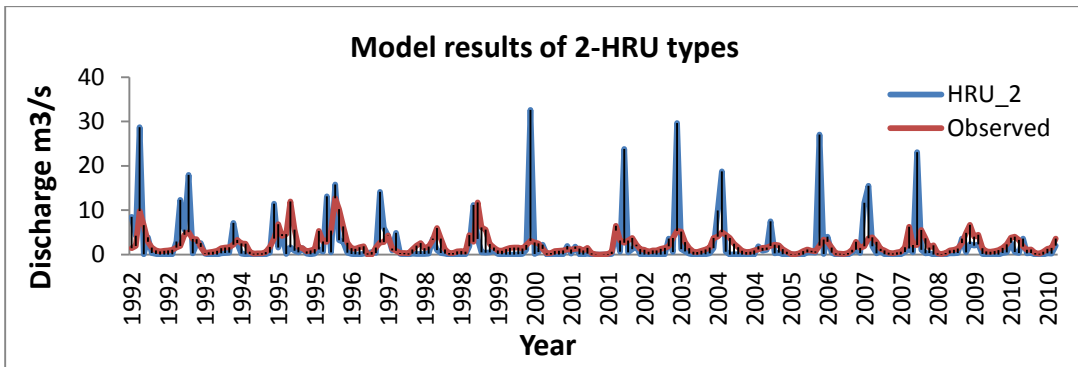


Figure 22 Model results of two-HRU types based on CN2 parameter

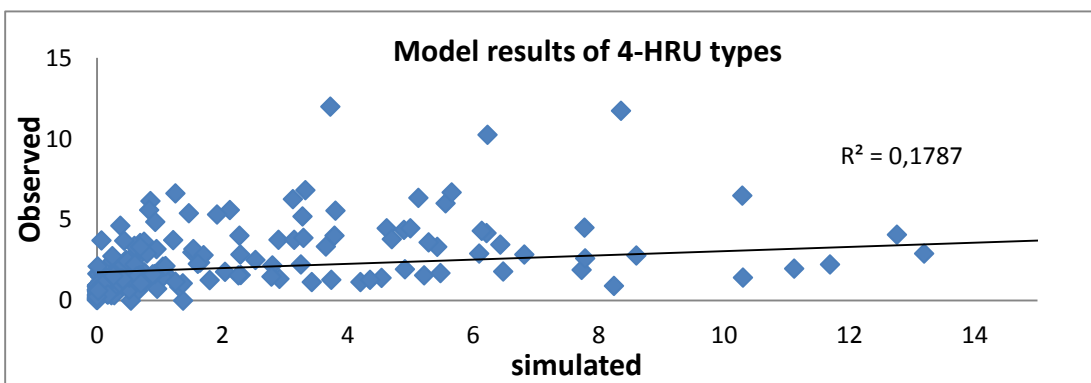
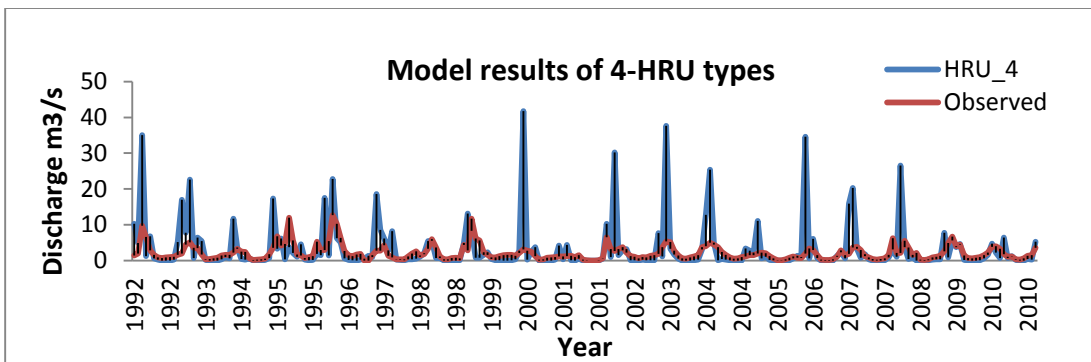


Figure 23 Model results of four-HRU types based on CN2 parameter

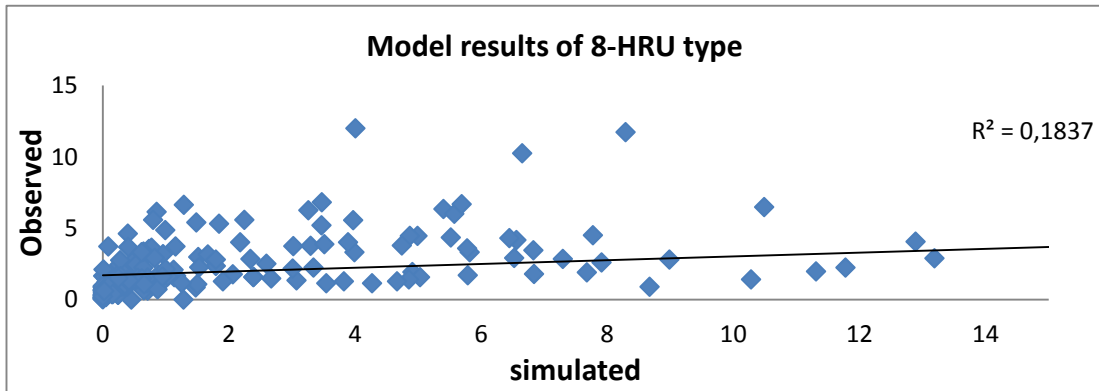
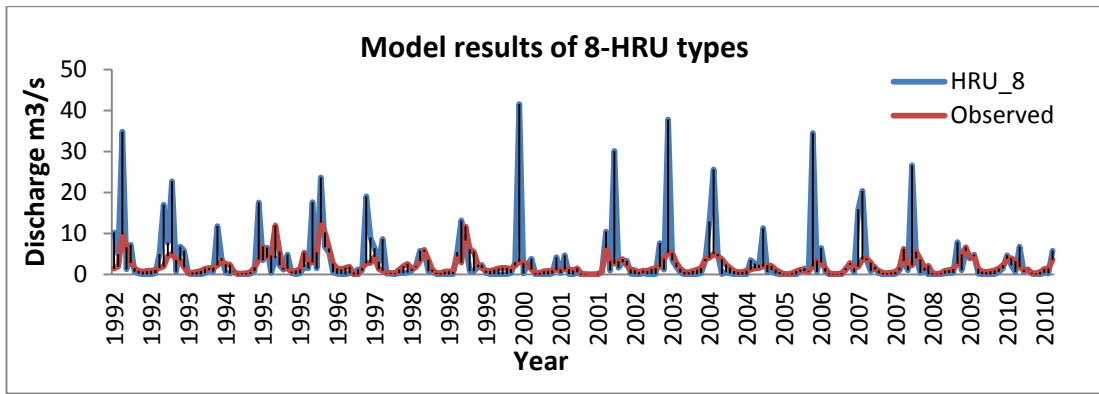


Figure 24 Model results of eight-HRU types based on CN2 parameter

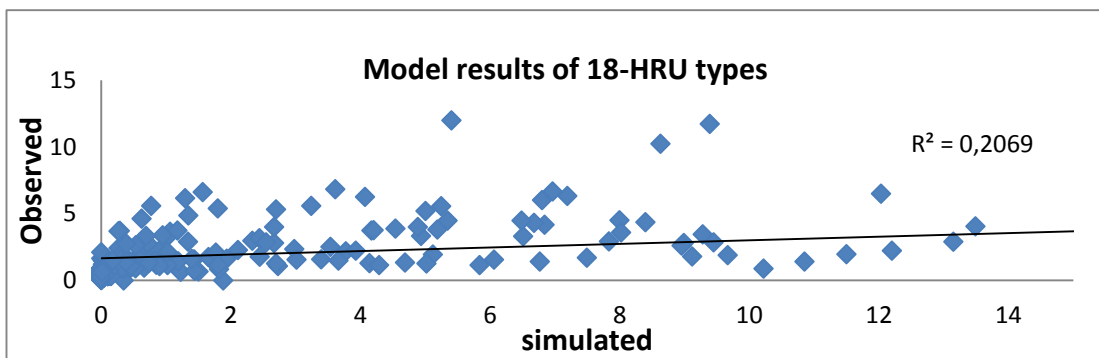
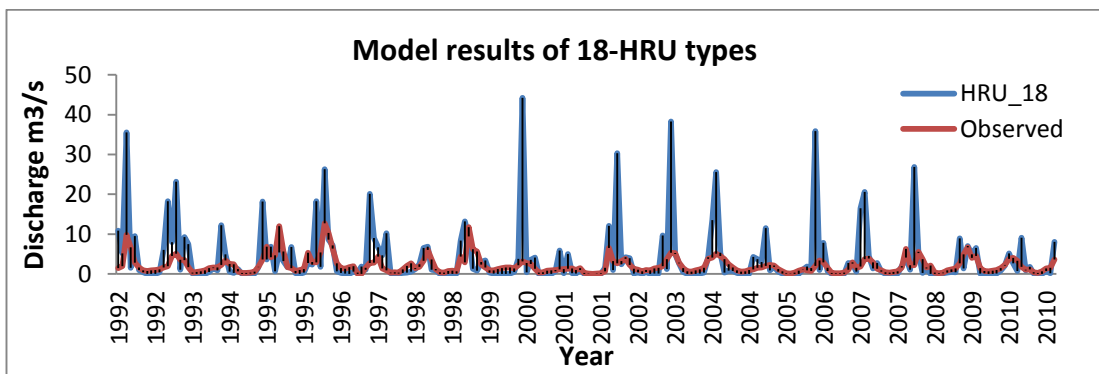


Figure 25 Model results of eighteen-HRU types based on CN2 parameter

When results at different levels of HRU detail are evaluated, four-HRU and eight-HRU types have similar results. If we increase HRU types to eighteen-HRUs, we obtain $r^2=0.20$ with respect to two-HRU case, $r^2=0.13$. It should be noted that all HRU types have the same peak from year 2000 to 2008. In order to see performance of calibration for each HRU, we calibrated them individually. For calibration, sixteen most important parameters which have greatest impact on hydrology (Table 15) were chosen. A Fast and Full Automatic Calibration Tool, which was developed in MATLAB based on SUFI-2 methodology, was used in order to perform one full the calibration from beginning to end without any user interaction. By using 250 simulation count, the models at each HRU level were calibrated. The goodness of fit of calibration was evaluated by NSE. The model efficiency as a fraction of the measured stream flow variance reproduced by the model is determined. NSE function was preferred since it represents not only the relationship simulated and observed discharge but also the amount of water. If NSE value is close to unity, the estimation of the stream flow by the model is best. When $NSE \geq 0.75$, it is a perfect approximation, and an NSE value between 0.75 and 0.36 is considered to be adequate (Motovilov et al., 1999). When the RMSE value is close to zero, the estimation is best. While increasing HRU detail level, we reached better results, from two-HRU to eighteen-HRU types calibration performance ranged from $r^2=0.43$ to $r^2=0.58$ (Figure 26, Figure 27, Figure 28, Figure 29). NS values were between 0.35 and 0.50. When comparing calibration performance of HRU levels, we reached best calibration values according to p-factor, NS and r^2 at eighteen-HRUs (Table 16).

Table 15 Calibration parameters and their ranges

PARAMETERS	MIN VALUE	MAX VALUE
CN2	-0.2	0.2
SOL_AWC	-0.2	0.1
SOL_K	-0.8	0.8
SOL_BD	-0.5	0.6
GWQMN	0	25
GW_REVAP	-0.1	0
REVAPMN	0	500
ALPHA_BF	0	1
GW_DELAY	30	450
ESCO	0.8	1
SFTMP	-20	20
SMTMP	-20	20
SMFMX	0	20
SMFMN	0	20
TIMP	0	1
SURLAG	0.05	24

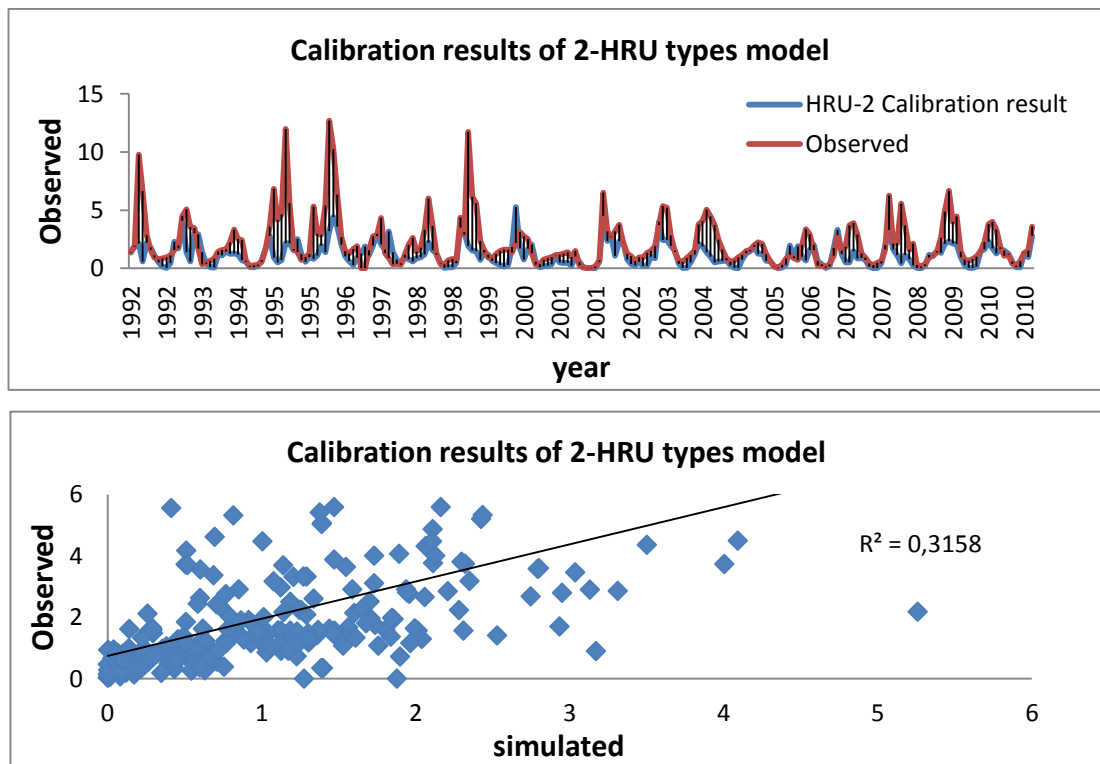


Figure 26 Calibration results of two-HRU types

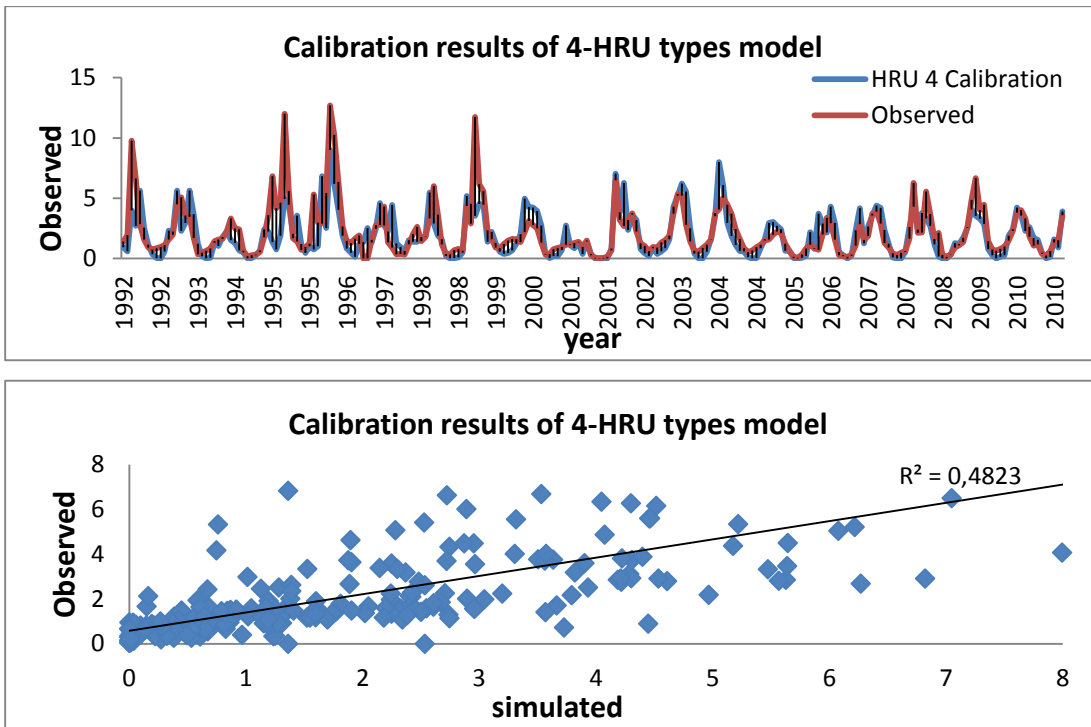


Figure 27 Calibration results of four-HRU types

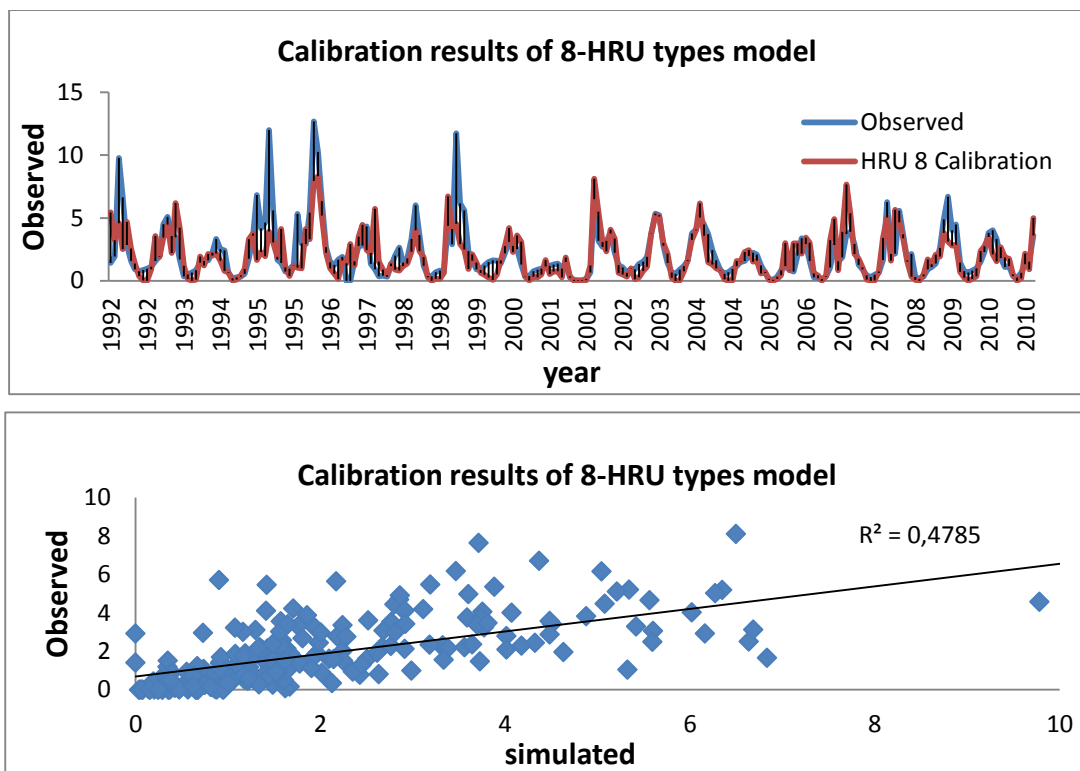


Figure 28 Calibration results of eight-HRU types

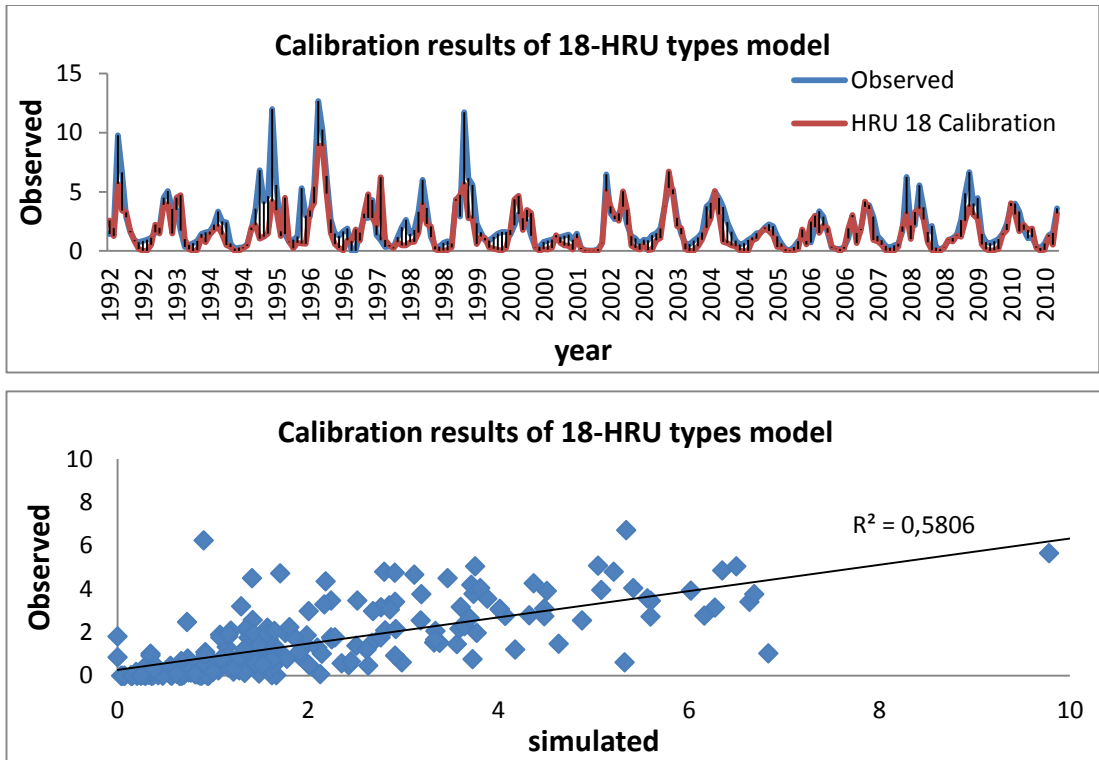


Figure 29 Calibration results of eighteen-HRU types

Table 16 Calibration results of HRU levels that are created based on the CN2 parameter

METHOD	CN2							
Variable	p-factor	r-factor	R2	NS	bR2	PBIAS	Mean(sim)	StdDev(sim)
2 HRUs TYPE	0,52	1,15	0,43	0,35	0,24	19,50	2.16 (1.74)	2.10 (1.81)
4 HRUs TYPE	0,75	1,50	0,48	0,45	0,29	10,50	2.16 (1.94)	2.10 (1.79)
8 HRUs TYPE	0,71	1,71	0,48	0,44	0,28	10,00	2.16 (1.95)	2.10 (1.78)
18 HRUs TYPE	0,93	2,85	0,58	0,50	0,35	27,30	2.16 (1.57)	2.10 (1.67)

4.4 HRU Creation based on SOL_K

The physical characteristics of the soil have an important impact on hydrological cycle. Especially, soil hydrologic group (A, B, C, D), available water capacity of the soil layer, moist bulk density and saturated hydraulic conductivity have great effect on the cycling of water within the HRU since the movement of water and air through the profile within an HRU are managed by these properties. These physical parameters are explained below.

According to the U.S Natural Resource Conservation Service (NRSC), soils are divided into four hydrologic groups with respect to infiltration capacity. Soil properties effect runoff potential, which is the rate of infiltration for a bare soil after prolonged wetting without freezing. Soils that have the same runoff capacity under similar meteorological and cover conditions are defined in same hydrologic group. Runoff potential depends on water table depth, saturated hydraulic conductivity, and layer depth. Available water capacity of the soil (mm H₂O/mm soil) is computed by taking out the fraction of water store at persistent wilting point from that store at field capacity. Saturated hydraulic conductivity (mm/hr), K_{sat} represents the ratio of soil water flow rate to the hydraulic gradient, and is a measure of how easily the water flows inside the soil. The ratio of the mass of solid particles to the total volume of the soil shows the soil bulk density. When the mass of the soil is the oven dry weight and total volume of the soil is measured when soil is at near field capacity, soil bulk density can be measured. Bulk density values are between 1.1 and 1.9 Mg/ m³.

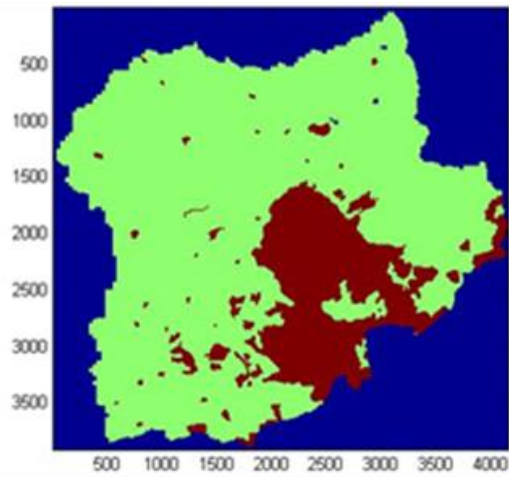
When soils physical properties that have important effect on hydrologic process were evaluated, soils hydraulic conductivity (SOL_K) was chosen for creating HRU types. At the first step of the SOL_K HRU creation method similar to CN2 HRU creation, HRUs were separated in two-HRU types according to soil hydraulic conductivity values of the soils. Each HRU types were further divided into two-HRUs). If soil bulk density, available water capacity and soil hydraulic conductivity values are examined, similar soil hydraulic conductivity values have similar bulk density and hydraulic conductivity values. Moreover, soils types that have the same soil properties are in the

same hydrologic group. At the first step of HRU division, SOL_K=10.15 was chosen for the threshold value based on soil types in the study area in order to separate soil types with respect to its infiltration capacity.

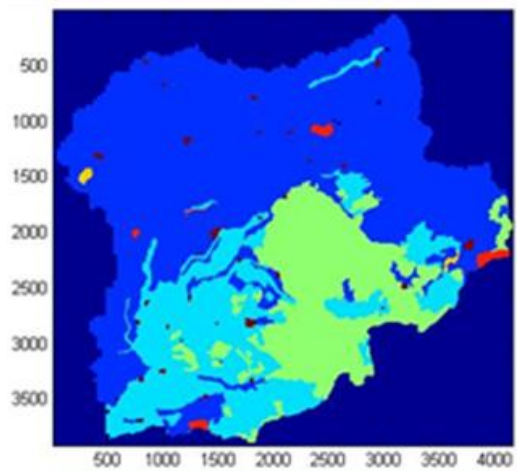
Table 17 HRU division based on SOL_K parameter

SNAM	HYDGRP	TEXTURE	SOL BD	SOL_AWC	SOL_K	2 HRU	4 HRU	18 HRU	
D	D	CLAY	1,35	0,1	3,3	K<=10.15	K=3.3	D	
C	D	CLAY	1,35	0,1	3,3			C	
F	D	CLAY LOAM- CLAY	1,35	0,1	3,3			F	
KBIR	D	CLAY	1,35	0,1	3,3			KBIR	
B	D	CLAY	1,35	0,1	3,3			B	
B	D	CLAY	1,35	0,1	3,3			B	
KALTI	D	CLAY LOAM	1,45	0,17	10,15		K=10.15	KALTI	
M	D	CLAY LOAM	1,45	0,17	10,15			M	
M	D	CLAY LOAM	1,45	0,17	10,15			M	
ABIR	D	SILTY CLAY LOAM	1,5	0,19	10,15			ABIR	
UONBES	D	CLAY LOAM	1,45	0,17	10,15			UONBES	
NO	D	CLAY LOAM	1,45	0,17	10,15			NO	
N	B	LOAM	1,5	0,18	33			K>10.15	N
MIKI	B	SILTY LOAM	1,5	0,21	33				33
UONIKI	B	LOAM	1,5	0,18	33	UONIKI			
KYEDI	A	SANDY LOAM	1,55	0,13	101,6	101,5	KYEDI		
AUC	A	SANDY LOAM	1,55	0,13	101,6		AUC		
CK	D	UWB	2,5	0,01	180	K>180	180		CK
YR	D	VAR	1,5	0,1	500		500	YR	

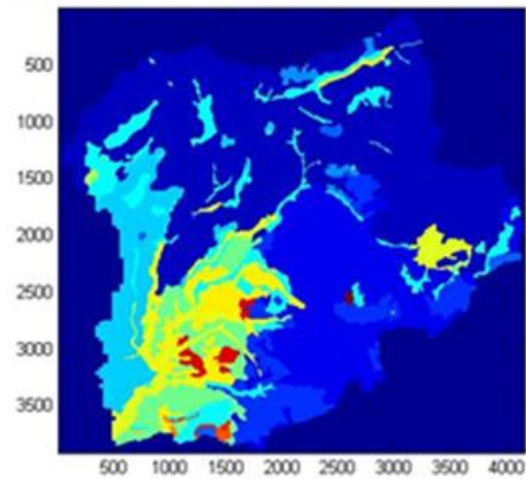
Bare rocks and urban areas are accepted as one HRU since the size of these areas are very small. HRUs were divided based on the soil hydraulic conductivity until eighteen types are reached (Figure 30).



2 HRU types



4 HRU types



18 HRU types

Figure 30 HRU types based on SOL_K parameter division

When each HRU type's model results were evaluated, unfortunately, almost same results were obtained. The results of HRU types which were generated with respect to soil hydraulic conductivity are under our expectations (Table 18). The r^2 values ranged from 0.12 to 0.19 (Figure 31, Figure 32, Figure 33). Each HRU level was calibrated individually in order to understand calibration performance for each HRU level. Calibration results of HRU types from two-HRU types to four-HRUs ranged from $r^2=0.43$ to 0.44 (Figure 34, Figure 35, Figure 36, Figure 37), and HRUs which included all soil types had $r^2=0.36$ (Figure 38). Although two-HRU and four-HRU type models based on soil hydraulic conductivity values have approximately the same calibration results, the calibration performance of HRUs created depending on all soil types decline.

Table 18 Calibration results of HRU types which are divided according to SOL_K parameter

METHOD	SOL_K									Mean (sim)	StdDev (sim)
	p-factor	r-factor	R2	NS	bR2	MSE	PBIAS	RSR			
2 HRU TYPE (SM=250)	0,74	1,41	0,43	0,43	0,19	2,50	-2,20	0,76	2.16 (2.21)	2.10 (1.41)	
4 HRUs TYPE (SM=250)	0,84	2,37	0,44	0,35	0,27	2,80	16,90	0,80	2.16 (1.80)	2.10 (1.91)	
4 HRUs TYPE(use initials) (SM=250)	0,87	2,95	0,34	0,20	0,19	3,50	-1,00	0,90	2.16 (2.19)	2.10 (2.00)	
4 HRUs TYPE(use initials) (SM=500)	0,96	4,22	0,34	0,30	0,16	3,10	-1,10	0,84	2.16 (2.19)	2.10 (1.67)	
ALL soil types	0,85	2,56	0,36	-	0,24	4,60	-	1,02	2.16 (2.85)	2.10 (2.38)	
ALL soil types(use initials) (SM=250)	0,72	3,48	0,37	0,19	0,23	3,50	-4,30	0,90	2.16 (2.26)	2.10 (2.14)	
ALL soil types(use initials) (SM=500)	0,86	3,90	0,34	0,22	0,18	3,40	14,70	0,88	2.16 (1.85)	2.10 (1.88)	
ALL soil types(use initials) (SM=750)	0,82	3,11	0,32	0,26	0,15	3,30	5,90	0,86	2.16 (2.04)	2.10 (1.73)	

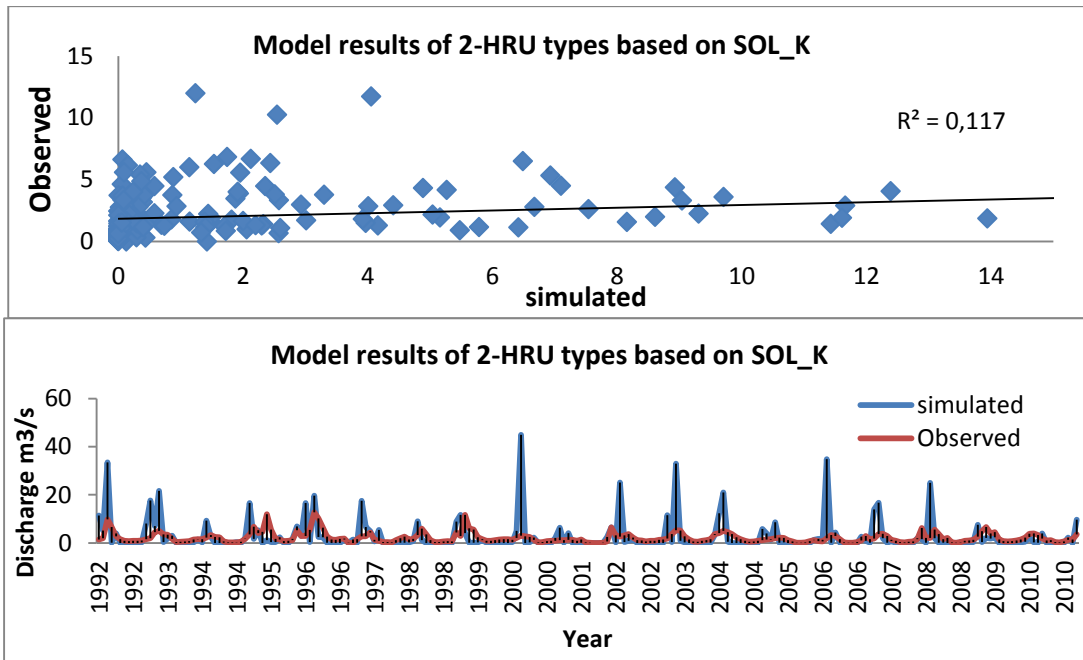


Figure 31 Model results of two-HRU types based on SOL_K parameter

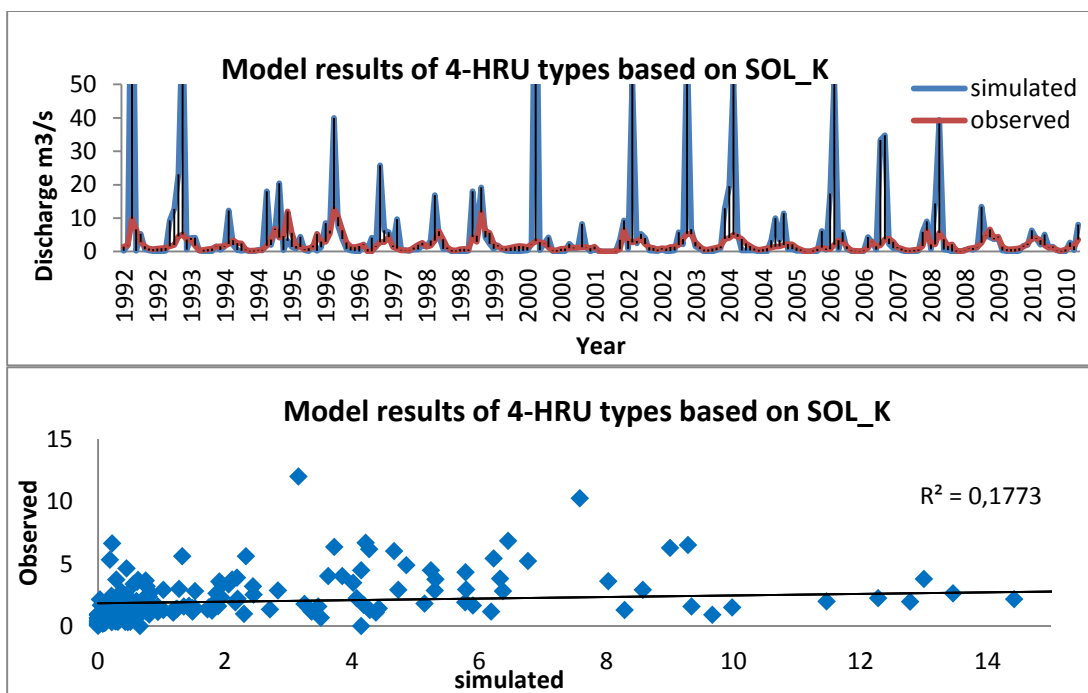


Figure 32 Model results of four-HRU types based on SOL_K parameter

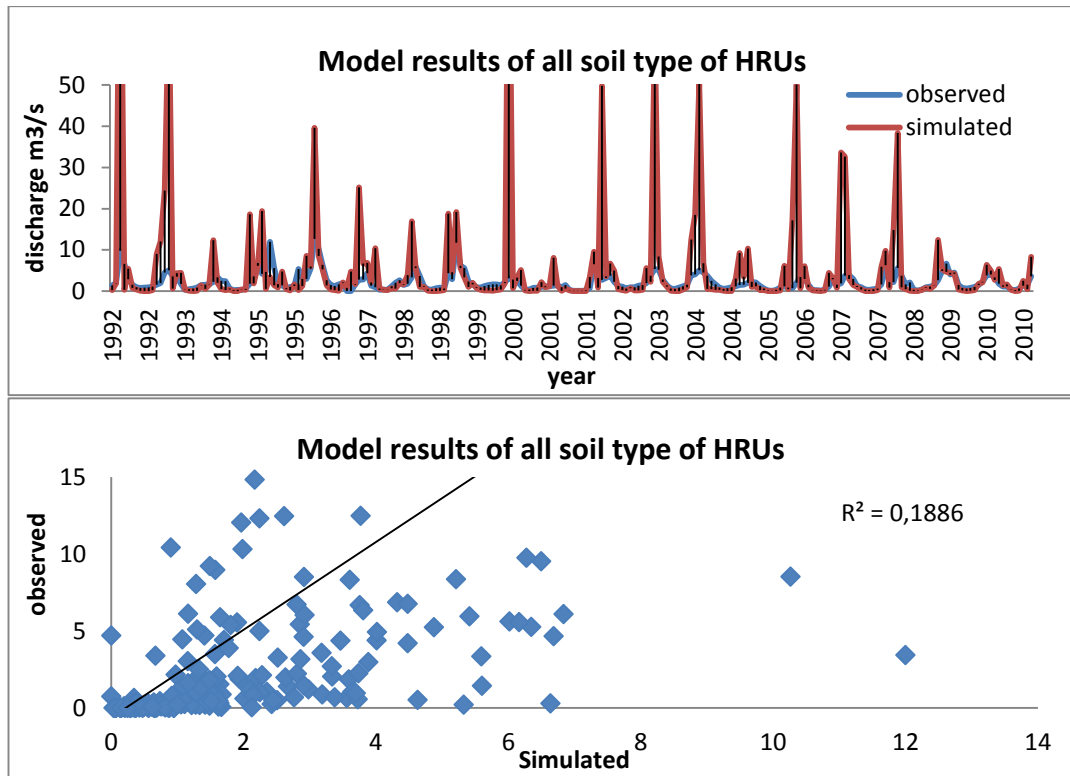


Figure 33 Model results of all HRU types based on SOL_K parameter

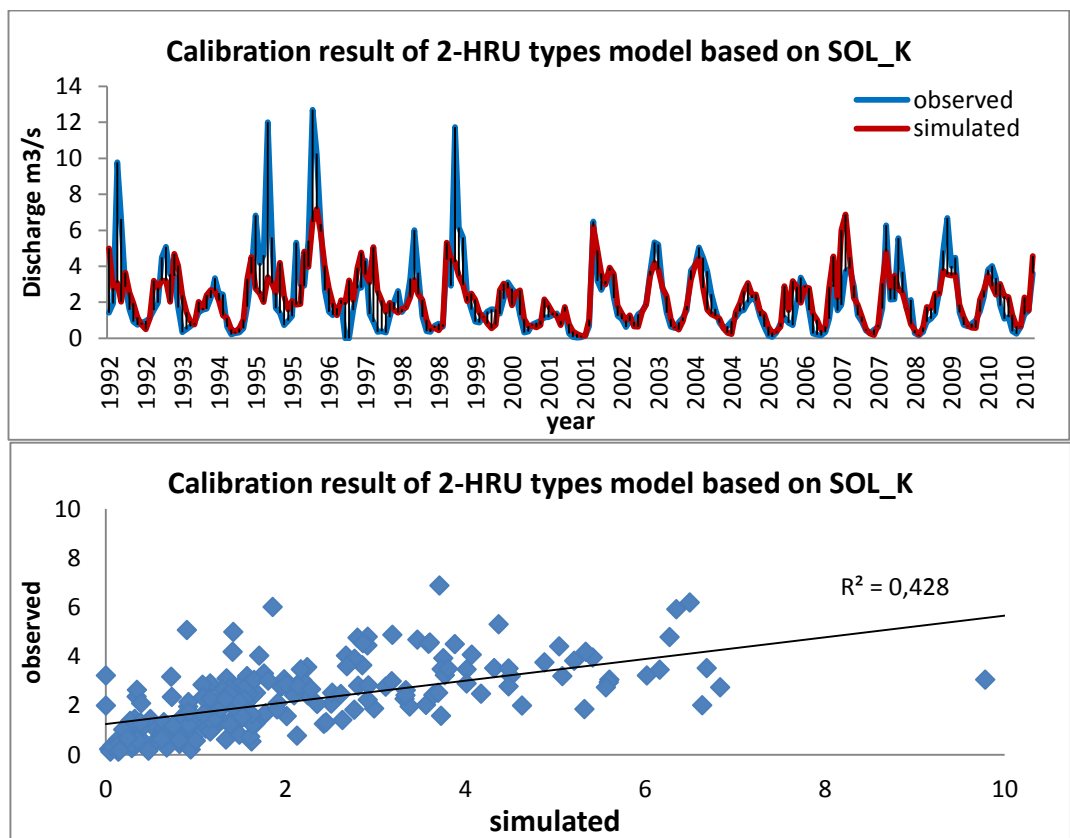


Figure 34 Calibration results of two-HRU types model.

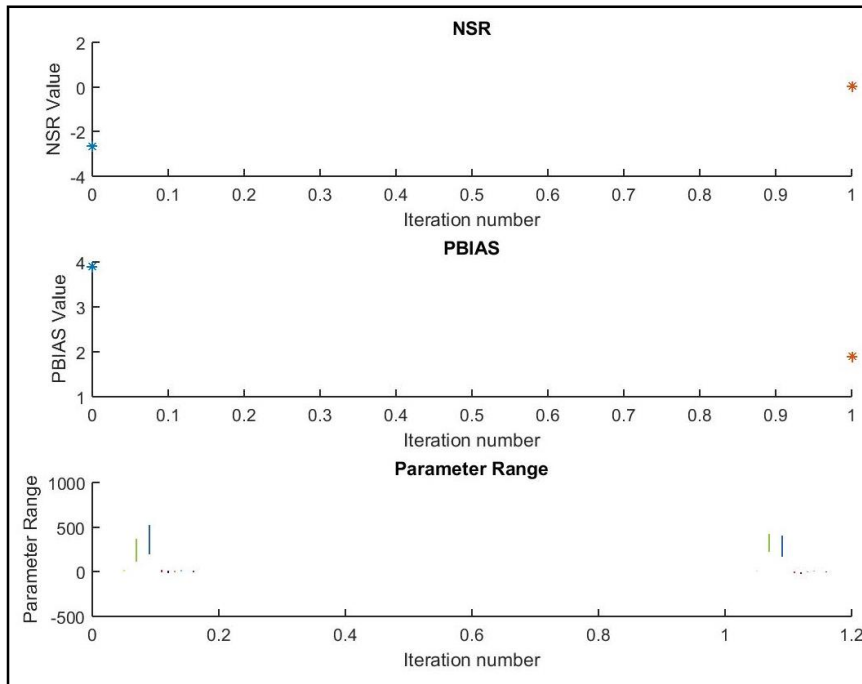


Figure 35 Calibration steps of two-HRU based on SOL_K parameter

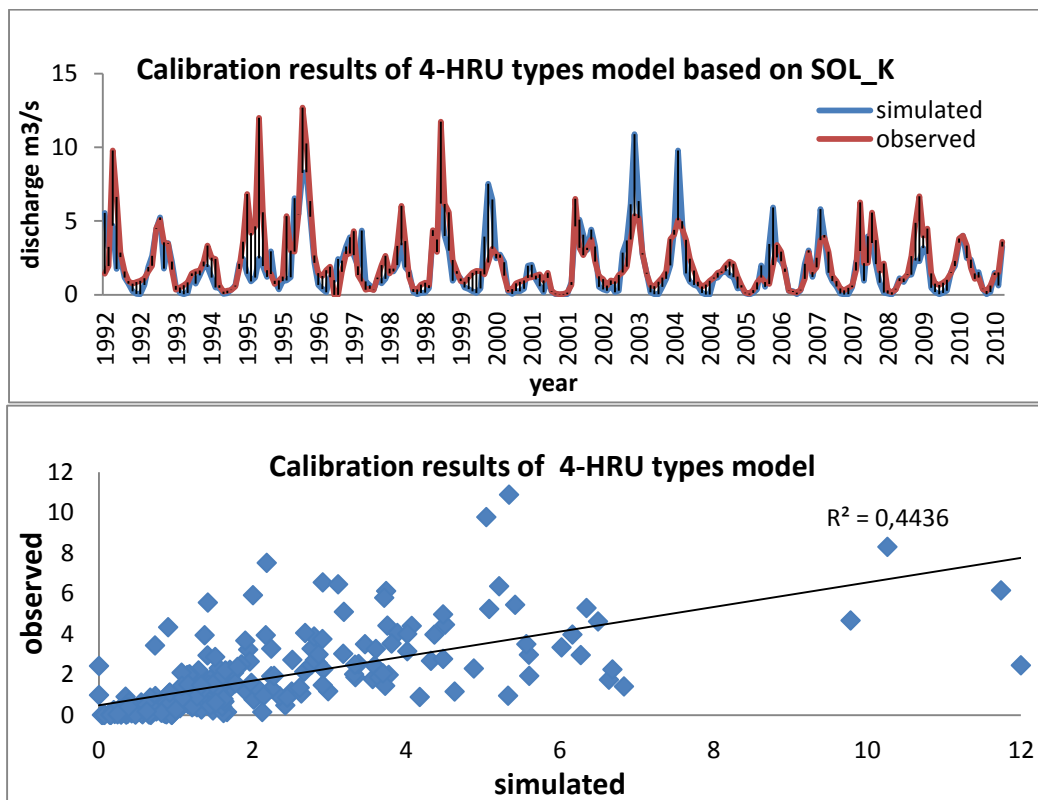


Figure 36 Calibration results of four-HRU types model (based on SOL_K)

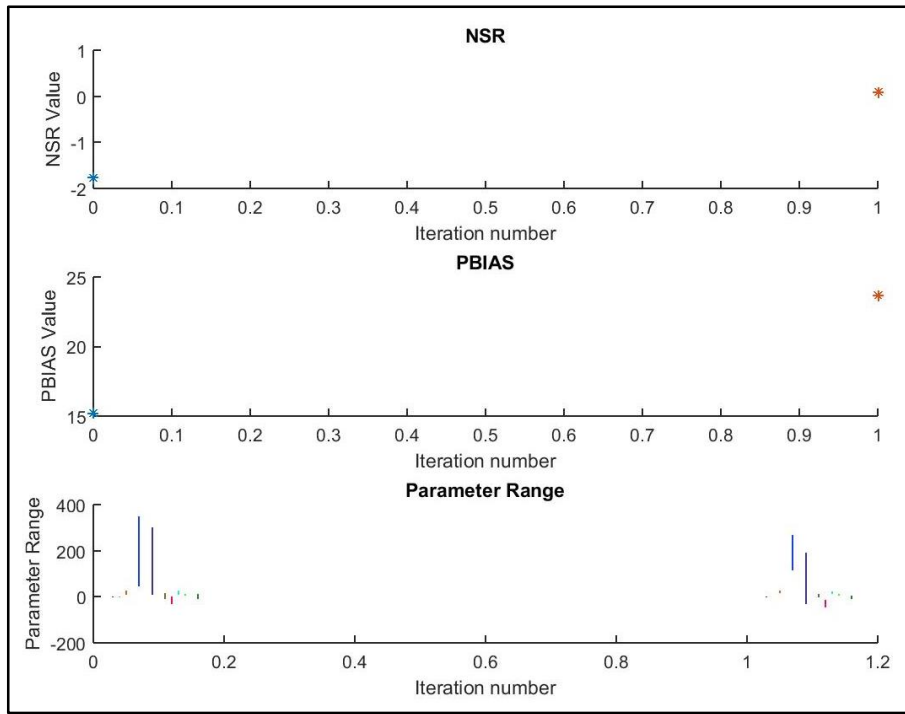


Figure 37 Calibration steps of four-HRU types based on SOL_K parameter

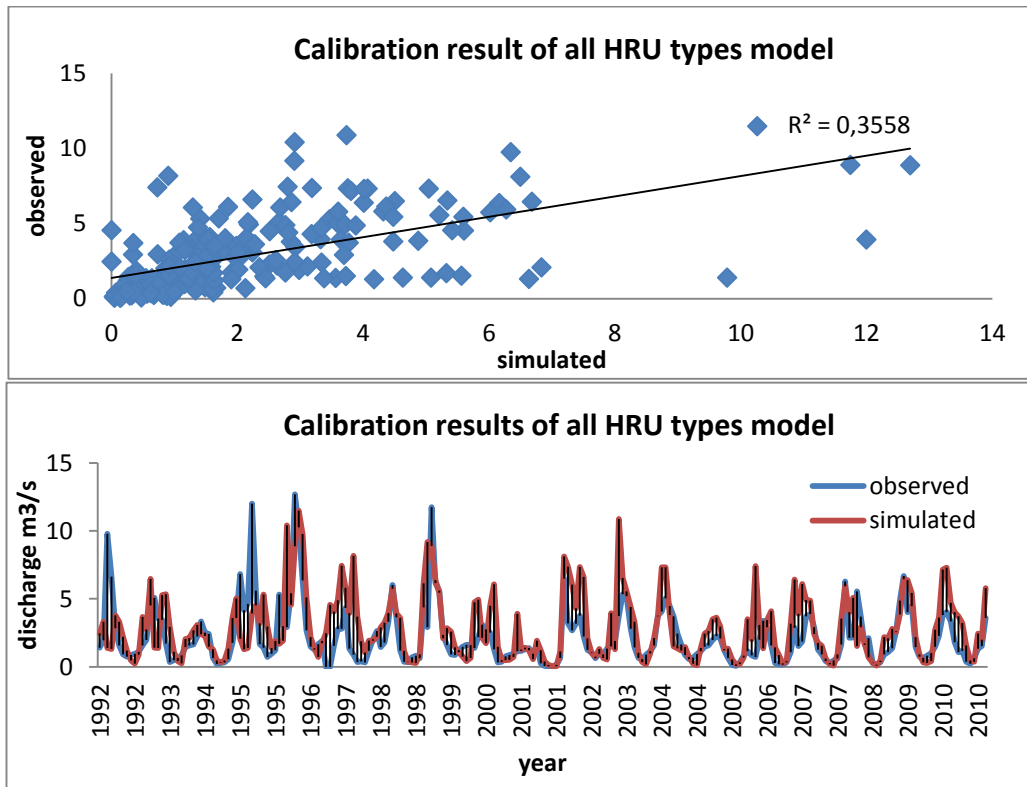


Figure 38 All HRU types model calibration results (based on SOL_K)

In order to increase the performance of the model and decrease the computational time for calibration procedure, the calibrated parameter values of two-HRU types were assigned as initial values to four-HRU types. The four-HRU types did not give us good model accuracy: $r^2=0.23$ (Figure 39). The model was improved to $r^2=0.34$, NS=0.20 after the calibration by using 250 simulation count (Figure 40 and Figure 41). Although the calibration model results of two-HRU types gave us NS=0.43, $r^2=0.43$ values, when HRU types were divided further and the calibrated parameter values of two-HRUs were used as initials to four-HRUs, the model performance declined. However, when the simulation count was increased to 500, similar calibration results with four-HRU without including initials were obtained (NS=0.34, $r^2=0.30$).

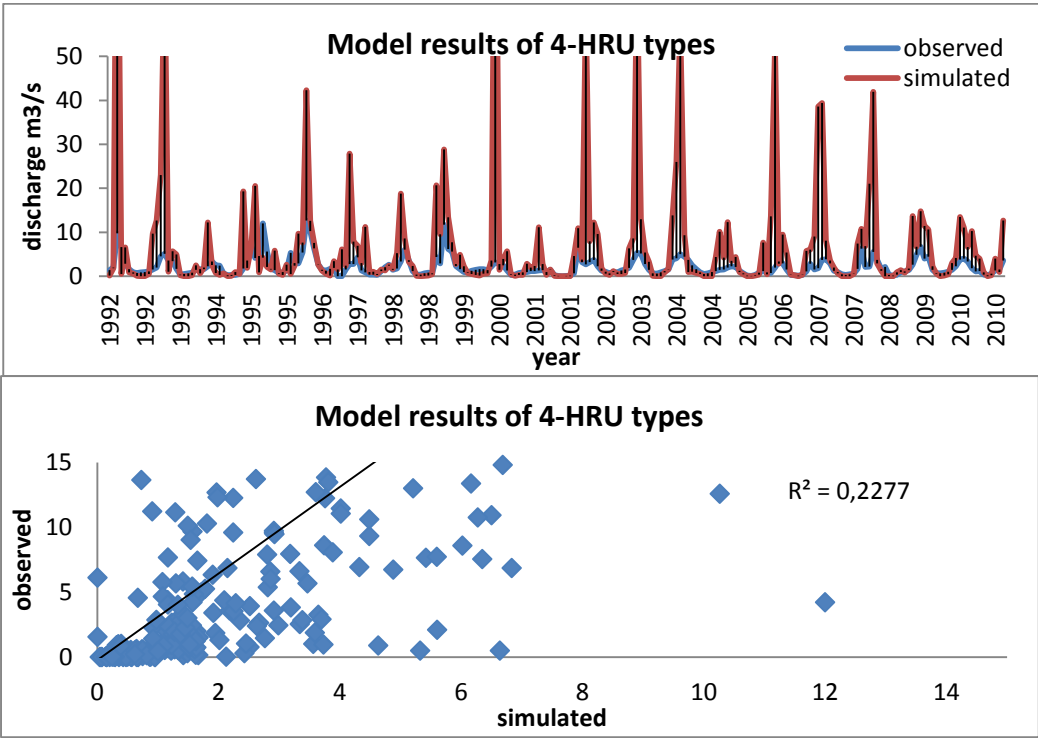


Figure 39 Model results of four-HRU types (calibrated parameters values of two-HRU types used as an initials for four-HRUs)

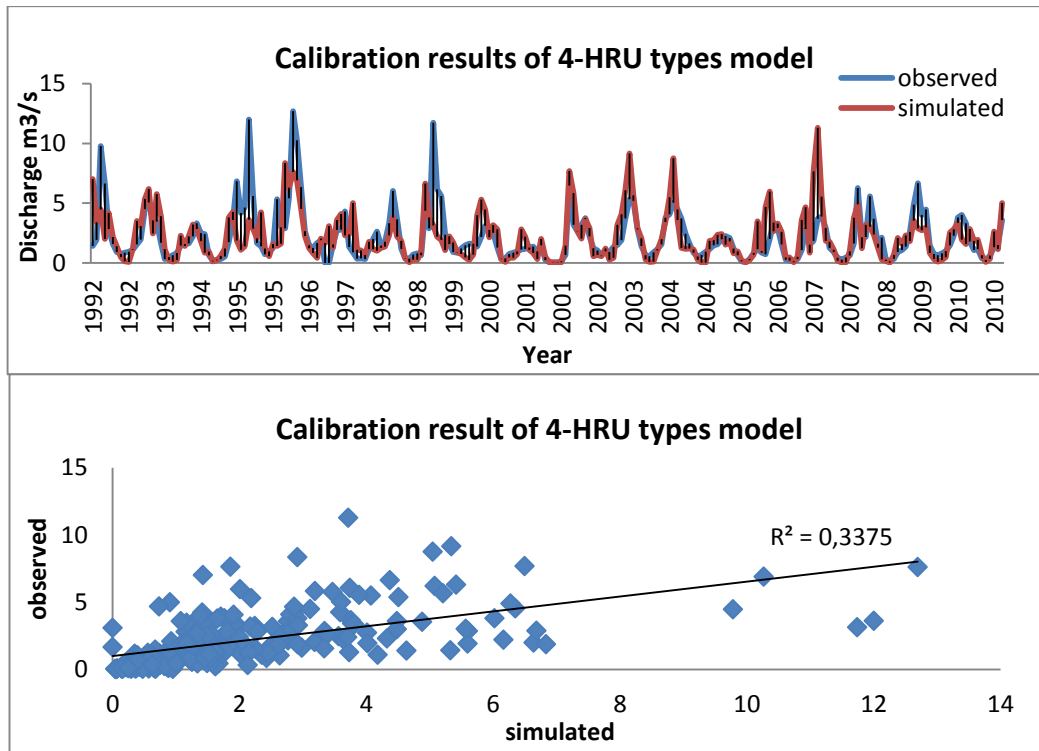


Figure 40 Calibration results of 4-HRU types model (initial value of 4 HRUs obtained from calibrated 2-HRU types model parameters)

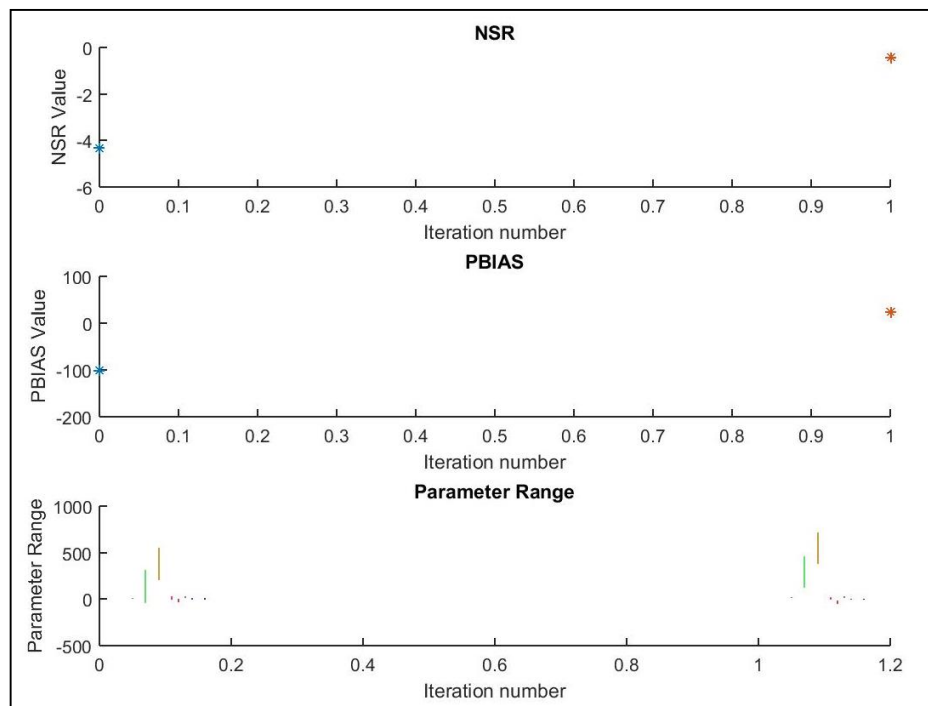


Figure 41 Calibration steps of four-HRU types model (initial value of 4 HRUs obtained from calibrated two-HRU types model parameters)

When calibrated parameters values of two-HRU types model used as an initials for all soils HRU types, the model was improved to $r^2=0.32$, NS=0.26 after the calibration by using 750 simulation count (Figure 42).

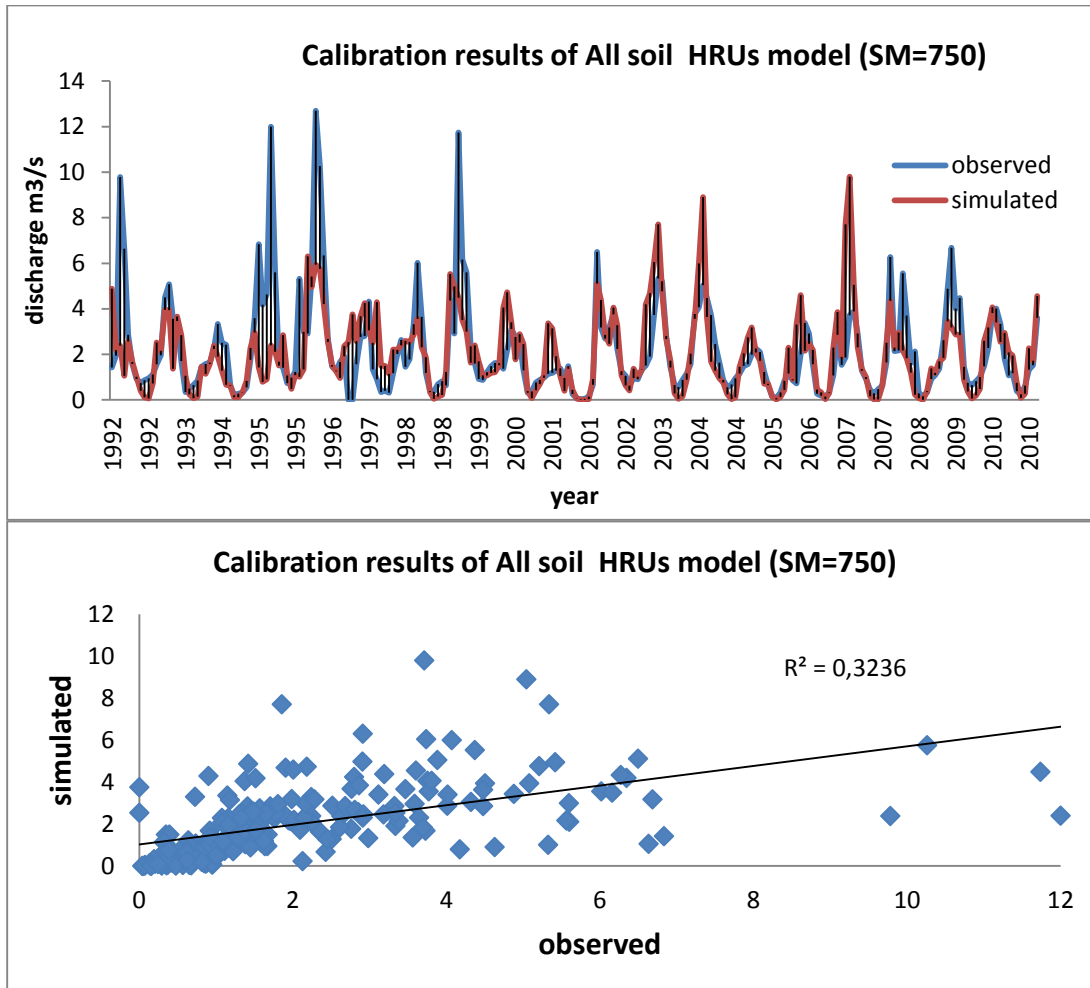


Figure 42 Calibration result of all soil HRU types model based on SOL_K classification (initial value of four HRUs obtained from calibrated two HRU types model parameters)

4.5 HRU Creation based on CN2+SOL_K+Slope Classification Parameters

Using CN2 and soil hydraulic conductivity parameters for HRUs creation independently did not give us enough model accuracy. Since some parameters have great impact in water cycle in HRUs, like curve number, the available water capacity

or the bulk density, combination of curve number and soil hydraulic conductivity and slope classification were used for generating HRU types. According to soil hydrologic group and land use/land cover type, CN2 value are determined (Figure 43). Threshold values for the combination parameters was chosen depending on study area properties. According to the area characteristics, at the first step of HRU division, HRUs were divided into two-HRUs which are the combination of the low infiltration capacity of soils and the high surface runoff characteristic of land use/land cover, and the high infiltration capacity of soils and surface runoff characteristics of land use/land cover.

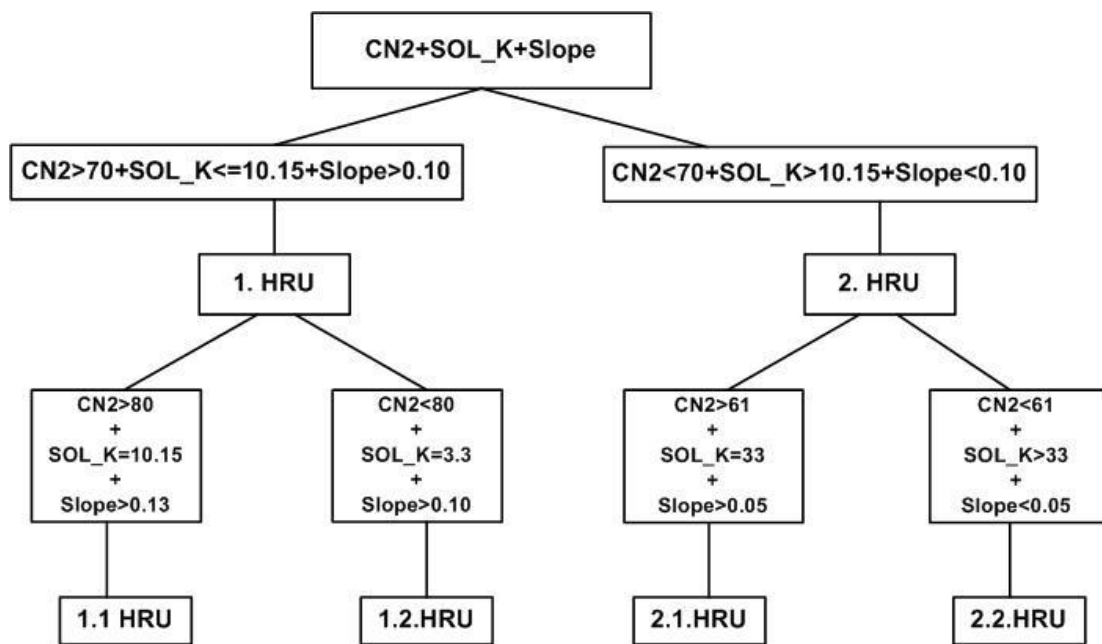


Figure 43 HRU division methodology for Sarisu-Eylikler Stream Basin

4.5.1 Two-HRU Types which were Created Based on Slope, CN2 and SOL_K parameters results

Firstly, according to combination of curve number, soil hydraulic parameters and two slope classifications, HRUs were divided on two types (Figure 44, Figure 45, Figure 46). The model performance was $r^2=0.32$ with total 13 HRUs number when the model was run depending on two-HRU types (Figure 47).

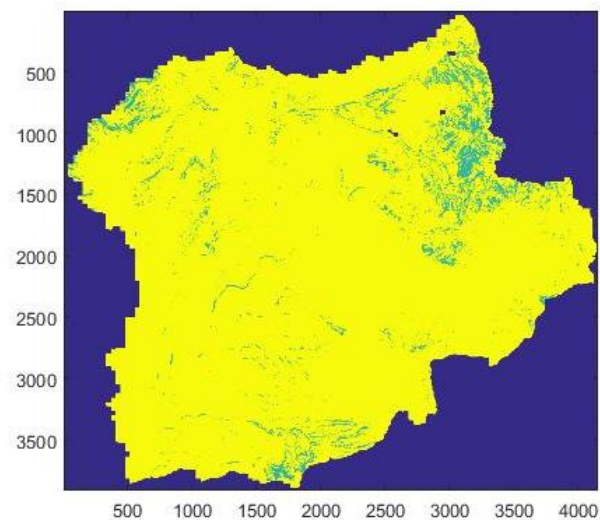


Figure 44 Two-HRU types division based on SOL_K, CN2 and slope parameters

```
if (curv_no>70) && (sol_k<=10.15) && (slope_class>0.10)
    hru_image(ii, jj) = 1;
else
    hru_image(ii, jj) = 2;
end
```

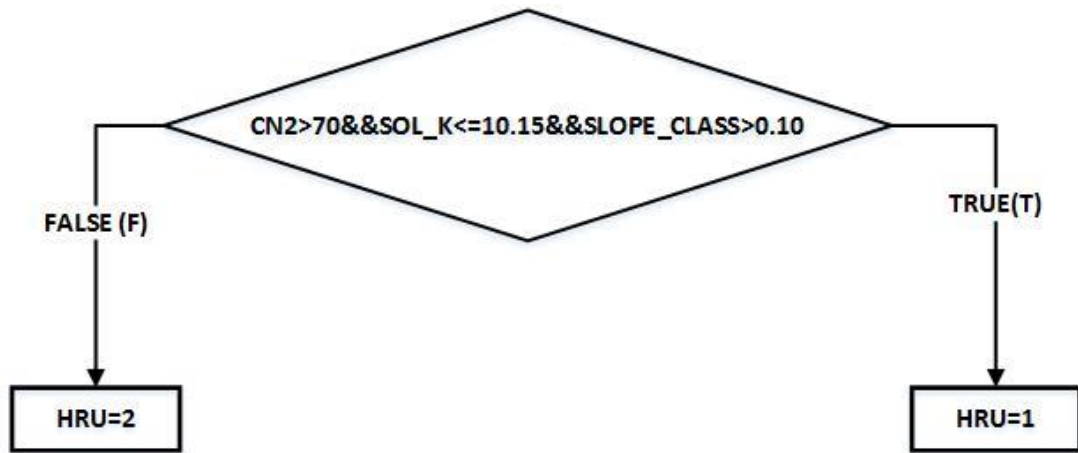


Figure 45 The flowchart of two-HRU types generation.

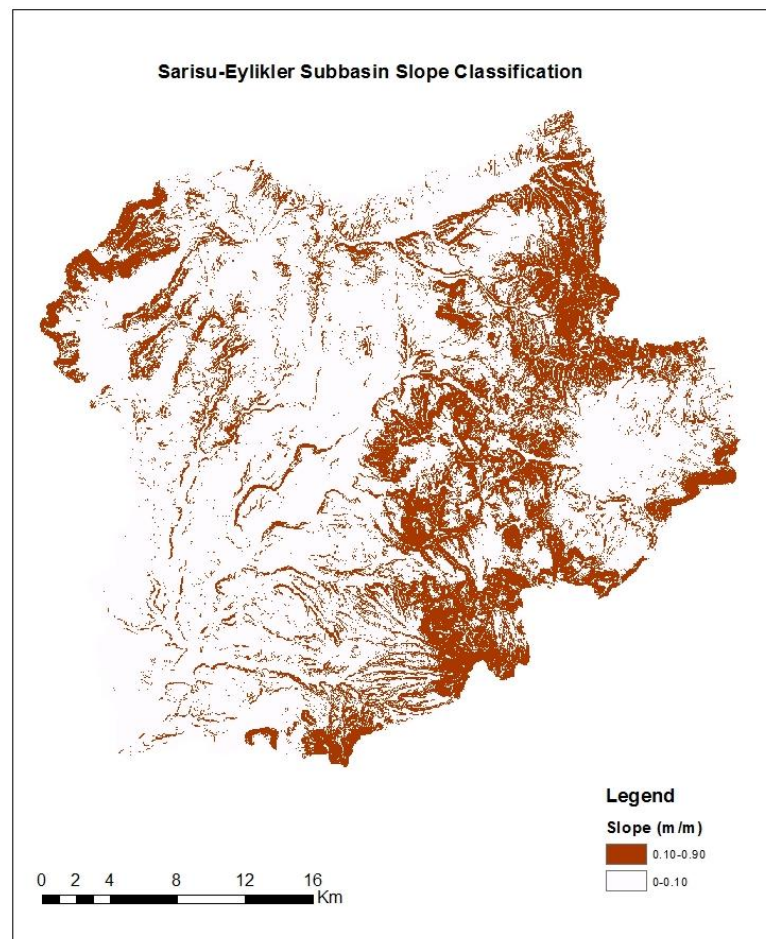


Figure 46 The slope classification of the study area

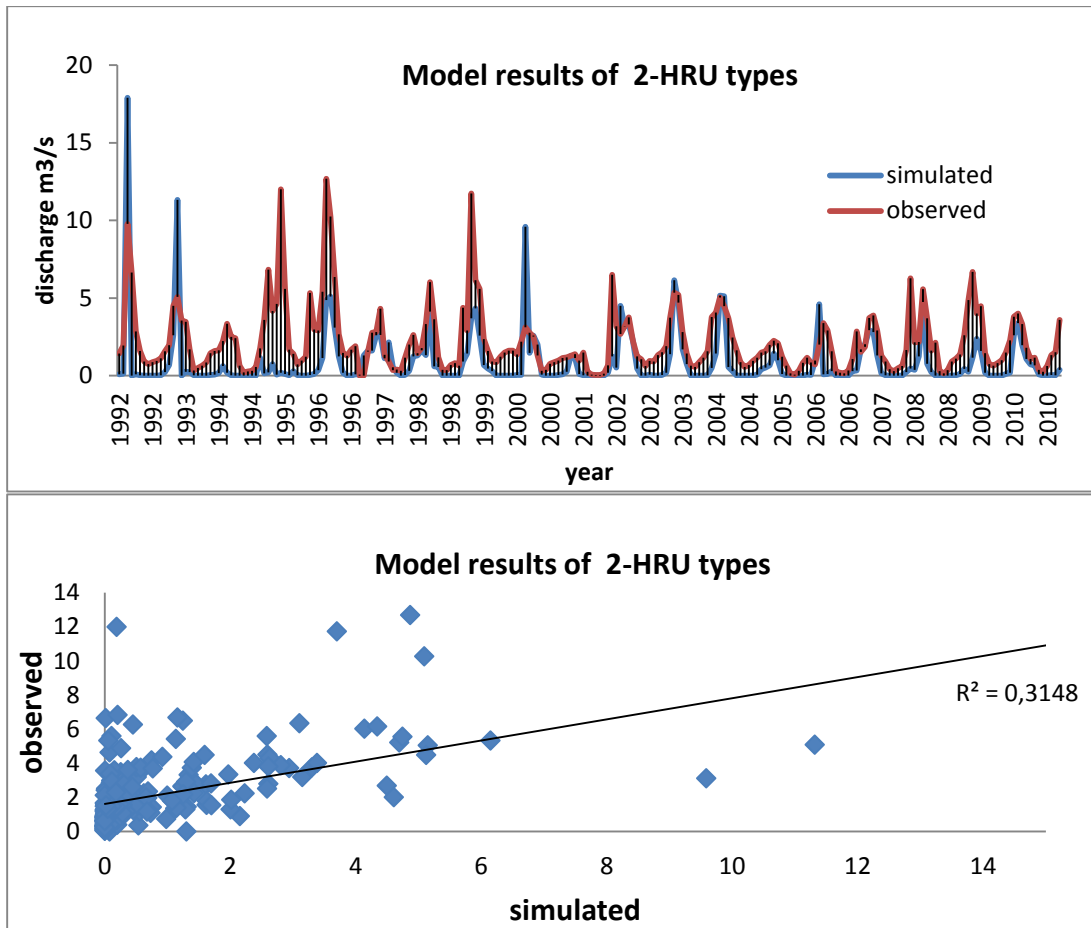


Figure 47 Model results of two-HRU types (based on soil hydraulic conductivity, CN2 and slope classification)

At the first step of the calibration, the two-HRU model was calibrated by using 100 simulation counts. Since the model accuracy of the model was not good ($NS=0.45$, $r^2=0.45$) at the end of that step, while increasing simulation count from 250 to 750, calibrated model results were assessed (Table 19). If the model was calibrated by using 250 simulation count, $r^2 = 0.53$ and $NS = 0.52$ values were obtained (Figure 48).

Table 19 Two-HRU types model calibration results depending on simulation count

METHOD	CN2+SOL_K+SLOPE							
Variable	p-factor	r-factor	R2	NS	bR2	PBIAS	Mean (sim)	StdDev (sim)
2 HRUs TYPE (SM=100)	0,71	1,16	0,45	0,45	0,19	1,40	2.16(2.13)	2.10(1.30)
2 HRUs TYPE (SM=250)	0,65	0,99	0,53	0,52	0,33	-0,30	2.16(2.17)	2.10(1.75)
2 HRUs TYPE (SM=500)	0,68	1,27	0,50	0,49	0,29	3,80	2.16(2.08)	2.10(1.70)
2 HRUs TYPE (SM=750)	0,36	0,61	0,49	0,44	0,30	-15,20	2.16(2.49)	2.10(1.83)

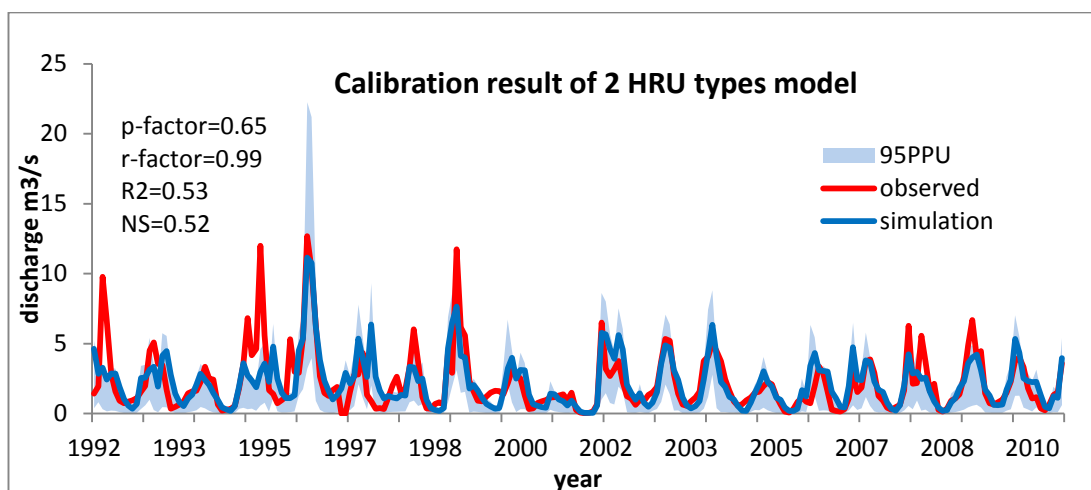


Figure 48 Two-HRU types model calibration results (SM=250), which are generated by CN2+SOL_K+Slope.

4.5.2 Four-HRU Types which were created with respect to Slope, CN2 and SOL_K parameters results

Each child of two-HRU level was further divided into two-HRUs, at the end of the division we obtained four-HRU types with a total of 16 HRUs (Figure 49, Figure 50). The MATLAB script is given below. Four-HRU types model without including calibrated values of two-HRUs was calibrated by using 250, 500 and 750 simulation counts (Table 20) in order to reach acceptable accuracy of the model. When the results of simulation counts were assessed, 500 simulation counts gave us better results. Initial

results of the model run was $r^2=0.41$, $NS=0.11$ (Figure 51) and improved to $r^2= 0.51$, $NS = 0.51$ after the calibration (Figure 52).

Table 20 Four-HRU types model calibration results depending on simulation count

METHOD	CN2+SOL_K+SLOPE							
Variable	p-factor	r-factor	R2	NS	bR2	PBIAS	Mean(sim)	StdDev(sim)
4 HRUs TYPE (SM=250)	0.84	1.20	0.48	0.48	0.25	-0.2	2.16(2.17)	2.10(1.57)
4 HRUs TYPE (SM=500)	0.95	2.47	0.51	0.51	0.24	6.5	2.16(2.02)	2.10(1.52)
4 HRUs TYPE (SM=750)	0.75	0.99	0.51	0.48	0.25	18.7	2.16(1.76)	2.10(1.44)

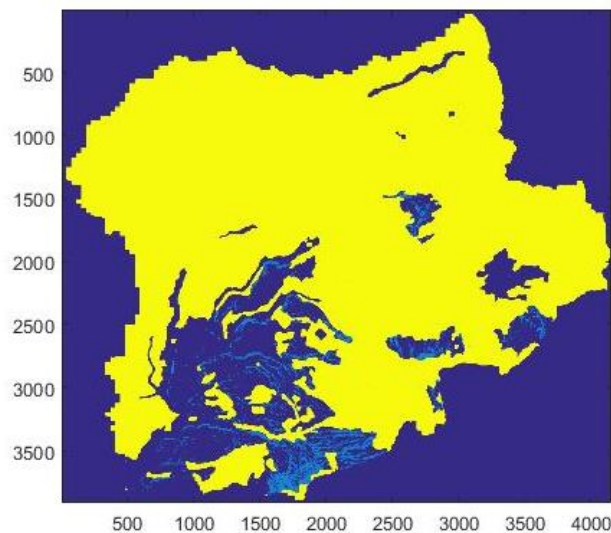


Figure 49 Four-HRU types division depending on SOL_K, CN2 and Slope

```

if (curv_no>70) && (sol_k<=10.15)
    if (curv_no<=94&&curv_no>=80)&&(sol_k>=3.3&&sol_k<=10.15)&&(slope_class>=0.13)
        hru_image(ii, jj) = 1;
    elseif (curv_no<80&&curv_no>=73)&&(slope_class>=0.10&&slope_class<0.13)
        hru_image(ii, jj)=2;
    end
else
    if (curv_no<70&&curv_no>=61)&&(sol_k==33)&&(slope_class>=0.5&& slope_class>0.10)
        hru_image(ii, jj)=3;
    else
        hru_image(ii, jj)=4;
    end
end

```

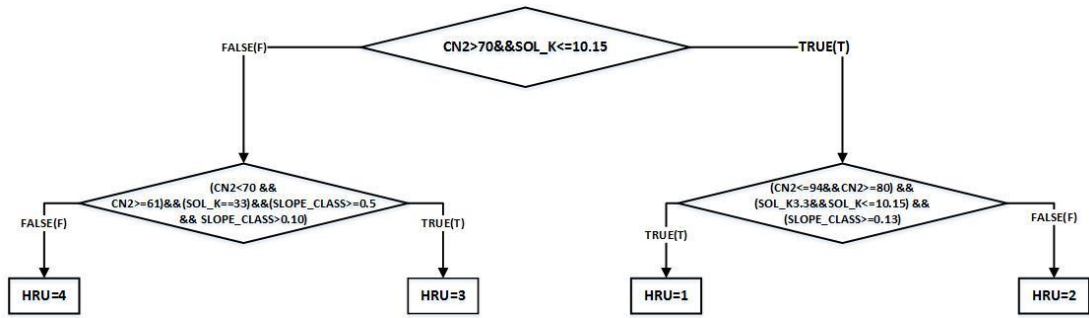


Figure 50 The flowchart of four-HRU types generation.

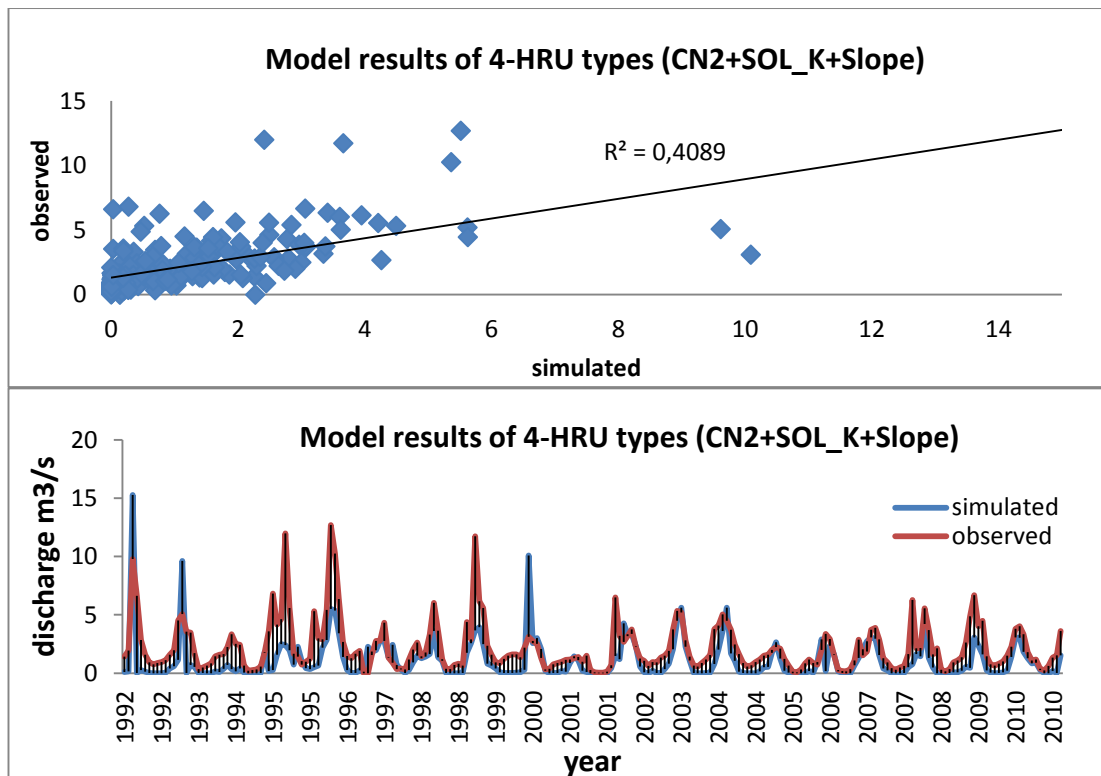


Figure 51 Four-HRU types model results without including initial values which are calibrated model parameters of two HRU types

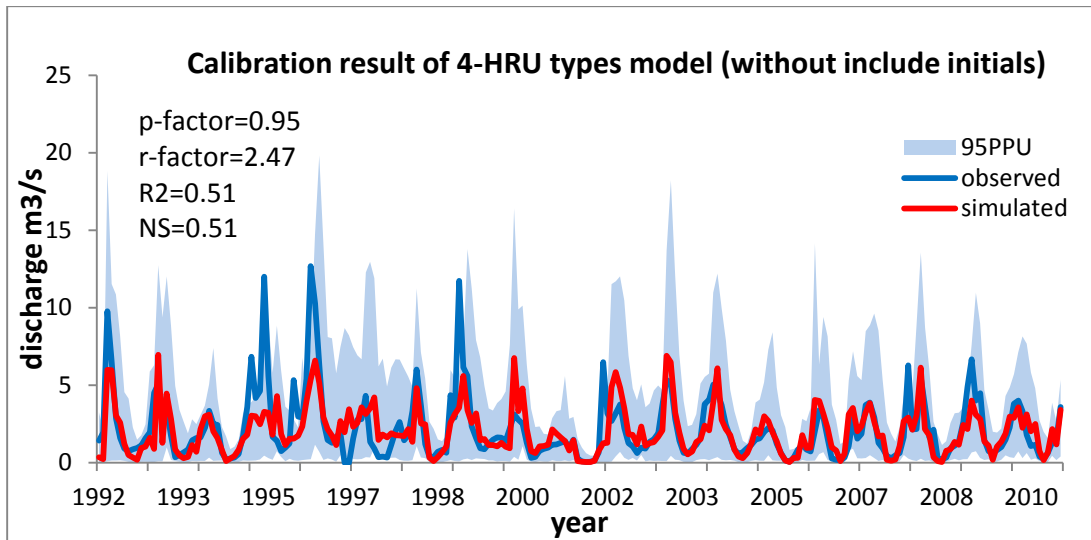


Figure 52 Four-HRU types calibration model results (simulation count =500)

The four-HRU type model was run with the calibrated parameters of the two-HRU types model and obtained $r^2=0.53$, NS=0.31 (Figure 53). When calibration performances were compared by using 100, 250, 500, 750, 1000 and 1250 simulation counts, the simulation 500 count gave the best model accuracy (Table 21). The model was improved to $r^2=0.59$ and NS=0.57 (Figure 54) after the calibration.

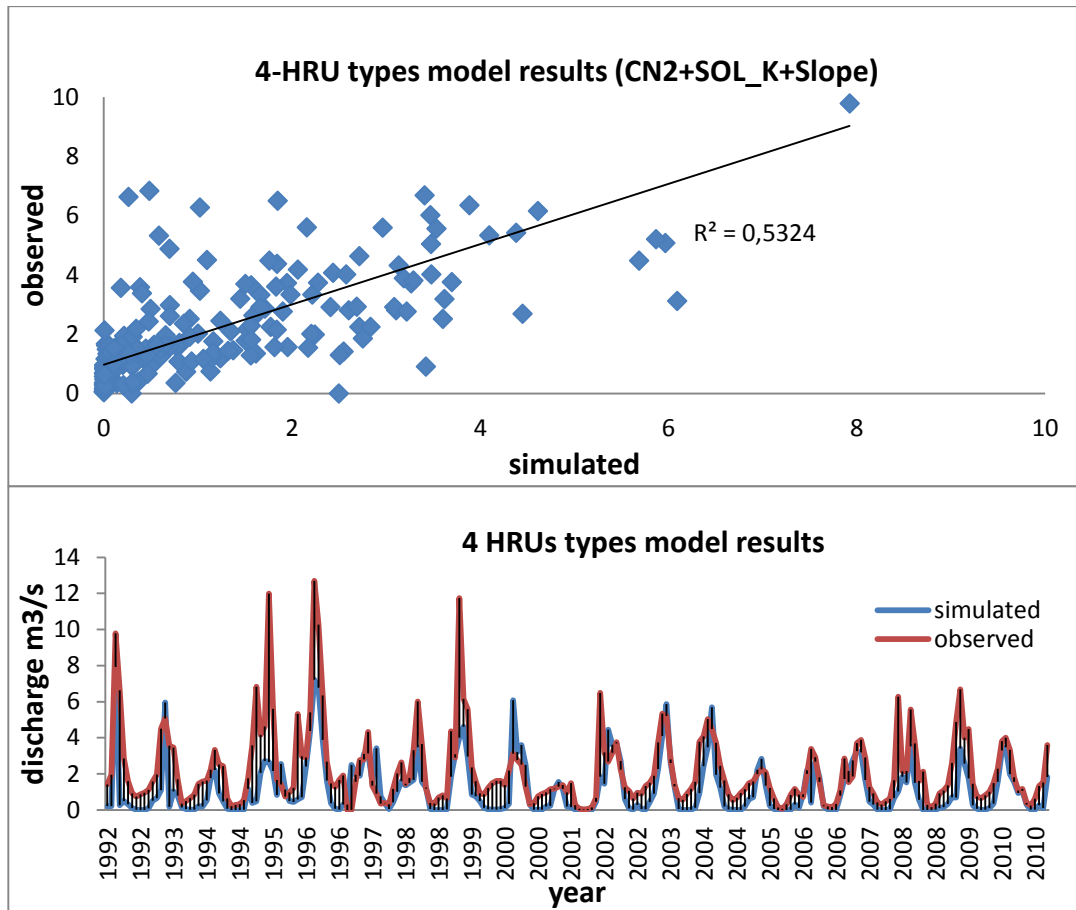


Figure 53 Four-HRU types model results by using calibrated parameters values of two-HRUs as initial values

Table 21 Four-HRU types model calibration results depending on simulation count

METHOD	CN2+SOL_K+SLOPE (using calibrated parameters of 4 HRUs as initial for 8 HRU)							
	p-factor	r-factor	R2	NS	bR2	PBIAS	Mean(sim)	StdDev(sim)
4 HRUs TYPE (SM=100)	0.89	2.06	0.53	0.50	0.3238	-14.3	2.16(2.47)	2.10(1.74)
4 HRUs TYPE (SM=250)	0.96	2.41	0.54	0.53	0.3113	0.4	2.16(2.15)	2.10(1.67)
4 HRUs TYPE (SM=500)	0.72	1.32	0.59	0.57	0.4101	-4.1	2.16(2.25)	2.10(1.90)
4 HRUs TYPE (SM=750)	0.82	1.79	0.57	0.56	0.3378	9.2	2.16(1.97)	2.10(1.64)
4 HRUs TYPE (SM=1000)	0.84	2.08	0.59	0.58	0.3687	5.6	2.16(2.04)	2.10(1.71)
4 HRUs TYPE (SM=1250)	0.96	2.37	0.56	0.55	0.3098	8.4	2.16(1.98)	2.10(1.55)

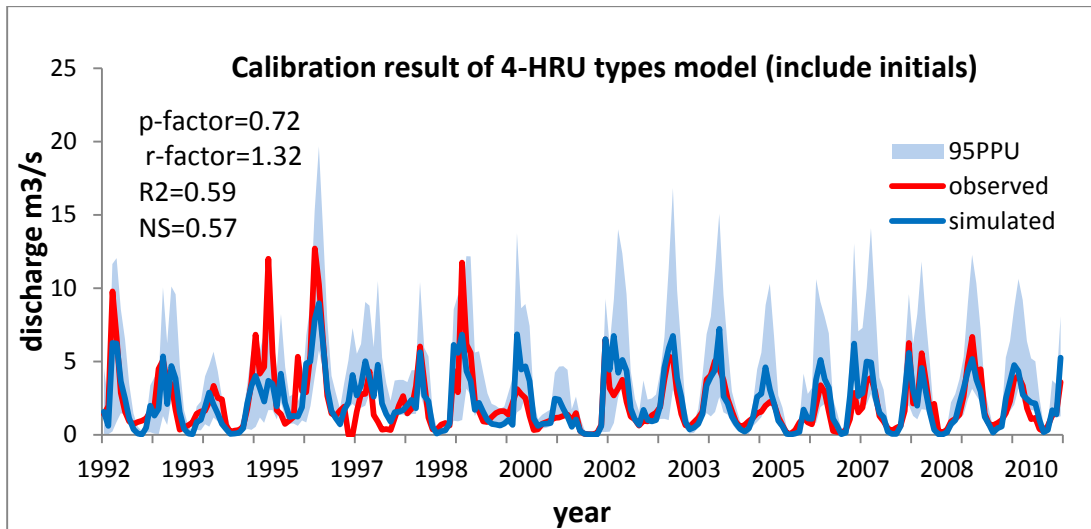


Figure 54 Four-HRUs calibration model results (simulation count =500) calibrated two HRU types model parameters used as an initials for four HRUs

In order to verify the four-HRU types model which includes initials, firstly the model was run for 1998-2010 years. After calibration of the model for this period (Figure 55), the model was verified with calibrated parameters between 1992 and 1994 years. According to the results, the model performance is $r^2=0.6045$ for this period (Figure 56).

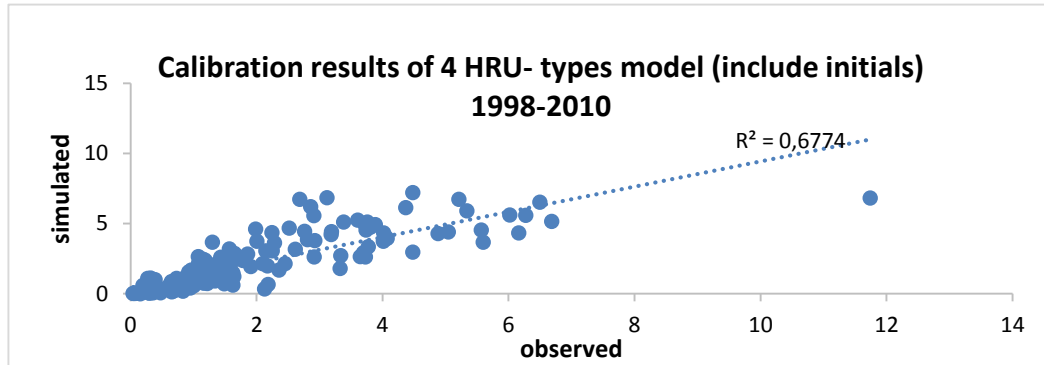
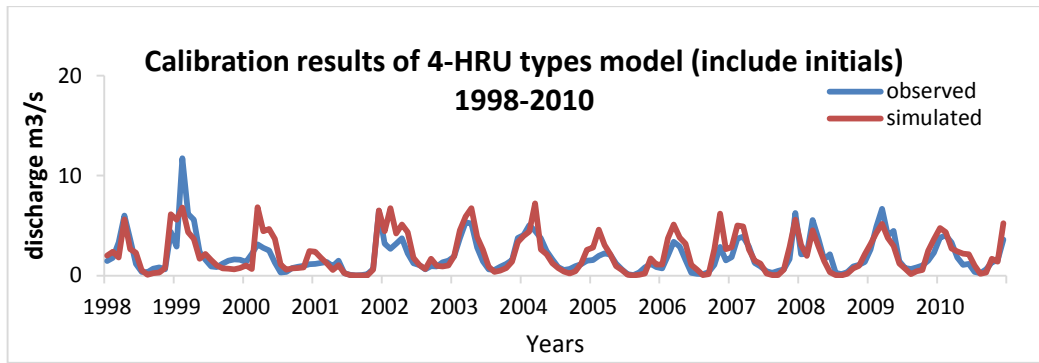


Figure 55 Calibration performance of the model between 1998 and 2010 years

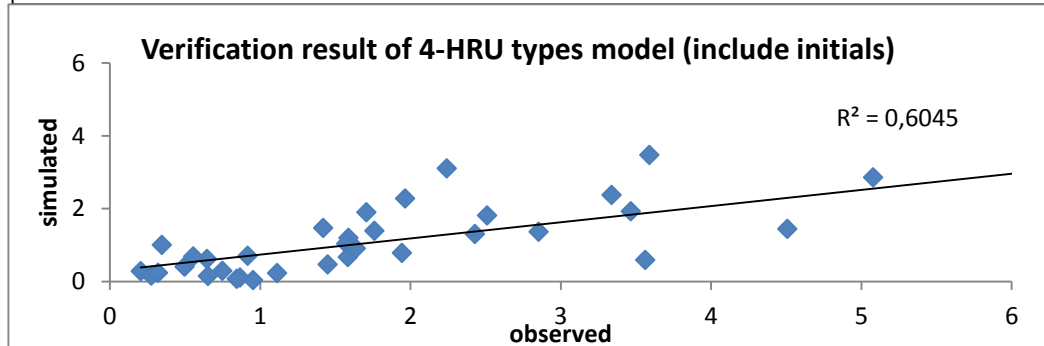
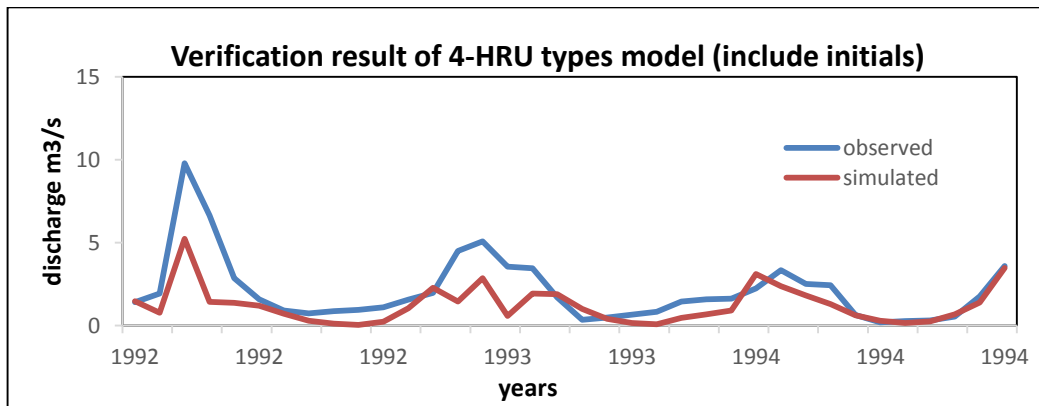


Figure 56 Four-HRU types model performance after verification

4.5.3 Eight-HRU Types which were created with respect to Slope, CN2 and SOL_K parameters results

In order to find an optimum HRU number, the HRUs in the four-HRU types model was further divided into two-HRUs resulting in the eight-HRU types model (Figure 57). The accuracy of the eight-HRU type model was initially $r^2=0.21$, $NS=-0.21$ (Figure 58). In order to see the calibration performance of the model which does not include any initials, the model was calibrated by using 250, 500, 750 and 1000 simulation counts (Table 22). Best calibration result was given by 500 simulation count. The model was calibrated to produce $r^2=0.56$ and $NS=0.51$ (Figure 59). Introducing the parameters of the calibrated parameters of the four-HRU model into the eight-HRU model, the initial run produced $r^2 = 0.24$, $NS = -0.10$ (Figure 60). If eight-HRU types model that includes initials was calibrated by applying 250, 500, 750 and 1000 simulation count (Table 23), 750 simulation count gave better calibration results. It produced $r^2=0.53$, $NS=0.52$ and (Figure 61).

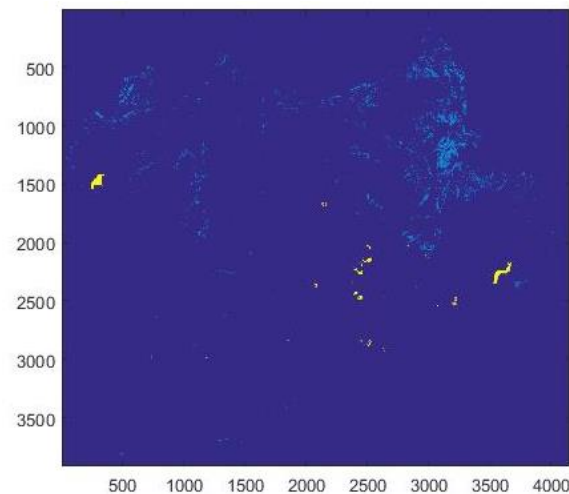


Figure 57 Eight-HRU types division depending on SOL_K, CN2 and slope classification

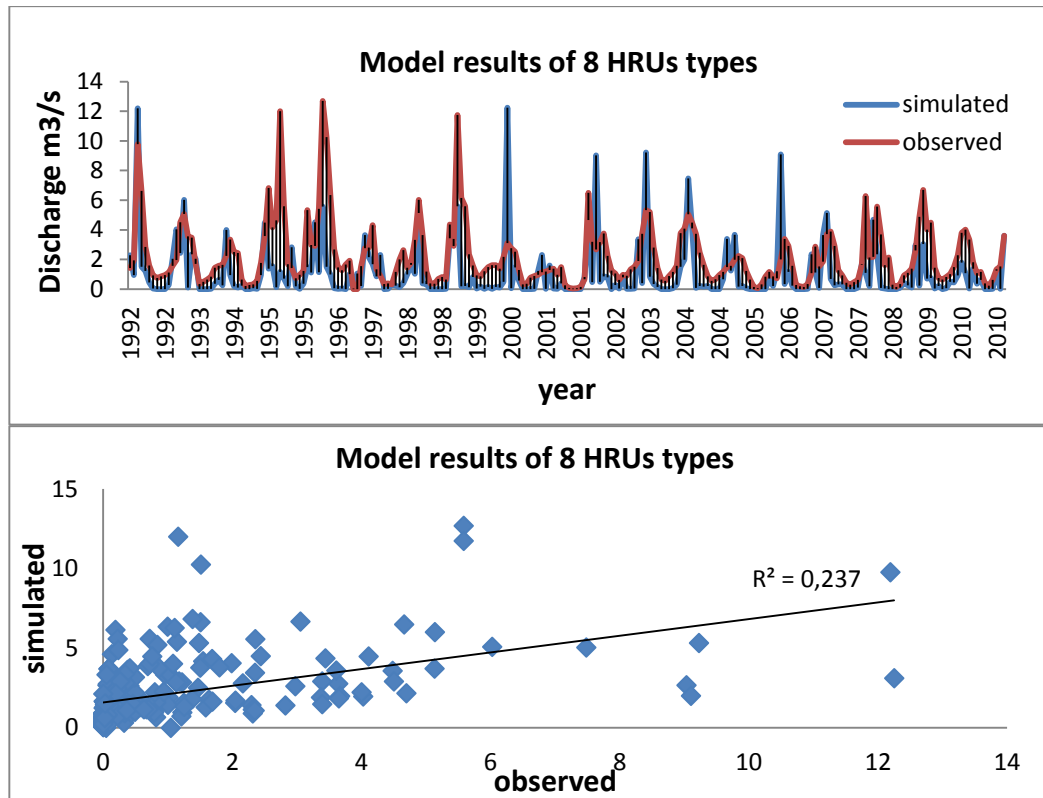


Figure 58 Model results eight-HRU types which are produced by combining CN2, SOL_K and slope classification.

Table 22 8 HRU types model calibration results depending on simulation count

METHOD	CN2+SOL_K+SLOPE							
	p-factor	r-factor	R2	NS	bR2	PBIAS	Mean(sim)	StdDev(sim)
8 HRUs TYPE (SM=250)	0,72	1,38	0,56	0,51	0,41	9,40	2.16(1.96)	2.10(2.03)
8 HRUs TYPE (SM=500)	0,91	2,03	0,55	0,54	0,29	8,60	2.16(1.98)	2.10(1.49)
8 HRUs TYPE (SM=750)	0,77	1,10	0,60	0,54	0,33	22,10	2.16(1.69)	2.10(1.52)
8 HRUs TYPE (SM=1000)	0,87	1,86	0,54	0,49	0,31	22,50	2.16(1.68)	2.10(1.64)

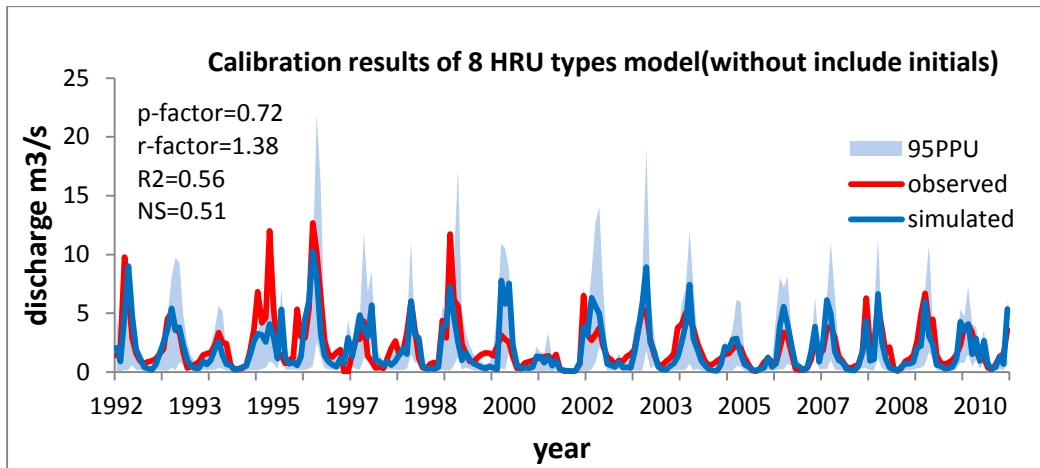


Figure 59 Calibration results of 8 HRU types model that are produced by combining CN₂, SOL_K and slope classification

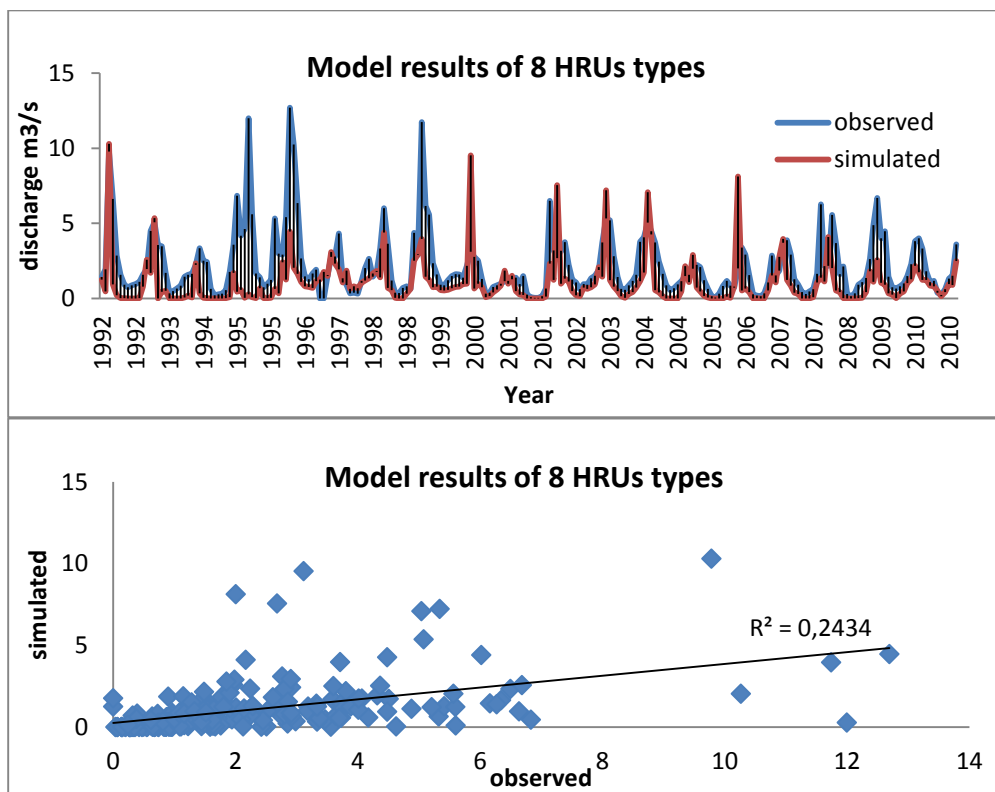


Figure 60 Model results of 8 HRU types which are produced by combining CN₂, Sol_K and slope classification (calibrated parameters values of 4 HRU types model as initials for 8 HRUs).

Table 23 8 HRU types model calibration results which include calibrated parameter values of 4 HRUs depending on simulation count

METHOD	CN2+SOL_K+SLOPE (using calibrated parameters of 4 HRUs as initial for 8 HRU)							
	p-factor	r-factor	R2	NS	br2	PBIAS	Mean(sim)	StdDev(sim)
8 HRUs TYPE (SM=250)	0,78	1,07	0,51	0,45	0,28	23,60	2.16(1.65)	2.10(1.62)
8 HRUs TYPE (SM=500)	0,85	1,92	0,52	0,51	0,28	8,40	2.16(1.98)	2.10(1.57)
8 HRUs TYPE (SM=750)	0,90	1,79	0,53	0,52	0,26	-2,00	2.16(2.21)	2.10(1.44)
8 HRUs TYPE (SM=1000)	0,77	1,49	0,56	0,53	0,38	11,00	2.16(1.93)	2.10(1.88)

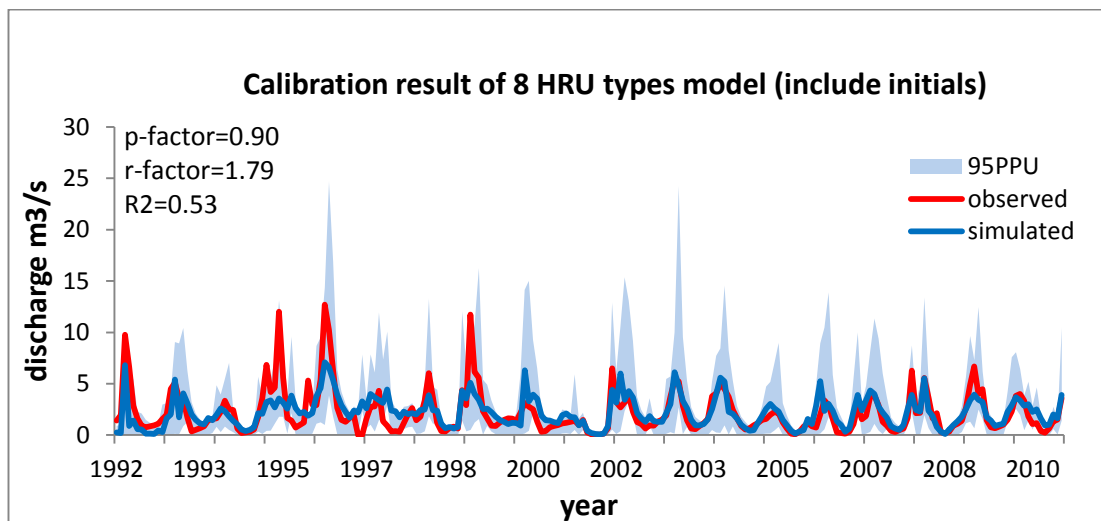


Figure 61 Calibration results of 8 HRU types model which are produced by combining CN2, SOL_K and slope classification (calibrated parameters values of 4 HRUs type model as initials for 8 HRUs).

4.6 2. Case Study: Namazgah Dam Basin, Kocaeli, TURKEY

Namazgah Dam Basin is located at 40°55'-41°04' north latitude and 30°00'-30°25' in Kandıra and İzmit District boundaries. The dam was constructed on Namazgah river in the Marmara Region. The area of the basin is 100,64 km². The dam was built in order to provide irrigation, drinking and usage water demand of tourist settlements on the Black Sea coast and the town center Kandıra, Derince, the villages and towns of İzmit and Körfez district (Figure 62).

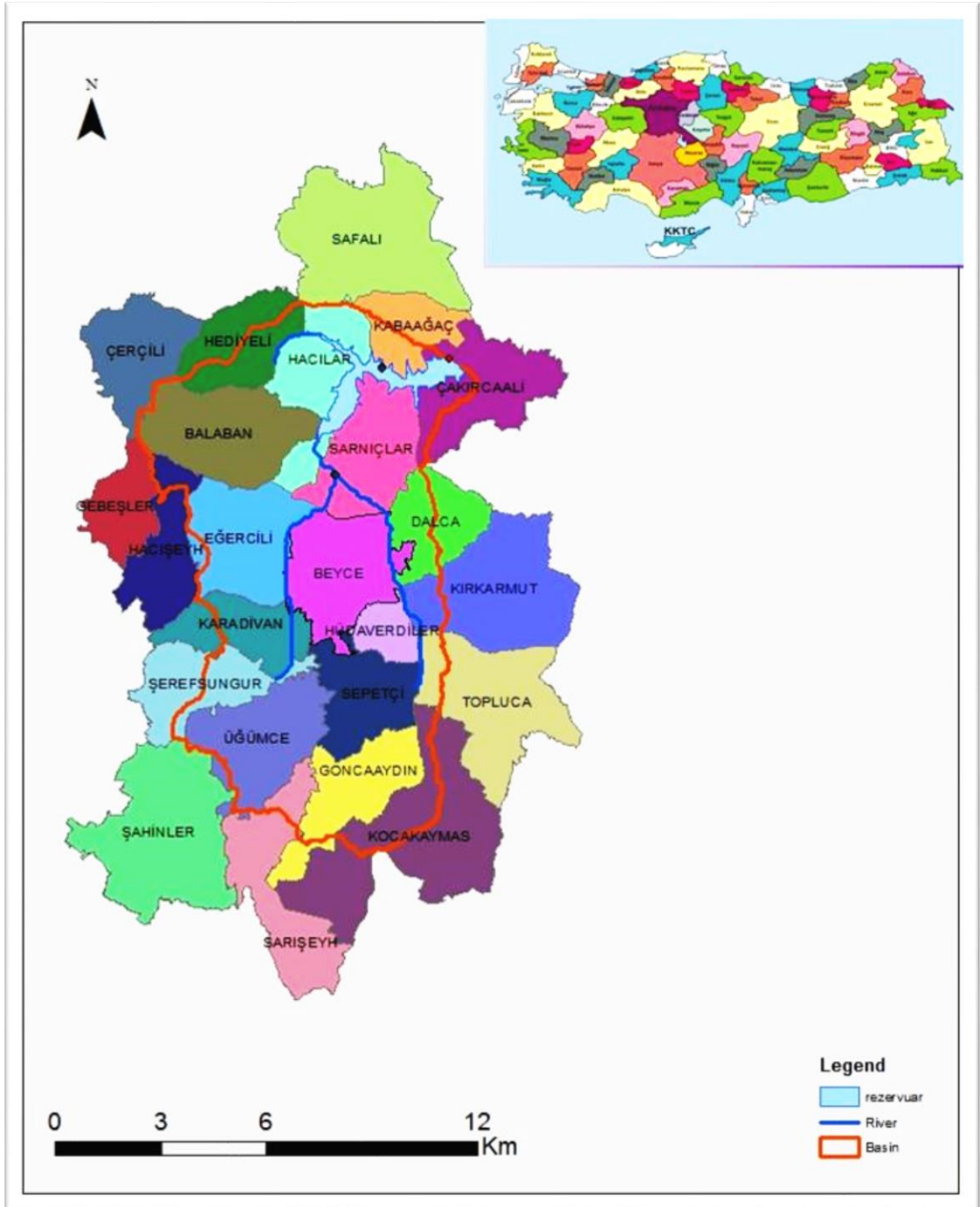


Figure 62 2. Case Study Area

4.6.1. SWAT Input Layers

Input layers of SWAT for Namazgah Dam Basin are digital elevation model, soils, land use, and slopes.

4.6.1.1 Delineation of Watershed

The Digital Elevation Model of Namazgah Dam Basin is given in (Figure 63). DEM was produced from 1:25 000 scale topographic maps. The DEM properties were given in Table 24.

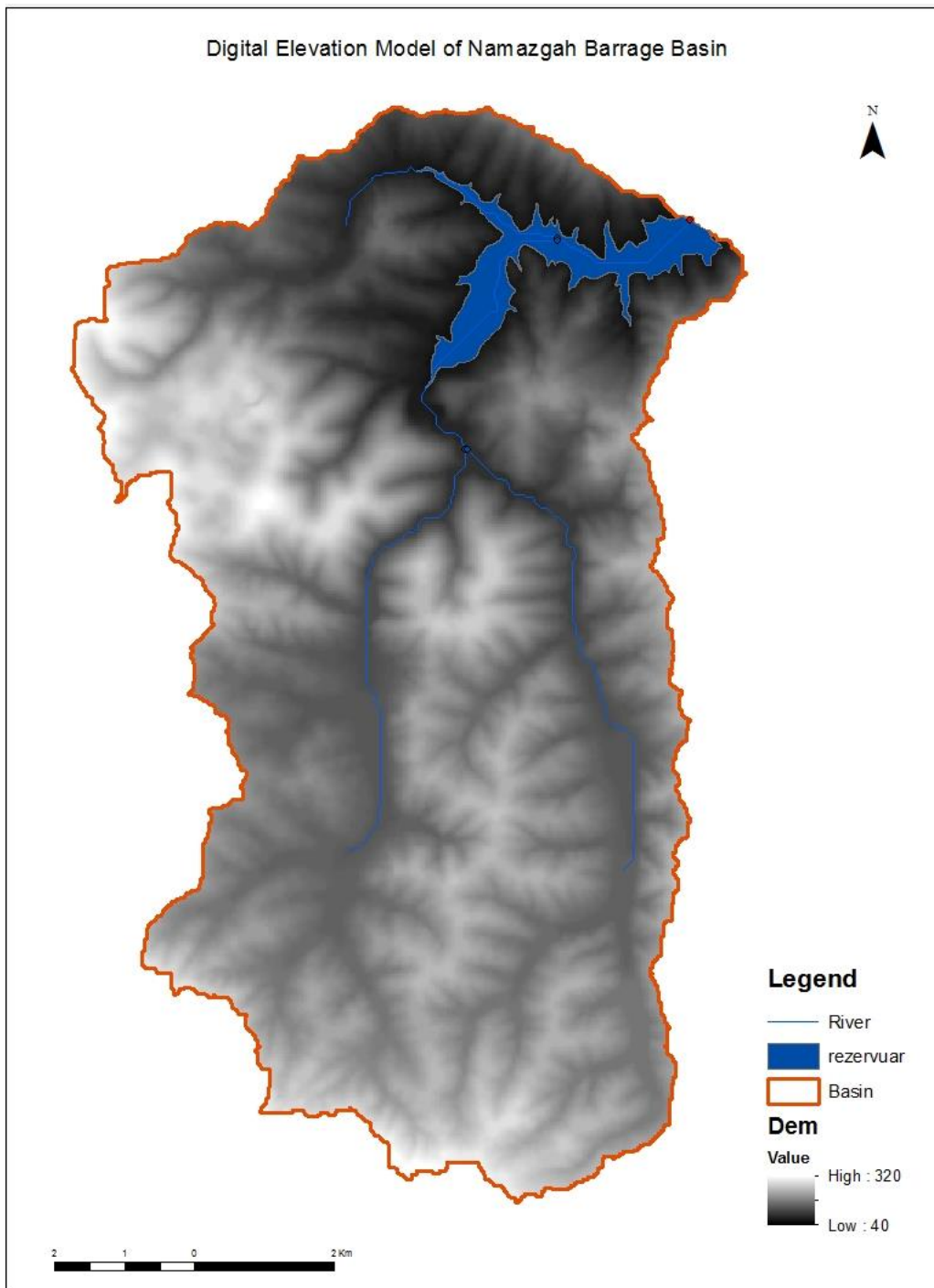


Figure 63 Digital Elevation Model of Namazgah Dam Basin

Table 24 DEM Characteristics of Namazgah Dam Basin

Metadata parameter	Value
Projection	Universal Transverse Mercator (UTM)
False Northing	500000
False Easting	0.000000
Central Meridian	27
Scale Factor	0.9996
Reference Latitude	0.000000
Geographic Coordination System	WGS_1984_35 N
Column/Row count	323/ 524
Cell size (X/Y) (m/m)	30/30
Bits per pixel	32

In order to produce sub-basins of the watershed from DEM, many operations were applied on DEM. Firstly, when the preprocessing of DEM was completed; minimum, maximum, and suggested sub-watershed areas in hectares were calculated as 52, 10340 and 1000, respectively. Secondly, streams and outlets were defined by SWAT. One outlet was added manually. The outlet was close to Namazgah stream gauging station in the watershed. This choice enables us to compare between the results of models and observation data. At the end of watershed delineation, we acquired five sub-basins (Figure 64), and SWAT calculated minimum, maximum, mean and standard deviation elevation values which were 40, 350, 165.437 and 53.72, respectively.

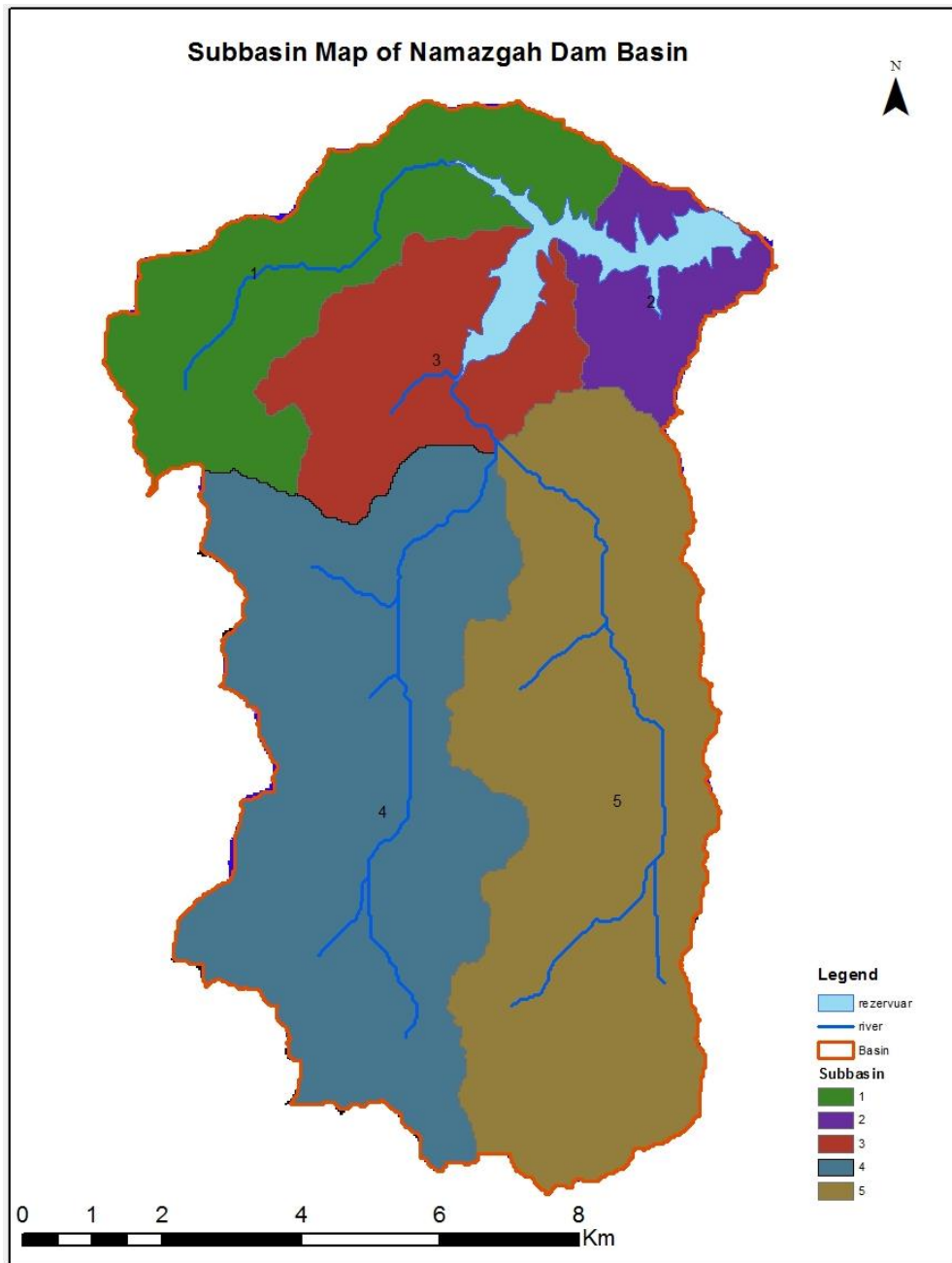


Figure 64 Sub-basins of Namazgah Dam Basin

4.6.1.2 Soil Class Layer

The soil map of the study area (Scale: 1/25,000) was supplied by a Kocaeli Metropolitan Municipality project. Soil data is classified according to major soils groups (Table 25).

Table 25 Major Soils Group in Namazgah Dam Basin.

Soil Classification	Explanation
R	Rendzina
N	Limeless brown forest soil
K	Colluvial soils
YR	Kolluvial
A	Alluvial

The soil map used in SWAT is given in Figure 65. Soil class distribution in the area was observed from Figure 66. There are mostly N and R group of soils, Limeless brown forest soils and Rendzina Soils, in the area. Properties of the soil were entered in SWAT soil user database (Table 26).

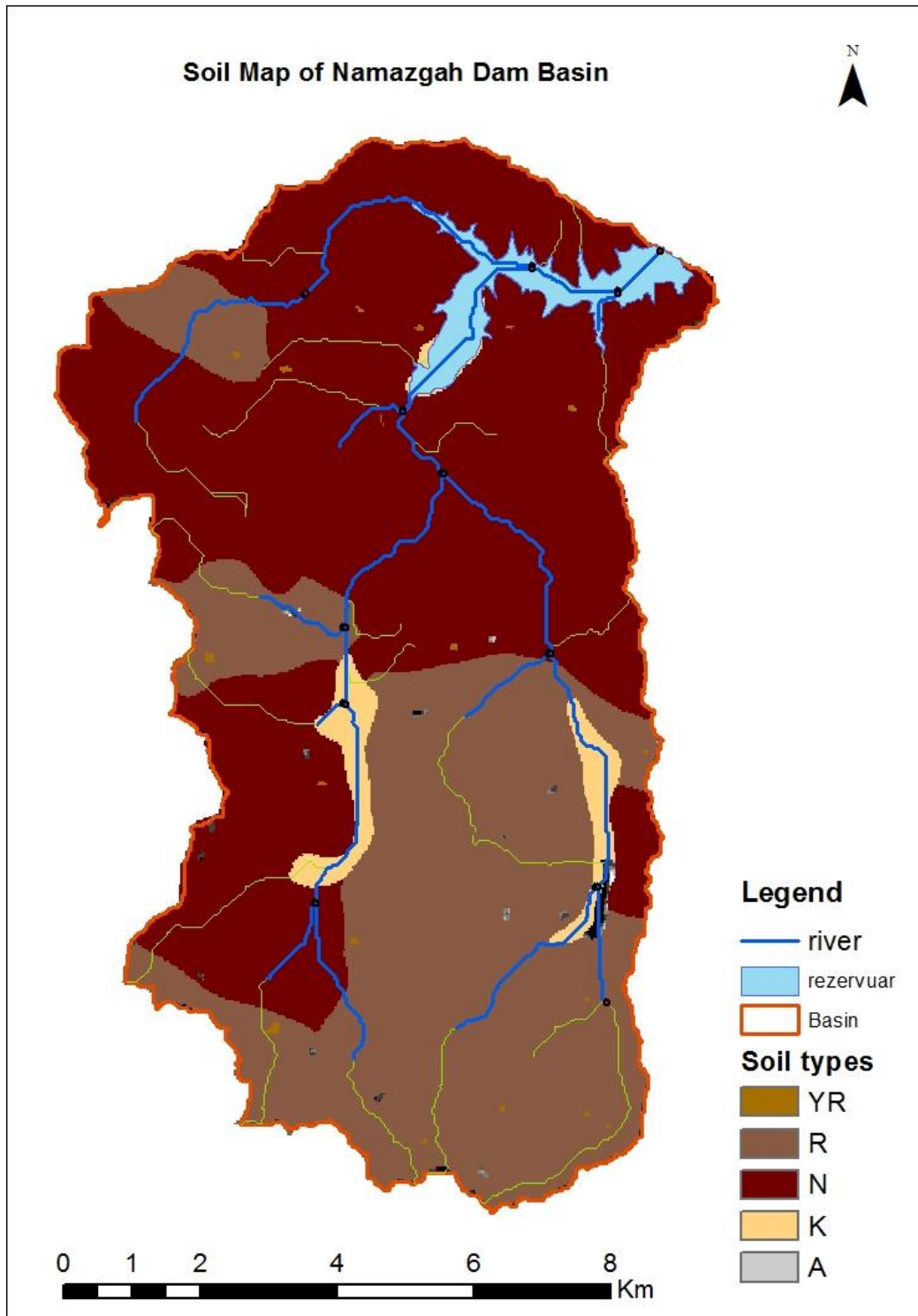


Figure 65 Soil Map of Namazgah Dam Basin.

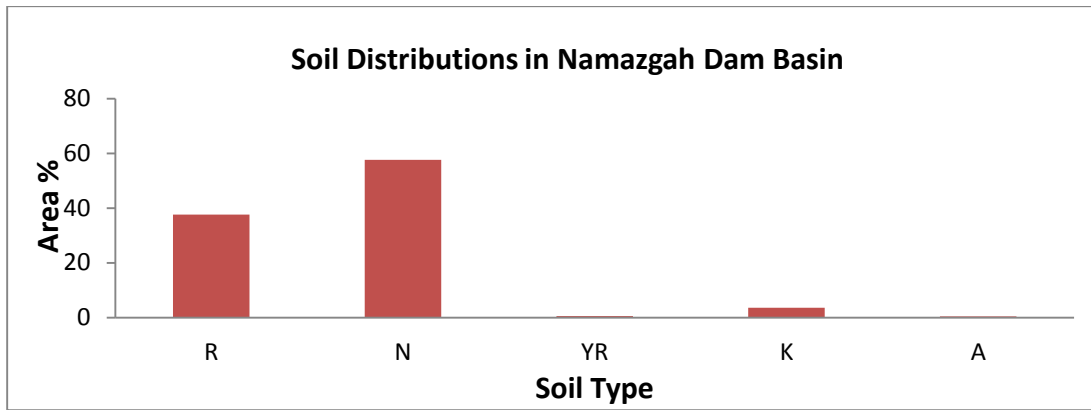


Figure 66 Soil type histogram representation of the study area.

Table 26 User soil database in SWAT for Namazgah Dam Basin

SNAM	NLAYERS	HYDGRP	SOL_ZMX	ANION_EXCL	SOL_CRK	TEXTURE	SOL_Z1	SOL_BD1	SOL_AWC1	SOL_K1	SOL_CBN1	CLAY1	SILT1	SAND1
R	2	C	500	0.5	0.5	CLAY	200	1.45	0.17	10.15	3.07	39	51	10
N	2	D	900	0.5	0.5	SANDY/CLAY LOAM	500	1.4	0.19	3.3	0.21	40	10	60
YR	1	D	152	0.5	0.5	VAR	152	1.5	0.1	500	2.97	15	30	55
K	1	D	900	0.5	0.5	CLAY	900	1.35	0.1	3.3	2.97	40	40	20
YR	1	D	152	0.5	0.5	VAR	152	1.5	0.1	500	2.97	15	30	55
YR	1	D	152	0.5	0.5	VAR	152	1.5	0.1	500	2.97	15	30	55
A	1	D	900	0.5	0.5	SILTY CLAY LOAM	900	1.5	0.19	10.15	0.48	40	40	20

4.6.1.3 Land use/Land cover Layer

Land use layer was obtained from the framework of a Ministry of Forestry and Water Affairs project. Land use/land cover data was clipped and reprojected by using the ArcSWAT project database. (Figure 67). Land use/land cover map resolution is 30/30 meters. There are eight land use/land cover class in the study area (Table 27). The most dominant type of land use is Agricultural area, which covers %67.31 of watershed area (

Figure 68). Other dominant land use/land cover area is Broad-leaved forest.

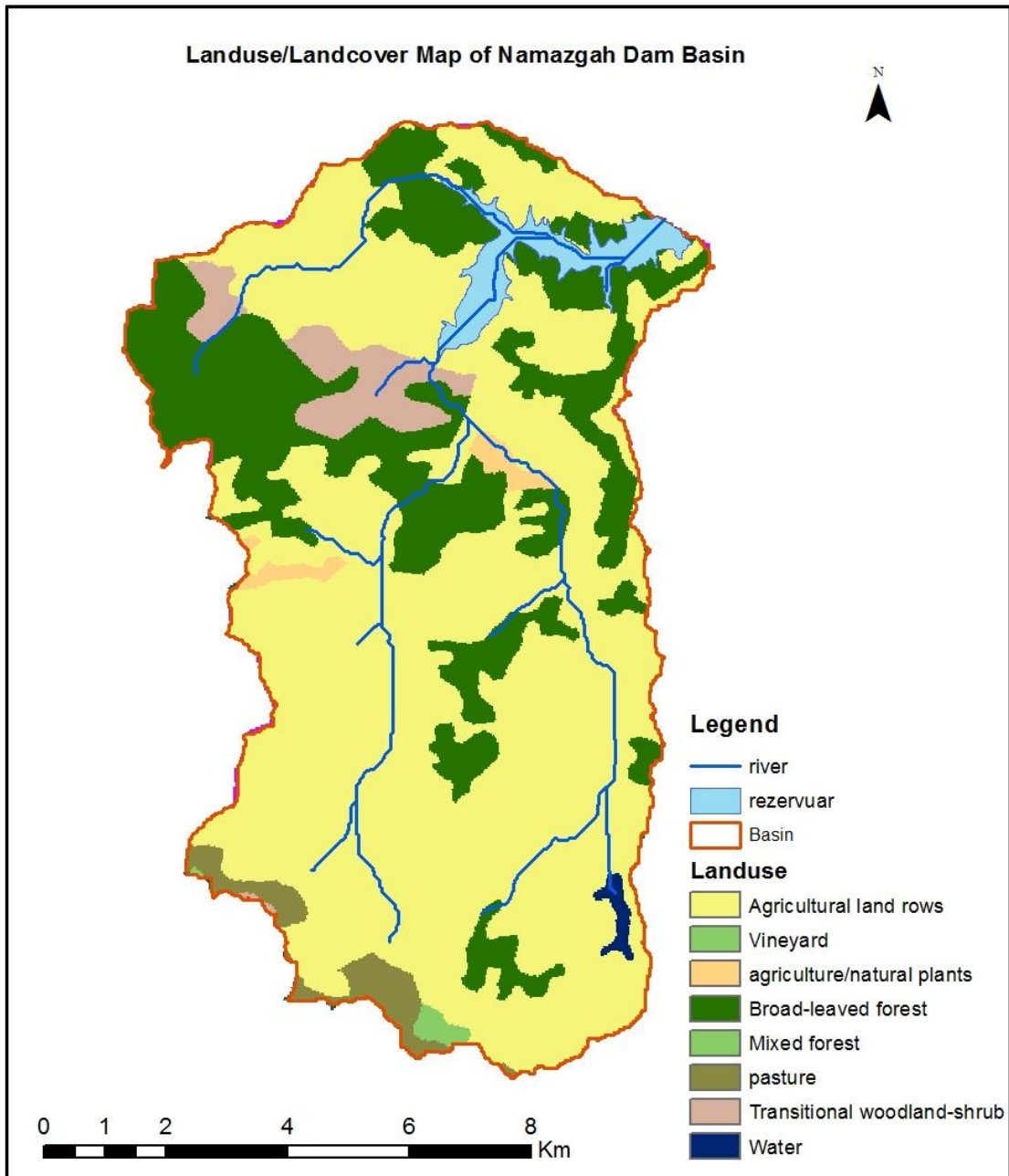


Figure 67 Land use/Land cover Map of Namazgah Dam Basin

Table 27 Land use/ land cover distribution in Namazgah Dam Basin

Land use/Land cover Type	Symbol	(%)Water shed Area
pasture	PAST	2.19
agriculture/natural plants	CRWO	1.10
Broad-leaved forest	FODB	24.90
Mixed forest	FOMI	0.37
Transitional woodland-shrub	MIGS	3.71
Water	WATR	0.40
Agricultural land rows	AGRR	67.31
Vineyard	GRAP	0.02

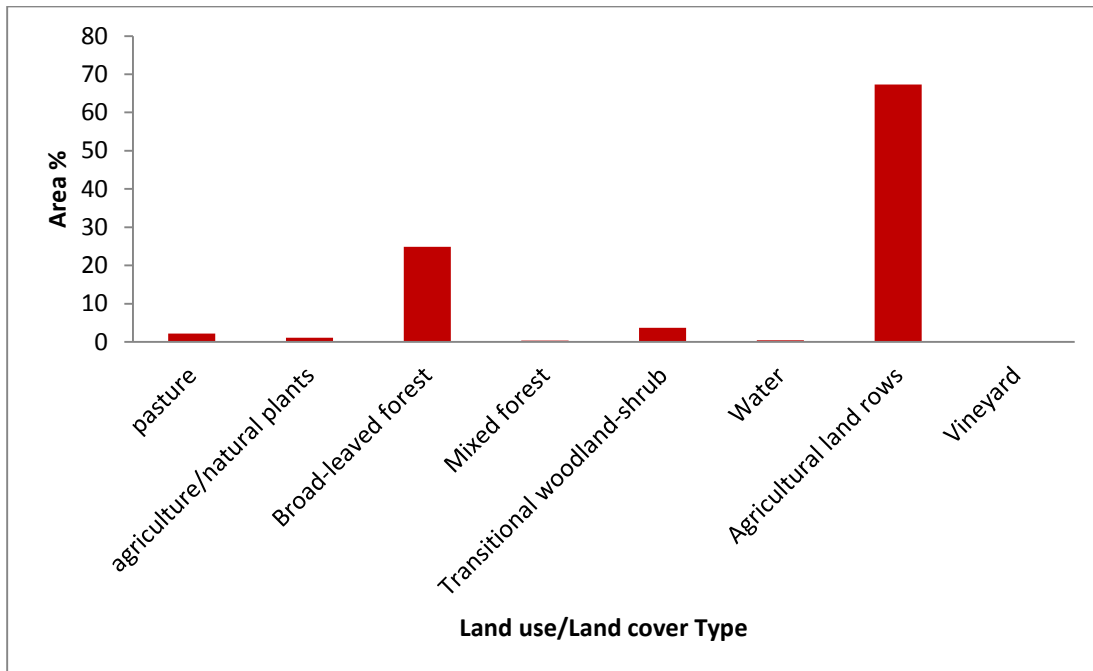


Figure 68 Land use/land cover type histogram representation of Namazgah Dam Basin.

4.6.1.4 Slope Layer

Slope characterization is based upon the DEM defined in the watersheds delineation (Figure 69).

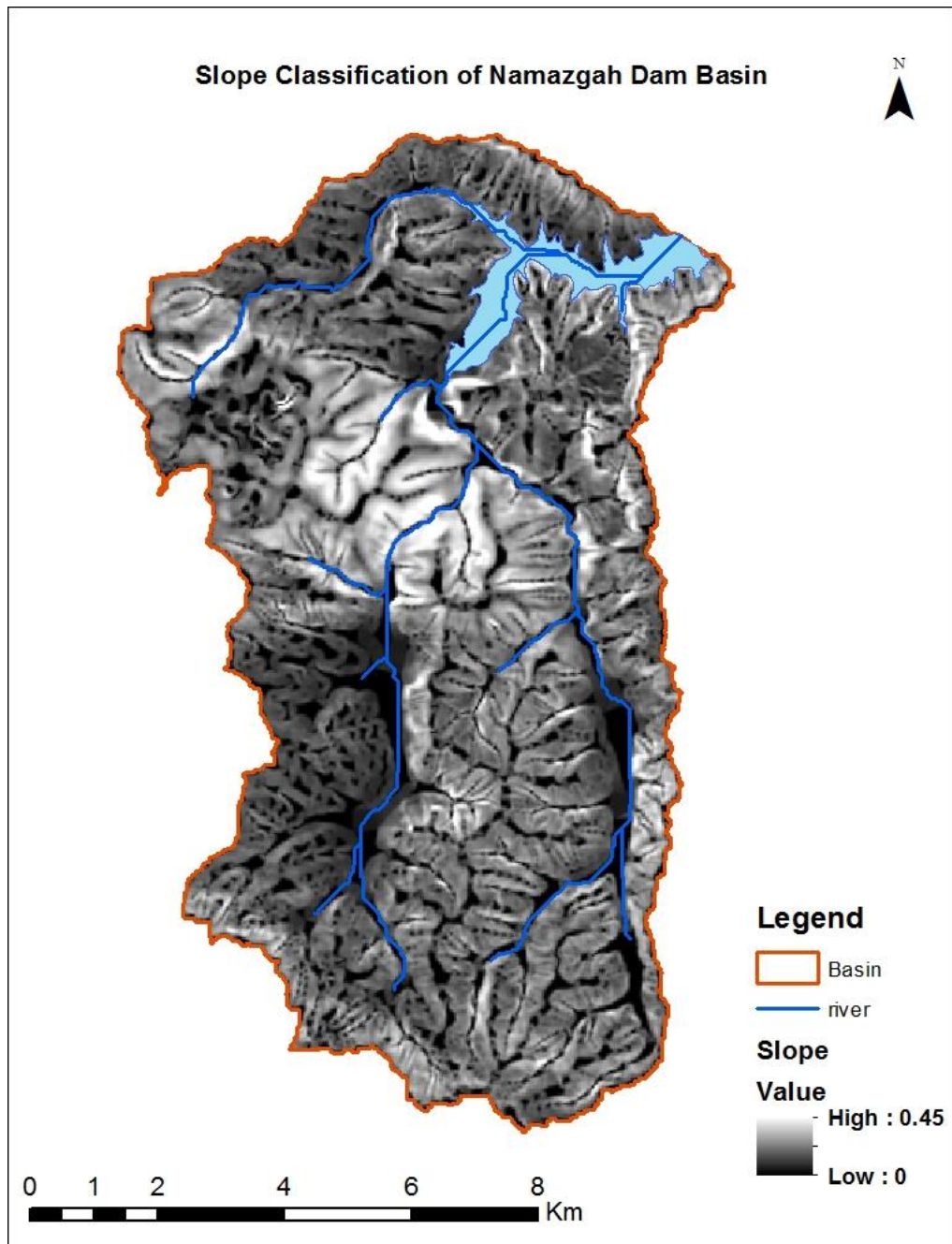


Figure 69 Slope Map of Namazgah Dam Basin

4.6.1.5 Meteorological Data

SWAT needs some important daily meteorological data such as minimum and maximum temperatures, precipitation, solar radiation, wind speed and relative humidity data. Meteorological data used in Namazgah Stream was obtained from NCEP/CFSR (The National Centers for Environmental Prediction/Climate Forecast System Reanalysis) data. It is available along with in situ measurements from several ground stations. Reanalysis data is used since in situ data has continuity problems. One meteorological station which was near the study area was used. Weather data obtained from global meteorological stations in the area was between 1979 and 2010 years. In order to assign meteorological data in the model, the data files were prepared in *.txt format. Long-term monthly averages of data is used in SWAT. When there is the missing observation data and the input data, lack of data is accomplished by statistical parameters produced from these long term daily data (Table 27).

The needed data for the weather generator are:

- Mean daily maximum air temperature for month (°C)
- Mean daily minimum air temperature for month (°C)
- Standard deviation for daily maximum air temperatures in month (°C)
- Standard deviation for daily minimum air temperature in month (°C)
- Mean total monthly precipitation (mm H₂O)
- Standard deviation for daily precipitation in month (mm H₂O/day).
- Skewness coefficient for daily precipitation in month.
- Probability of a wet day following a dry day in the month.
- Probability of a wet day following a wet day in the month.
- Mean number of days of precipitation in month.
- Mean daily solar radiation for month (MJ/m²/day).
- Mean daily dew point temperature in month (°C).
- Mean daily wind speed in month (m/s).

Table 28 Statistical Values of Meteorological Data

OBJECTID	STATION	TMPMX1	TMPMX2	TMPMX3	TMPMX4	TMPMX5	TMPMX6	TMPMX7	TMPMX8	TMPMX9	TMPMX10	TMPMX11	TMPMX12
1	p411300wgn	8.367723	8.791184	11.76964	16.93165	21.90777	26.50012	28.33543	28.42928	24.98051	19.96796	14.51822	10.0235
WLATITUDE	41.058	TMPMN1	TMPMN2	TMPMN3	TMPMN4	TMPMN5	TMPMN6	TMPMN7	TMPMN8	TMPMN9	TMPMN10	TMPMN11	TMPMN12
VLONGITUD	30	2.587635	2.218753	3.767604	6.613638	9.922231	13.95265	16.14762	16.72022	14.12415	11.38944	7.466173	4.462481
WELEV	152	TMPSTDMX1	TMPSTDMX2	TMPSTDMX3	TMPSTDMX4	TMPSTDMX5	TMPSTDMX6	TMPSTDMX7	TMPSTDMX8	TMPSTDMX9	TMPSTDMX10	TMPSTDMX11	TMPSTDMX12
RAIN_YRS	36	4.216229	4.981779	5.501248	5.277781	4.51159	3.626094	3.065076	3.127362	3.899444	5.076766	4.968755	4.170317
		TMPSTDMN1	TMPSTDMN2	TMPSTDMN3	TMPSTDMN4	TMPSTDMN5	TMPSTDMN6	TMPSTDMN7	TMPSTDMN8	TMPSTDMN9	TMPSTDMN10	TMPSTDMN11	TMPSTDMN12
		3.324241	3.779735	3.649838	3.650179	3.736305	2.924531	2.537765	2.469851	2.89719	3.206943	3.632773	3.392279
		WNDV1	WNDV2	WNDV3	WNDV4	WNDV5	WNDV6	WNDV7	WNDV8	WNDV9	WNDV10	WNDV11	WNDV12
		3.762871	3.835361	3.694384	3.347005	3.340656	3.558232	3.84006	3.810617	3.512196	3.430532	3.356773	3.816047
		PCPMM1	PCPMM2	PCPMM3	PCPMM4	PCPMM5	PCPMM6	PCPMM7	PCPMM8	PCPMM9	PCPMM10	PCPMM11	PCPMM12
		115.2356	98.47276	90.12451	59.59363	47.78748	37.68852	38.54046	43.42759	54.08229	98.47534	100.7484	117.1558
		PCPSTD1	PCPSTD2	PCPSTD3	PCPSTD4	PCPSTD5	PCPSTD6	PCPSTD7	PCPSTD8	PCPSTD9	PCPSTD10	PCPSTD11	PCPSTD12
		5.655748	5.419052	5.164611	4.040562	3.447406	3.548194	3.869533	4.684351	4.62458	6.848008	5.95314	6.141749
		PCPSKW1	PCPSKW2	PCPSKW3	PCPSKW4	PCPSKW5	PCPSKW6	PCPSKW7	PCPSKW8	PCPSKW9	PCPSKW10	PCPSKW11	PCPSKW12
		2.711104	2.806436	2.951064	3.899492	3.528167	5.276297	4.660065	4.754622	4.319499	3.621555	2.783552	2.822944
		PR_W1_1	PR_W1_2	PR_W1_3	PR_W1_4	PR_W1_5	PR_W1_6	PR_W1_7	PR_W1_8	PR_W1_9	PR_W1_10	PR_W1_11	PR_W1_12
		0.5405405	0.4744898	0.4801444	0.4194444	0.3279022	0.2491909	0.1912145	0.1970706	0.2819615	0.3791349	0.3506097	0.4887892
		PR_W2_1	PR_W2_2	PR_W2_3	PR_W2_4	PR_W2_5	PR_W2_6	PR_W2_7	PR_W2_8	PR_W2_9	PR_W2_10	PR_W2_11	PR_W2_12
		0.8747203	0.8769793	0.8474374	0.7763889	0.75	0.6406927	0.5730994	0.5568863	0.6784969	0.7817919	0.8490305	0.8700234
		PCPD1	PCPD2	PCPD3	PCPD4	PCPD5	PCPD6	PCPD7	PCPD8	PCPD9	PCPD10	PCPD11	PCPD12
		24.83333	22.80556	23.30556	20	17.33333	12.83333	9.5	9.542857	13.68571	19.77143	20.62857	24.4
		SOLARAV1	SOLARAV2	SOLARAV3	SOLARAV4	SOLARAV5	SOLARAV6	SOLARAV7	SOLARAV8	SOLARAV9	SOLARAV10	SOLARAV11	SOLARAV12
		5.596886	8.691776	13.6443	19.59435	24.46763	27.86041	28.09176	24.91563	18.74233	11.3068	7.071417	4.733597
		DEWP1	DEWP2	DEWP3	DEWP4	DEWP5	DEWP6	DEWP7	DEWP8	DEWP9	DEWP10	DEWP11	DEWP12
		0.8385895	0.8308618	0.7833003	0.7241173	0.6934124	0.6401212	0.6620137	0.6772357	0.6884864	0.7394965	0.777979	0.8245591

4.6.2 SWAT Model Results of Namazgah Dam Basin by using the current methodology for HRU division SWAT

According to the current methodology for generating HRU in SWAT, the total number of 5, 12 and 17 HRUs in five subbasins were compared. While using dominant land use/land soil and slope combination approach, we obtained five HRUs in total. The initial model run of five-HRU had $r^2=0.3784$, $NS=-1.37$ and improved to $r^2=0.69$, $NS=0.56$ after the calibration. When the total number of HRUs was increased to 12 by using 20%/20%/60% threshold values for land use/soil/slope combination, the initial model run had $r^2=0.37$, $NS=-1.34$ and improved to $r^2=0.70$, $NS = 0.58$ after the calibration. When 10%/10%/80% threshold values for land use/soil/slope combination were used, the total number of HRUs was 17. The initial model run had $r^2=0.39$, $NS=-1.33$ and improved to $r^2=0.68$, $NS = 0.57$ after calibration.

4.6.3 HRUs division depending on CN2 parameter

Since the CN2 curve number is a function of the soil's permeability, land use and antecedent soil water conditions, CN2 was chosen for dividing HRU types (Table 29). A threshold on CN2 found from LU/Soil tables is used to divide a sub-basin into two-

HRUs. This guaranties that the two-HRUs are more or less uniform within itself with respect to CN. Then, each HRU is further divided into two-HRUs (Figure 70, Figure 71). In contrast to combination of CN2, soil hydraulic conductivity in order to create HRUs, HRU generation with respect to just CN2 give us better model results.

Table 29 HRUs division based on CN2 parameter on Namazgah Dam basin

Landuse	Symbol	HYRD	CN2	HRU 2	HRU 4	HRU 8
Water	WATR	CN2A	92	CN2>79	CN2>85	CN2=92
Water	WATR	CN2B	92			
Water	WATR	CN2C	92			
Water	WATR	CN2D	92			
Agricultural Land-Row Crops	AGRR	CN2D	89			
Agricultural Land-Row Crops	AGRR	CN2C	85			
Pasture	PAST	CN2D	84		CN2<85	82<CN2<85
CROPLAND/WOODLAND MOSAIC	CRWO	CN2D	83			
DECIDUOUS BROADLEAF FOREST	FODB	CN2D	83			
Vineyard	GRAP	CN2D	83			
MIXED GRASSLAND/SHRUBLAND	MIGS	CN2D	82			
Pasture	PAST	CN2C	79			
MIXED FOREST	FOMI	CN2D	79			
CROPLAND/WOODLAND MOSAIC	CRWO	CN2C	78			
Agricultural Land-Row Crops	AGRR	CN2B	78	CN2<79	CN2>65	CN2>73
DECIDUOUS BROADLEAF FOREST	FODB	CN2C	77			
Vineyard	GRAP	CN2C	77			
MIXED GRASSLAND/SHRUBLAND	MIGS	CN2C	76,5			
MIXED FOREST	FOMI	CN2C	73			
Pasture	PAST	CN2B	69			
CROPLAND/WOODLAND MOSAIC	CRWO	CN2B	68,5		CN2<65	CN2>49
Agricultural Land-Row Crops	AGRR	CN2A	67			
DECIDUOUS BROADLEAF FOREST	FODB	CN2B	66			
Vineyard	GRAP	CN2B	66			
MIXED GRASSLAND/SHRUBLAND	MIGS	CN2B	65			
MIXED FOREST	FOMI	CN2B	60			
CROPLAND/WOODLAND MOSAIC	CRWO	CN2A	51,5			
Pasture	PAST	CN2A	49			
DECIDUOUS BROADLEAF FOREST	FODB	CN2A	45	CN2<45		
Vineyard	GRAP	CN2A	45			
MIXED GRASSLAND/SHRUBLAND	MIGS	CN2A	44			
MIXED FOREST	FOMI	CN2A	36			

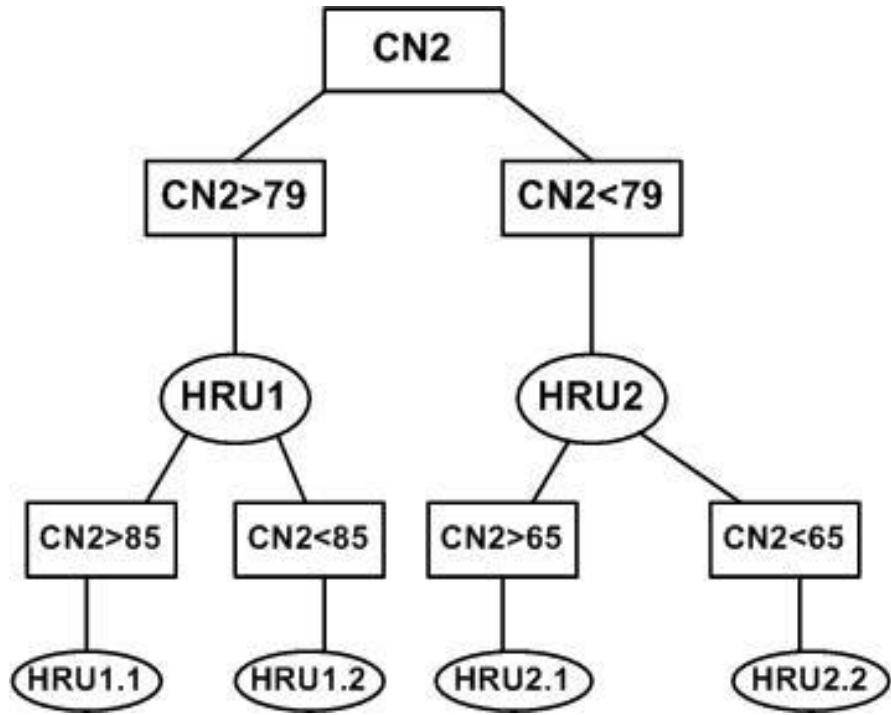


Figure 70 HRU division methodology for Namazgah Dam Basin

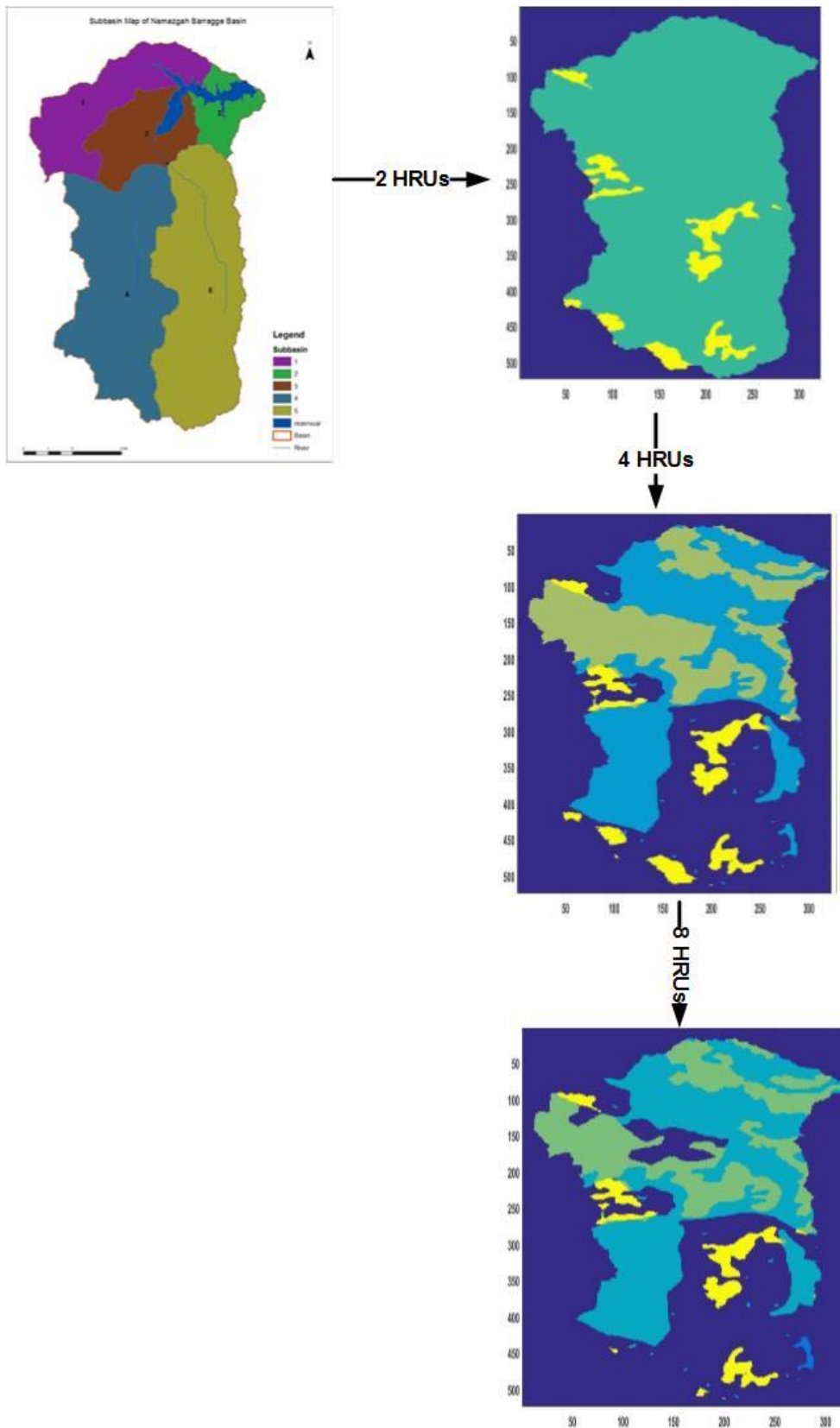


Figure 71 HRU type division based on CN2 on Namazgah Dam Basin.

4.6.3.1 Two-HRU Types which were created with respect to CN2 parameter results

Two-HRU type model was created in each of five subbasins resulting in eight HRUs. The initial run had $r^2=0.37$, NS=-1.47 (Figure 72). In order to increase model accuracy, the fastly calibrated SUFI-2 model was applied on the model by using 16 important parameters (Table 30). When 250 simulation count and 500 simulation counts were applied on the model for the calibration process (Table 31), 500 simulation count gave us better calibration results. The model improved to $r^2=0.71$, NS=0.71 after the calibration (Figure 73).

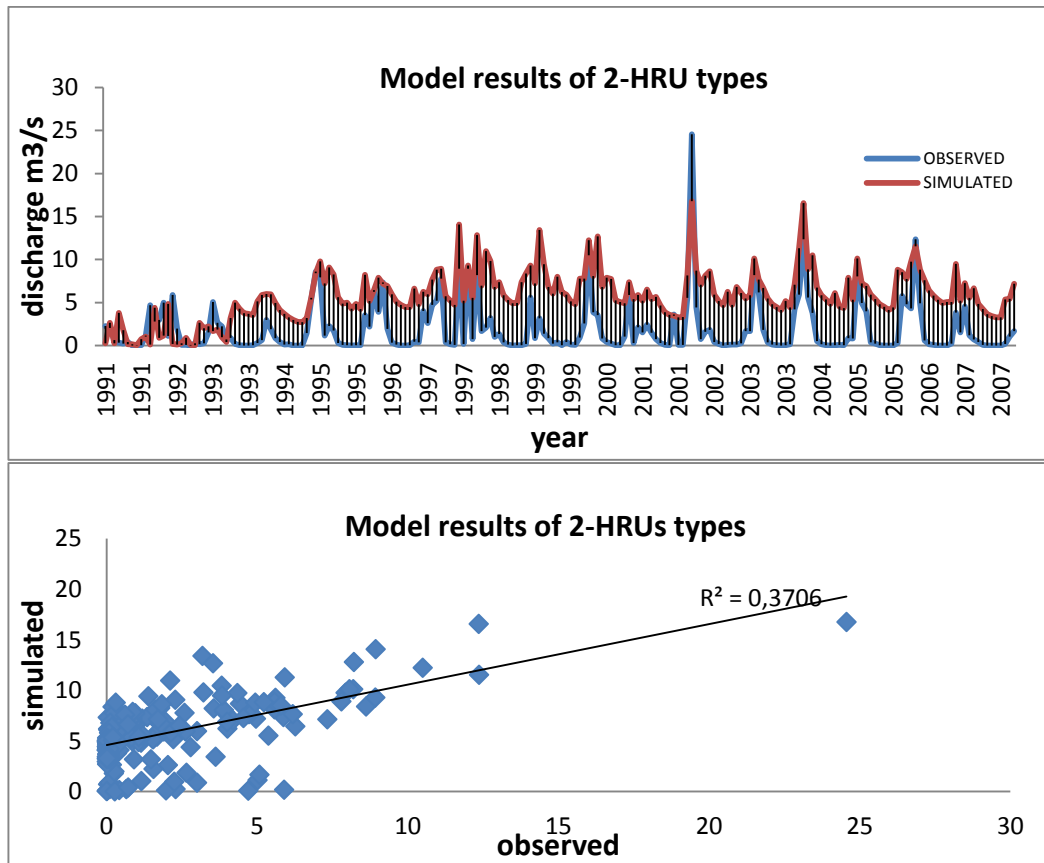


Figure 72 Model results of two-HRU types of Namazgah Dam Basin.

Table 30 Calibration parameters and their range

PARAMETERS	MIN VALUE	MAX VALUE	Definition	Process/ Layer
CN2	-0.2	0.2	Initial SCS runoff curve number	Surface runoff
SURLAG	0.05	24	Surface runoff lag time.	
SOL_AWC	-0.2	0.1	Available water capacity of the soil layer	Soil
SOL_K	-0.8	0.8	Saturated hydraulic conductivity (mm/hr)	
SOL_BD	-0.5	0.6	Moist bulk density (Mg/m ³ or g/cm ³)	
GWQMN	0	25	Threshold depth of water in the shallow aquifer required for return flow to occur (mm H ₂ O)	Baseflow
GW_REVAP	-0.1	0	Groundwater “revap” coefficient	
REVAPMN	0	500	Threshold depth of water in the shallow aquifer for “revap” or percolation to the deep aquifer to occur (mm H ₂ O)	
ALPHA_BF	0	1	Baseflow alpha factor (days)	
GW_DELAY	30	450	Groundwater delay time (days)	
ESCO	0.8	1	Soil evaporation compensation factor.	
SFTMP	-20	20	Snowfall temperature (°C)	Snow
SMTMP	-20	20	Snowmelt base temperature (°C)	
SMFMX	0	20	Melt factor for snow on June 21 (mm H ₂ O/°C-day)	
SMFMN	0	20	Melt factor for snow on December 21 (mm H ₂ O/°C-day)	
TIMP	0	1	Snow pack temperature lag factor.	

Table 31 Calibration results of 2 HRU types depending on simulation counts.

METOD	CN2							
	p-factor	r-factor	R2	NS	bR2	PBIAS	Mean(sim)	StdDev(sim)
2 HRUs TYPE (SM=250)	0,25	1,08	0,51	0,14	0,4336	54,80	1.90(2.95)	2.98(3.59)
2 HRUs TYPE (SM=500)	0,82	3,48	0,72	0,71	0,5713	-3,80	1.90(1.97)	2.98(2.80)

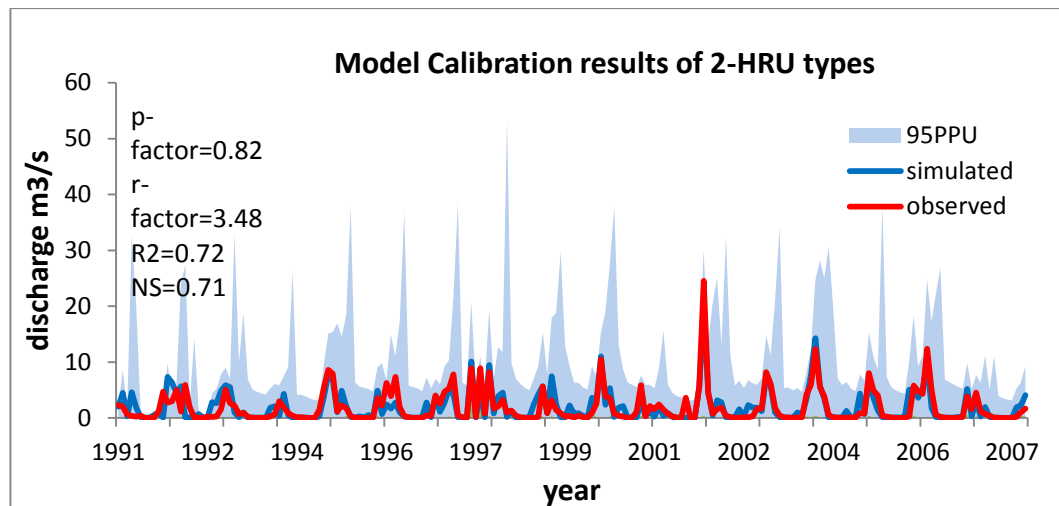


Figure 73 Model calibration results of two-HRU types which were divided according to CN2 values.

4.6.3.2 Four-HRU types which were created with respect to CN2 parameter results

In the later stage, we produced a four-HRUs model with initial results $r^2=0.43$, $NS=-0.79$ (Figure 74). 250 and 500 simulation count was applied on the model in order to see performance of the calibration during calibration (Table 32). The model improved to $r^2=0.74$ and $NS=0.74$ after the calibration if 500 simulation count was used (Figure 75).

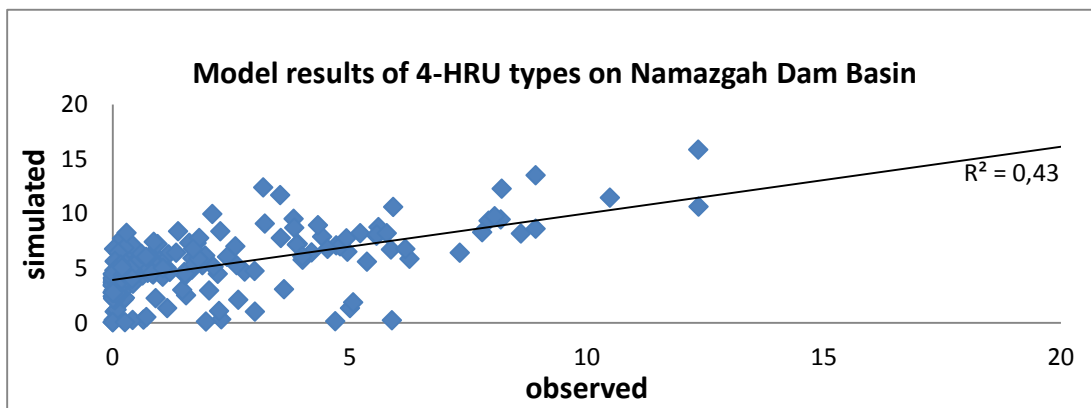
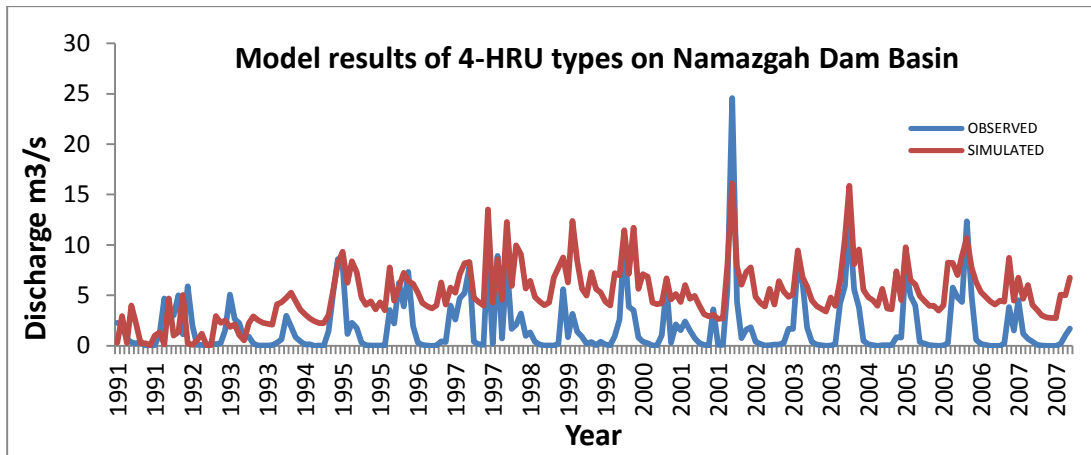


Figure 74 Model results of four-HRU types on Namazgah Dam Basin

Table 32 Calibration results of four-HRU types depending on simulation counts.

METOD	CN2							
	p-factor	r-factor	R2	NS	bR2	PBIAS	Mean(sim)	StdDev(sim)
4 HRUs TYPE (SM=250)	0,81	1,97	0,72	0,71	0,57	7,70	1.90(1.76)	2.98(2.81)
4 HRUs TYPE (SM=500)	0,66	1,67	0,74	0,74	0,58	3,80	1.90(1.83)	2.98(2.72)
4 HRUs TYPE (SM=250) int HRU	0,79	2,14	0,74	0,73	0,54	16,60	1.90(1.59)	2.98(2.58)

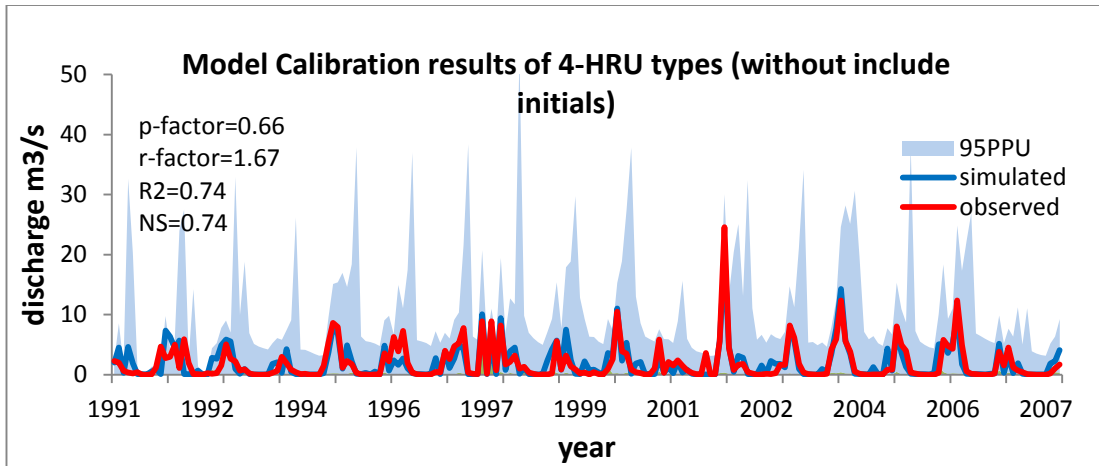


Figure 75 Calibration results of four-HRU types model on Namazgah Dam Basin (SM=500)

When the four-HRU type model was used with the calibrated parameters of the two-HRU type model, the model accuracy was $r^2=0.59$, NS=0.10 and improved to $r^2=0.74$ and NS=0.73 after calibration (Figure 76).

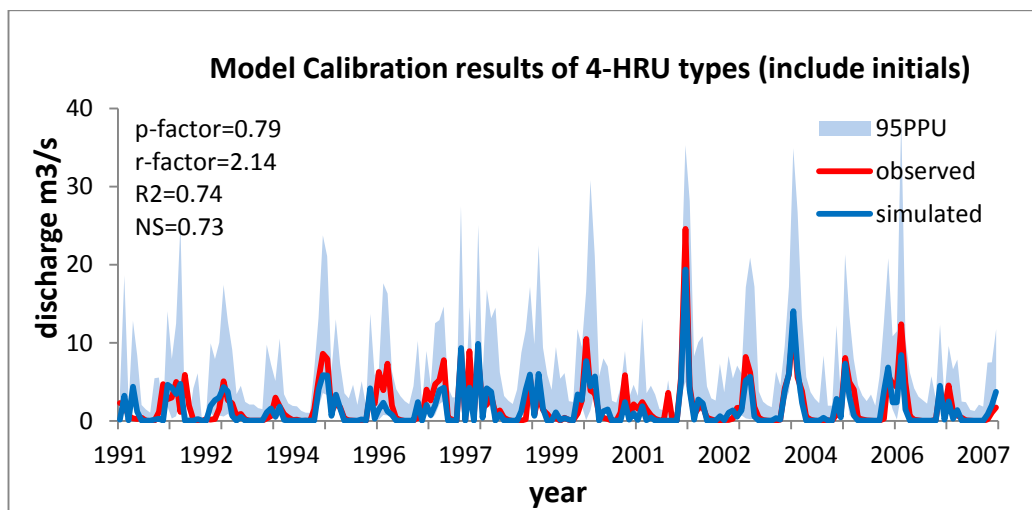


Figure 76 Model calibration results of four-HRU types (include initials)

4.6.3.2 Eight-HRU types which were created with respect to CN2 parameter results

In order to find optimum HRU numbers, eight-HRU type model was created. The model accuracy of eight-HRU types was initially $r^2=46$, NS= -0.14 (Figure 77). When the eight-HRU type model was calibrated by applying 100, 250, 500 and 1000 simulation count in order to decide which simulation count gave better the model accuracy (Table 33), 500 simulation count was gave best calibration results. Thus, the model improved to $r^2=73$ and NS=72 after the calibration (Figure 78).

Table 33 Calibration results of eight-HRU types model depending on simulation counts.

METOD	CN2							
	p-factor	r-factor	R2	NS	bR2	PBIAS	Mean(sim)	StdDev(sim)
8 HRUs TYPE (SM=100)	0,68	1,72	0,68	0,67	0,4929	14,30	1.90(1.63)	2.98(2.59)
8 HRUs TYPE (SM=250)	0,76	1,59	0,67	0,66	0,489	4,50	1.90(1.82)	2.98(2.65)
8 HRUs TYPE (SM=500)	0,8	1,88	0,73	0,72	0,5138	17,50	1.90(1.57)	2.98(2.45)
8 HRUs TYPE (SM=1000)	0,75	2,06	0,74	0,73	0,4944	9,10	1.90(1.73)	2.98(2.31)

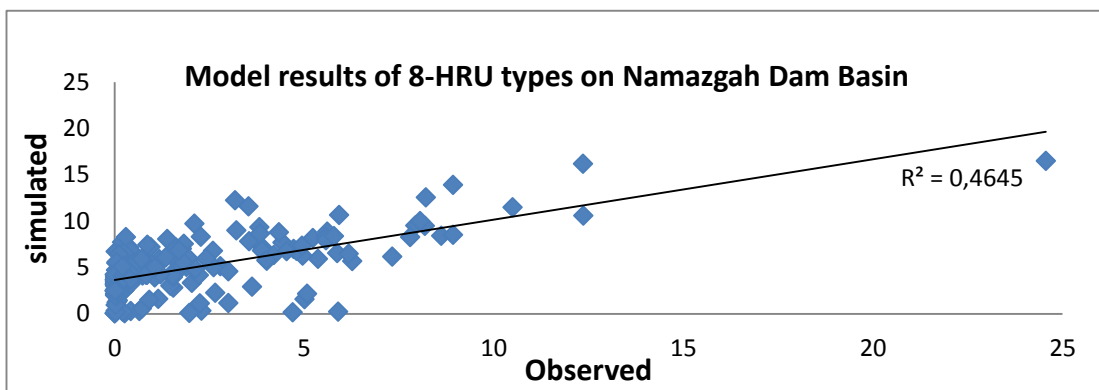
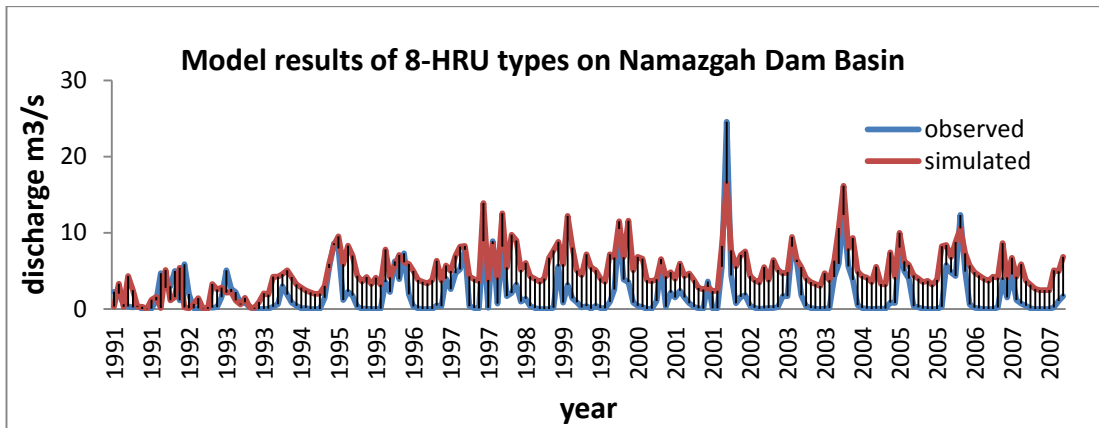


Figure 77 Model results of eight-HRU types on Namazgah Dam Basin

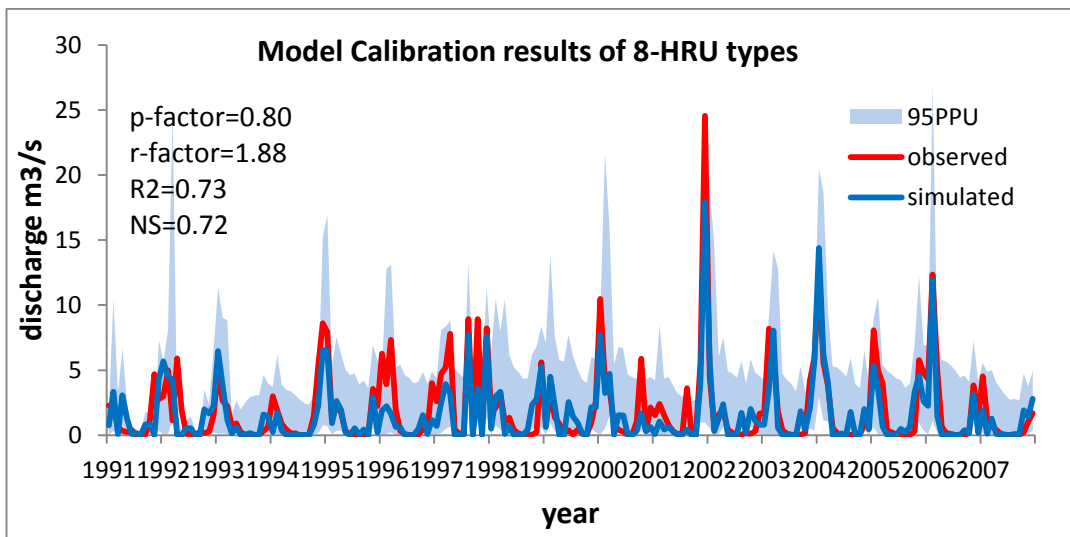


Figure 78 Calibration results of eight-HRU types model which are produced by division of CN2 (calibrated parameter values of 4 HRUs type model as initials for 8 HRUs).

CHAPTER 5

SUMMARY AND DISCUSSION

As the current HRU methodology in SWAT is based on user-defined thresholds of soil land use, and slope classification combinations, it may result in ignoring some important combinations, which may have great impact on hydrological process in a watershed. As a result, the model performance declines and calibration takes a long time. The error caused by lumping effects (Geza and McCray, 2008) is reduced by using small and relatively uniform HRUs, but it makes calibration more difficult and increases required computation time. In this work, we adopt a hierarchical approach, similar to many other optimization problems in order to increase performance and reduce computational complexity simultaneously. For hierarchical optimization, each sub-basin is divided into two-HRUs and optimize with respect to some important hydrological processes parameters. Then, each HRU is further divided into two. Each child HRU inherits the optimum parameters of the parent HRU as its initial values. Thus, we expect to decrease the total calibration time and increase the performance of the model.

Hierarchical approach to hydrological model was applied on two different test areas in Turkey with different hydrologic, topographic, hydrogeologic conditions. Although the maximum elevation in the Sarısu-Eylikler Basin is 2400 m, in Namazgah Dam Basin the maximum elevation is 320 m. There are 17 different soil types in Sarısu-Eylikler Basin. The most dominant soil types in the basin is Reddish-Chestnut and Limeless Brown soils. There are mostly agricultural, grarigue and pasture area in the basin. When assessed the area properties, the area represents heterogeneous properties. The characteristics of the area effects the choice of the HRU generation method. When SOL_K and CN2 parameters were chosen independently for division HRU types, the model performance was not so good. Since these parameters individually couldn't represent all hydrological processes in the watershed area, combination of these parameters which are CN2, SOL_K and slope classification was preferred.

Namazgah Dam Basin has more homogeneous properties than Sarısu-Eylikler Basin. The most dominant soil type is limeless brown forest soil, which has approximately %60 of the watershed area. There are two dominant land cover in the basin which are agricultural land and broad-leaved forest area, the areas of land cover are % 67.31 and %24.90, respectively. There are many karstic areas in Namazgah Dam Basin where groundwater is recharged from surface water (Altuntas et al., 2015). Since topography of the basin is distinct from Sarısu-Eylikler basin, the area of Namazgah Dam basin is smaller than Sarısu-Eylikler basin, moreover, Namazgah Dam basin shows homogenous characteristics, one important parameter for generating HRU types, CN2, can represent all hydrological processes in the watershed area. When four-HRU were separated further into two-HRU types in Sarısu-Eylikler Basin, total number of HRUs in the model did not increase much, and further division caused many gaps in the model. In other words, when eight-HRU types were generated, some combinations for producing HRU types were not in the most sub-basins. Although the model performance was getting worse, model calibration performance was getting better. This results show that the optimum division of HRU types should be four-HRUs for Sarısu-Eylikler Basin. With increasing complexity of the model, the uncertainties increase. Thus, more HRU types cause more uncertainties in the model (Table 34).

When CN2 division approach is tested in Namazgah Dam Basin, the model gives us better r^2 values from two-HRU to four-HRU. However, calibration results of two-HRU and four-HRU are approximately same. If we use calibrated parameter values of two-HRU for four-HRU as an initials, our model is getting better and computational time for calibration declines. If four-HRUs were divided into two children, model performance and calibration effort for eight-HRU were similar to four-HRUs since the total number of HRUs in the basin during generation of eight-HRU types didn't increase much. In other words, although the total HRU number of four-HRU type is 13, the total HRU number of eight-HRU types is 14. Thus, we stopped HRU division further because optimum HRU type division was eight (Table 35).

In the current HRU methodology, while trying to reach from simple to complex model with increasing HRU number, we got relatively same model results and calibration

performance. If we compare our HRU generation approach with the current methodology, Hierarchic HRU methodology gives us better model and calibration performance. When we need much more detailed hydrological models, especially for applying water management policy in the watershed, Hierarchical approach for HRU division gives us better model performance and easy calibration processes. It should be considered that before applying the methodology, the basin should be understood correctly with respect to its physical properties.

Table 34 Summary of results for Sarisu-Eylikler Basin.

Method	Total # of HRUs	Initial Model R², NS,PBIAS	After Calibration R², NS, PBIAS
ArcSWAT (Dominant land use/slope/soil)	7	0.33, -10, -164.669	0.36, 0.24, -27.5
ArcSWAT (25%/25%/50% threshold value for land use/soil/slope)	14	0.34, -10, -163.088	0.35, 0.32, -16.9
ArcSWAT (20%/20%/60% threshold value for land use/soil/slope)	21	0.34, -2.69, -161.168	0.36, 0.32, -42.5
CN2KS , 2 HRU types	13	0.32, -0.16, -2.07	0.50, 0.49, 3.8
CN2KS 4 HRU types	16	0.41, 0.11, 6.47	0.51, 0.51, 6.5
CN2KS 4 HRU types, initials from 2 HRU	16	0.53, 0.31, -4.14	0.59, 0.57, -4.1
CN2KS 8 HRU types,	18	0.21, -0.21, 9.36	0.56, 0.51, 8.6
CN2KS 8 HRU types, initials from 4 HRU	18	0.24, -0.10, -1.99	0.53, 0.52, -2.0

Table 35 Summary of results for Namazgah Dam Basin.

Method	Total # of HRUs	Initial Model R², NS, PBIAS	After Calibration R², NS, PBIAS
ArcSWAT (Dominant land use/slope/soil)	5	0.3784, -1.37, 39.22	0.69, 0.56, 32.1
ArcSWAT (20%/20%/60% threshold value for land use/soil/slope)	12	0.3755, -1.34, 38.47	0.70, 0.58, 30.9
ArcSWAT (10%/10%/80% threshold value for land use/soil/slope)	17	0.39, -1.33, 38.96	0.68, 0.57, 26.09
CN2, 2 HRU types	13	0.37, -1.47, -200.7	0.71, 0.71, -3.76
CN2 4 HRU types	13	0.43,-0.79, -167.35	0.73, 0.72, 7.7
CN2 4 HRU types, initials 2 HRU	13	0.59, 0.10, -103.25	0.74, 0.73, 16.6
CN2 8HRU types	14	0.46,-0.14,-156.41	0.73, 0.72, 17.5

CHAPTER 6

CONCLUSION

Hierarchical HRU approach to hydrological model calibration was developed in order to increase model performance and reduce computational complexity simultaneously. Although the first method for the approach is combination of parameters, second method for producing HRU types is one parameter division. The performance of the hierarchical methodology is shown on two basins: Sarisu-Eylikler Basin and Namazgah Dam Lake in Turkey. According to these methodologies, we have the following conclusions;

- 1- Combination of CN2, soil hydraulic conductivity and slope classification was chosen for first HRU generation method since these parameters may have great impact on hydrological processes in the watershed.
- 2- CN2 parameter was preferred for dividing HRU types.
- 3- First approach for generation HRU types gives better results in Sarisu-Eylikler Basin in contrast to the second method,
- 4- The model performance in the Basin improved from two to four-HRU types. Although, the model performance of the eight-HRU type did not improve the results, the computational time for calibration was reduced.
- 5- By using the second approach of hierarchical optimization, we reached better results on Namazgah Dam Basin. From the two-HRU type to the four-HRU type, the model performance increased and the computational complexity decreased.
- 6- The hydrological behavior is different in each study areas. Although surface runoff in Namazgah Dam Basin has mainly affected from land use variations, soil type, land use and topography are mainly affected hydrological processes in Sarisu-Eylikler Basin.

7-Each methodology for HRU generation gives us better results than the current HRU generation approach in SWAT.

8-Hierarchical approach to HRU generation is suitable for heterogeneous and large scale basins. When this approach is applied on small scale and homogeneous areas, one parameter should be preferred for hierarchical HRU generation method.

At the end of this study, developed methodology for generation HRU division in hydrological models can improve model accuracy and decrease computational complexity for calibration. Moreover, the results shows that further model complexity does not give more accurate model results. While using better available data, more accurate model prediction and smaller uncertainties can be reached by using the methodology. In the future, the proposed methodology should be applied on other semi-distributed models except from the SWAT model. In order to measure performance of the methodology, different optimization approach should be used.

REFERENCES

Abbaspour, K. C., Rouholahnejad, E., Vagnefi, S., Srinivasan, R., Yang, H., Love, B., 2015, A continental scale hydrology and water quality model for Europe: Calibration and uncertainty of high-resolution large scale SWAT model, *Journal of Hydrology* 524, 733-752.

Abbaspour, K. C., 2012 [interactive]. SWAT-CUP 2012: SWAT Calibration and Uncertainty Programs – A User Manual [previewed on 03 February 2014]. Available at: <http://www.neprashtechology.ca/Downloads/SwatCup/Manual/Usermanual_SwatCup.pdf>.

Abbaspour K. C., M. Vejdani, and S. Haghighat. 2007. SWATCUP calibration and uncertainty programs for SWAT. In Proc. Intl. Congress on Modelling and Simulation (MODSIM'07), 1603-1609. L. Oxley and D. Kulasiri, eds. Melbourne, Australia: Modelling and Simulation Society of Australia and New Zealand.

Abbott, M. B., J. C. Bathurst, A. Cunge, P. E. O'Connell, and J. Rasmussen. 1986. An introduction to the SHE 1: History and philosophy of a physically based, distributed modelling system. *J. Hydrol.* 87(1-2): 49-59.

Ardas, S., Creutzberg, D., 1995, Soil Reference Profiles of Turkey, Dept. of Soil Science-Faculty of Agriculture-Çukurova University, International Soil Reference and Information Centre, Country Report 3. Arnold, J.G., Srinivasan, R., Muttiah, R.S., Williams, J.R., 1998. Large area hydrologic modeling and assessment part I: model development. *Journal of the American Water Resources Association* 34 (1), 7389

Arnold, J.G., Allen, P.M., 1999. Automated methods for estimating base flow and ground water recharge from stream flow records. *Journal of the American Water Resources Association* 35 (2), 411–424.

Arnold, J.G., Fohrer, N., 2005. SWAT2000: current capabilities and research opportunities in applied watershed modeling. *Hydrol. Process.* 19 (3), 563–572.

Arnold, J.G., 2007. The soil and water assessment tool: historical development, applications, and future research directions. *Trans. ASABE* 50 (4), 1211–1250.

Arnold, J. G., Allen, P. M., Volk, M., Williams, J. R., Bosch, D. D., 2010, Assessment of different representations of spatial variability on SWAT model performance, *American Society of Agricultural and Biological Engineers*, Vo. 53(5),: 1433-1443.

Arnold, J. G., Moriasi, D. N., Gassman, P. W., Abbaspour, K. C., White, M. J., Srinivasan, R., Santhi, C., Harmel, R. D., Griensven, A., Liew, M. W. N., Jha, K., 2012, Soil & Water Division of ASABE

Ajami, N.K., Gupta, H., Wagener, T., Sorooshian, S., 2004. Calibration of a semidistributed hydrologic model for streamflow estimation along a river system. *Journal of Hydrology* 298 (1–4), 112–135.

Baker, T. J., Miller, N. S., 2013, Using the Soil and Water Assessment Tool (SWAT) to assess land use impact on water resources in an East African watershed, *Journal of Hydrology*, 486, 100-111.

Balascio, C. C., D. J. Palmeri, and H. Gao. 1998. Use of a genetic algorithm and multi-objective programming for calibration of a hydrologic model. *Trans. ASAE* 41(3): 615-619.

Beck, M.B., 1987. Water quality modeling: a review of the analysis of uncertainty. *Water Resour. Res.* 23 (8), 1393–1442.

Bedient, P.B., Huber, W.C., 1992. *Hydrology and Floodplain Analysis*, 2nd edition. Addison-Wesley Publishing Company. 692 pp.

Beven, K. J., and M. J. Kirby. 1979. A physically based variable contributing area model of basin hydrology. *Hydrol. Sci. Bull.* 24(1): 43-69.

Beven, K., Binley, A., 1992. The future of distributed models – model calibration and uncertainty prediction. *Hydrological Processes* 6 (3), 279–298.

Beven, K.J., 2000. *Rainfall–Runoff Modeling: The Primer*. John Wiley & Sons Press, New York.

Beven, K.J., Freer, J., 2001. Equifinality, data assimilation, and uncertainty estimation in mechanistic modeling of complex environmental systems. *Journal of Hydrology* 249, 11–29.

Beven, K.J., 2006. A manifesto for the enquiringly thesis. *Journal of Hydrology* 320, 18–36.

Bronstert, A., and E. J. Plate. 1997. Modelling of runoff generation and soil moisture dynamics for hillslopes and micro catchments. *J. Hydrol.* 198: 177-195.

Brown, D.G., Bian, L., Walsh, S.J., 1993. Response of a distributed watershed erosion model to variations in input data aggregation levels. *Computers and Geosciences* 19 (4), 499–509.

Butts, M.B., Payne, J.T., Kristensen, M., Madsen, H., 2004a. An evaluation of the impact of model structure on hydrological modelling uncertainty for streamflow simulation. *Journal of Hydrology* 298, 222–241.

Burrough, P. A. (1996). Opportunities and limitations of GIS-based modeling of solute transport at the regional scale. In application of GIS to the non-point source pollutants in the vadose zone, SSSA, Special Publication 48, D. Corning and K. Loague eds., Madison, WI.

Butts, M.B., Payne, J.T., Overgaard, J., 2004b. Improving streamflow simulations and flood forecasting with multimodel ensemble. In: Liang, P.B. (Ed.), 6th International Conference on Hydroinformatics. World Scientific Publishing, Singapore

Chaplot, V., 2005. Impact of DEM mesh size and soil map precision for the prediction of water, sediment and NO₃ loads in a watershed. *Journal of Hydrology* 312, 207–222.

Chen R, Pi L, Hsieh C. 2005. Application of parameter optimization method for calibrating tank model. *Journal of American Water Resources Association* 41(2): 389–402.

Chiew, F. H. S., M. J. Stewardson, and T. A. McMahon. 1993. Comparison of six rainfall runoff modeling approaches. *J. Hydrol.* 147: 1- 36.

Cooper VA, Nguyen VTV, Nicell JA. 1997. Evaluation of global optimization methods for conceptual rainfall-runoff model calibration. *Water Science Technology* 36(5): 53–60.

Duan, Q., S. Sorooshian, and V. K. Gupta. 1992. Effective and efficient global optimization for conceptual rainfall- runoff models. *Water Resources Res.* 28(4): 1015-1031.

Easton, M. Z., Fuka, D. R., Walter, M. T., Cowan, D. M., Schneinderman, E. M., Steenhuis, T. S., 2008, Re-conceptualizing the soil and water assessment toll (SWAT) model to predict runoff from variable source areas, *Journal of Hydrology*, 348,279-291.

Engel B., D. Storm, M. White, and J. G. Arnold. 2007. A hydrologic/water quality model application protocol. *J. American Water Resources Assoc.* (in press).

Faramarzi, M., K. C. Abbaspour, R. Schulin, and H. Yang. 2009. Modeling blue and green water availability in Iran. *Hydrol. Proc.* 23(3): 486-501.

Faramarzi, M., Srinivasan, R., Irvani, M., Bladon, K. D., Abbaspour, K. C., Zehnder, A. J. B., Goss, G., 2015, Setting up a hydrological model of Alberta: Data discrimination analyses prior to calibration, *Environmental Modeling&Software*, V 74, p 48-65.

Fenicia, F., Kavetski, D., Saveije, H. H. G., Pfister, L., (2016), From spatially variable hydrological models: Analysis of key modelling decisions, *Water Resources Research*. DOI: 10.1002/2015WR017398

Levick, L.R., Semmens, D.J., Guertin, D.P., Burns, I.S., Scott, S.N., Unkrich, C.L., Goodrich, D.C., 2004. Adding global soils data to the automated geospatial watershed assessment tool (AGWA). *Second International Symposium on Transboundary Waters Management, Tucson, AZ, 2004 November 16–19. CD Proceedings*, 8 pp.

Gassman, P.W., Reyes, M.R., Green, C.H., Arnold, J.G., 2007. The soil and water assessment tool: historical development, applications, and future research directions. *Trans. ASABE* 50 (4), 1211–1250.

Galbiati, L., Bouraoui, F., Elorza, F.J., Bidoglio, G., 2006. Modeling diffuse pollution loading into a Mediterranean lagoon: development and application of an integrated surface subsurface model tool. *Ecol. Model.* 193 (1–2), 4–18.

Geza, M., and McCray, J. E., 2008, Effects of soil data resolution on SWAT model stream flow and water quality predictions, *Journal of Environmental Management*, 88, 393-406.

Govender, M., and C. S. Everson. 2005. Modelling streamflow from two small South African experimental catchments using the SWAT model. *Hydrol. Proc.* 19(3): 683-692.

Gupta, H. V., S. Sorooshian, and P. O. Yapo. 1998. Toward improved calibration of hydrologic models: Multiple and noncommensurate measures of information. *Water Resources Res.* 34(4): 751-763.

Kirkby, M. J. 1998. Modelling across scales: The MEDALUS family of models. In *Modelling Soil Erosion by Water*, 161-173. J. Boardman and D. Favis- Mortlock, eds. Berlin, Germany: Springer/Verlag.

Krysanova, V., D. I. Muller, Wohlfeil, and A. Becker. 1998. Development and test of a spatially distributed hydrological/water quality model for mesoscale watersheds. *Ecol. Model.* 106(2-3): 261-289.

Lane, L. J., and M. A. Nearing, eds. 1989. USDA Water Erosion Prediction Project: Hillslope profile model documentation. NSERL Report No. 2. West Lafayette, Ind.: USDA/ARS National Soil Erosion Research Laboratory.

Jha MK, Kumar A, Nanda G, Bhatt G. 2006. Evaluation of traditional and nontraditional optimization techniques for determining well parameters from step-drawdown test data. *Journal of Hydrological Engineering* 11(6): 617–630.

Jung BS, Karney BW. 2006. Hydraulic optimization of Transient protection devices using GA and PSO approaches. *Journal of Water Resources Planning and Management* 132(1): 44–52.

Jürgen, S., Abbaspour, K.C., Srinivasan, R., Yang, H., 2008, Estimation of freshwater availability in the West African sub-continent using the SWAT hydrologic model, *Journal of Hydrology*, V: 35, p: 30-49.

Harbaugh AW, McDonald MG. User's for MODFLOW-96, an update to the U.S. Geological Survey modular finite-difference ground-water model. U.S. Geol. Surv. Open-File Rep; 1996. p. 96-485.

Huang, F., Wang, X., Lou, L., Zhou., Wu, J., 2010, Spatial variation and source apportionment of water pollution in Qiantang River (China) using statistical techniques, *Water Research* 44 (2010) 1562 – 1572

Ke, K.Y., 2013, Application of an integrated surface water-groundwater model to multi-aquifers modeling in Choushui River alluvial fan, Taiwan, *Hydrol. Process.* (2013), DOI: 10.1002/hyp.9678

Khakbaz, B., Imam, B., Hsu, K., Sorooshian, S., 2012, from lumped to distributed via semi-distributed: Calibration strategies for semi-distributed models. *Journal of Hydrology* 418-419 (2012), 61-77.

Khu, S. T., and Madsen. H., 2005. Multiobjective calibration with Pareto preference ordering: An application to rainfall/runoff calibration. *Water Resources Res.* 41: W03004, doi: 10.1029/2004WR003041.

Knisel, W.G., 1980, CREAMS, A field scale model for chemicals, runoff, and erosion from agricultural management systems. US Dept. Agric. Conserv. Res. Rept. No. 26.

Ko, C., Chenga, Q., 2004, GIS spatial modeling of river flow and precipitation in the Oak Ridges Moraine area, Ontario, *Computers & Geosciences* 30 (2004) 379–389.

Koren, V., Reed, S., Smith, M., Zhang, Z., Seo, D.-J., 2004. Hydrology laboratory research modeling system (HL-RMS) of the US national weather service. *Journal of Hydrology* 291, 297–318.

Kuczera G. 1997. Efficient subspace probabilistic parameter optimization for catchment models. *Water Resources Research* 33(1): 177–185.

Lenhart, T., Eckhardt, K., Fohrer, N., Frede, H.-G., 2002, Comparison of two different approaches of sensitivity analysis, *Physics and Chemistry of the Earth* 27 (2002) 645–654

Ley, T.W., Stevens, R.G., Topielec, R.R., Neibling, W.H., Soil Water Monitoring and Measurement, Pacific Northwest Cooperative Extension Bulletin – PNW0475, December 1994. (<http://cru.cahe.wsu.edu/CEPublications/pnw0475/pnw0475.html>; last access January 2005)

Liebetrau, A.M. and Doctor P.G., 1987. Uncertainty Analysis for Performance Assessments of Radioactive Waste Disposal Systems. Nuclear Energy Agency, OECD.

Ma, L., J. C. Ascough II, L. R. Ahuja, M. J. Shaffer, J. D. Hanson, and K. W. Rojas. 2000. Root Zone Water Quality Model sensitivity analysis using Monte Carlo simulation. *Trans. ASAE* 43(4): 883-895.

Marshall, L., Nott, D., Sharma, A., 2004. A comparative study of Markov chain Monte Carlo methods for conceptual rainfall– runoff modeling. *Water Resources Research* 40, W02501. doi:10.1029/2003WR002378.

Marquardt, D. W., 1963, “An algorithm for least-squares estimation of nonlinear parameters,” *Journal of the Society for Industrial and Applied Mathematics*, 11(2):431-441.

McKay, M. D., W. J. Conover and R. J. Beckman. 1979. A Comparison of Three Methods for Selecting Values of Input Variables in the Analysis of Output from a Computer Code. *Technometrics* 21: 239-245.

Menking, K.M., Syed, K.H., Anderson, R.Y., Shafike, N.G., Arnold, J.G., 2003. Model estimates of runoff in the closed, semiarid Estancia basin, central New Mexico, USA. *Hydrol. Sci. J.* 48 (6), 953–970.

Menking, K.M., Anderson, R.Y., Shafike, N.G., Syed, K.H., Allen, B.D., 2004. Wetter or colder during the last glacial maximum Revisiting the pluvial lake question in southwestern North America. *Quart. Res.* 62 (3), 280–288.

Moriasi, D. N., Arnold, J. G., Van Liew, M. W., Bingner, R. L., Harmel, R. D., Veith, T. L., 2007. Model Evaluation Guidelines for Systematic Quantification Of Accuracy In Watershed Simulations, *American Society of Agricultural and Biological Engineers*, Vol. 50(3): 885–900.

Motovilov, Y. G., L. Gottschalk, K. England, and A. Rodhe. 1999. Validation of distributed hydrological model against spatial observations. *Agric. Forest Meteorology* 98-99: 257-277.

Muleta, M.K., Nicklow, J.W., 2005. Sensitivity and uncertainty analysis coupled with automatic calibration for a distributed watershed model. *Journal of Hydrology* 306, 127–145.

Nash, J.E., Sutcliffe, J.V., 1970. River flow forecasting through conceptual models, part 1—a discussion of principles. *Journal of Hydrology* 10 (3), 282–290.

Neitsch, S.L., Arnold, J.G., Kiniry, J.R., Williams, J.R., 2005a. Soil and water assessment tool theoretical documentation, Version 2005, USDA.ARS Grassland, Soil and Water Research Laboratory, Temple, TX. Available at: <www.brc.tamus.edu/swat/doc.html> (accessed 01.11.2006.).

Neitsch, S.L., Arnold, J.G., Kiniry, J.R., Srinivasan, R., Williams, J.R., 2005b. Soil and water assessment tool input/output file documentation, Version 2005, USDA.ARS Grassland, Soil and Water Research Laboratory, Temple, TX. Available at: <www.brc.tamus.edu/swat/doc.html> (accessed 01.11.2006.).

Neitsch, S.L., Arnold, J.G., Kiniry, J.R., Williams, J.R., 2011. Soil and water assessment tool theoretical documentation, Version 2009, Agricultural Research Service Blackland Research Center, Texas Agrilife Research, Texas Water Resources Institute Technical Report no: 406, Texas A&M University System College Station, Texas.

Razavi, S., B. A. Tolson, L. S. Matott, N. R. Thomson, A. MacLean, and F. R. Seglenieks. 2010. Reducing the computational cost of automatic calibration through model preemption. *Water Resour. Res.* 46: W11523, doi: 10.1029/2009WR008957.

Refsgaard, J. C. 1997. Parameterisation, calibration, and validation of distributed hydrological models. *J. Hydrol.* 198(1): 69-97.

Rosewell, C.J., 1993, SOILOSS Technical Handbook, No.11, 2nd Edition.

Santhi, C, J. G. Arnold, J. R. Williams, W. A. Dugas, R. Srinivasan, and L. M. Hauck. 2001. Validation of the SWAT model on a large river basin with point and nonpoint sources. *J. American Water Resources Assoc.* 37(5): 1169-1188.

SCS (now NRCS). *Urban Hydrology for Small Watersheds*. US Dept. of Agric., Soil Conservation Service. 156 pgs. 1986.

Schuol, J., K. C. Abbaspour, H. Yang, R. Srinivasan, and A. J. B. Zhender. 2008b. Modeling blue and green water availability in Africa. *Water Resour. Res.* 44: W07406, doi: 10.1029/2007WR006609.

Setegn, S. G., R. Srinivasan, and B. Dargahi. 2009. Hydrological modelling in the Lake Tana basin, Ethiopia, using SWAT model. *Open Hydrol. J.* 2: 49-62.

Shafike, N.G., Flanigan, K.G., 1999. Hydrologic modeling of the Estancia basin, New Mexico. In: *New Mexico Geological Soc. Guidebook, 50th Field Conference, Albuquerque Geology, 409418*, New Mexico Geological Society, Socorro, New Mexico, USA.

Sharpley, A.N., Kleinman, P.J.A., McDowell, R.W., Gitau, M., Bryant, R.B., 2002. Modeling phosphorus transport in agricultural watersheds: processes and possibilities. *J. Soil Water Conserv.* 57 (6), 425–439.

Sorooshian S, Duan Q, Gupta VK. 1993. Calibration of rainfall runoff models: application of global optimization to the Sacramento soil moisture accounting model. *Water Resources Research* 29: 1185–1194.

Van Griensven, A., Meixner, T., 2006. Methods to quantify and identify the sources of uncertainty for river basin water quality models. *Water Science and Technology* 53 (1), 51–59

Vrugt JA, Gupta HV, Bouten W, Sorooshian S., 2003. A Shuffled Complex Evolution Metropolis algorithm for optimization and uncertainty assessment of hydrologic model parameters. *Water Resources Research* 39(8): 1201, DOI: 10.1029/2002WR001642.

Williams J.R., 1995. Chapter 25: The EPIC model. In V.P. Singh (ed) *Computer models of watershed hydrology*. Water Resources Publication, 909-1000.

Winchell, M., Srinivasan, R., Di Luzio, M. and Arnold, J. (2013) ArcSWAT (2013) interface for SWAT 2012 – User’s guide. Blackland Research and Extension Center Texas Agrilife Research & Grassland, Soil and Water Laboratory USDA Agricultural Research Service, Available at: Temple, Texas, USA.

Wischmeier, W.H., Smith, D.D., 1978, Predicting rainfall losses: A guide to conservation planning, USDA Agricultural Handbook No. 537. U.S. Gov. Print. Office, Washington, D. C.

Wischmeier, W.H., Smith, D.D., 1965, Predicting rainfall-erosion losses from cropland east of the Rocky Mountains, Agriculture Handbook 282, USDA-ARS.

Yang, J., Reichert, P., Abbaspour K.C., Xia J., Yang H., 2008. Comparing uncertainty analysis techniques for a SWAT application to the Chaohe Basin in China, Journal of Hydrology 358, 1– 23

Zhang, W., Montgomery, D.R., 1994. Digital elevation model grid size, landscape representation, and hydrologic simulations. Water Resources Research 30 (4).

Zhang, X., Srinivasan, R., Van Liew M., 2008, Multi- Site Calibration of the Swat Model for Hydrologic Modeling, American Society of Agricultural and Biological Engineers, Vol. 51(6): 2039-2049

Zhang, X., R. Srinivasan, and F. Hao. 2007. Predicting hydrologic response to climate change in the Luohe River basin using the SWAT model. Trans. ASABE 50(3): 901-910.

Zhang, X., R. Srinivasan, B. Debele, and F. Hao. 2008a. Runoff simulation of the headwaters of the Yellow River using the SWAT model with three snowmelt algorithms. J. American Water Resources Assoc. 44(1): 48- 61.

Zhang, X., R. Srinivasan, K. Zhao, and M. Van Liew. 2008b. Evaluation of global optimization algorithms for parameter calibration of a computationally intensive hydrologic model. Hydrol. Process. (in press)

Van Liew, M. W., and J. Garbrecht. 2003. Hydrologic simulation of the Little Washita River experimental watershed using SWAT. J. American Water Resour. Assoc. 39(2): 413-426.

Vrugt JA, Gupta HV, Bouten W, Sorooshian S. 2003. A Shuffled Complex Evolution Metropolis algorithm for optimization and uncertainty assessment of hydrologic model parameters. Water Resources Research 39(8): 1201, DOI: 10.1029/2002WR001642.

Wang G, Guo X, Shen Y, Cheng G. 2003. Evolving landscapes in the headwaters area of the Yellow River (China) and their ecological implications. *Landscape Ecology* 18: 363–375.

Williams, J.R., Nicks, A.D., Arnold, J.G., 1985. SWRRB, Simulator for water resources in rural basins. *J. Hydrol. Eng. ASCE* 111 (6), 970–986.

Wischmeier, W.H., Smith, D.D. 1965. Predicting rainfall-erosion losses from cropland east of the Rocky Mountains. *Agriculture Handbook* 282. USDA-ARS.

Wischmeier W.H., Smith D.D., 1978. Predicting rainfall erosion losses. *Agr. Handbook* 537, USDA, Washington D.C.

Pereira, A. and Broed, R., 2006, *Methods for Uncertainty and Sensitivity Analysis. Review and recommendations for implementation in Ecolego*, Dept. of Physics, AlbaNova University Center, Stockholm Center of Physics, Astronomy and Biotechnology, Stockholm, Sweden.

Zhang, W., Montgomery, D.R., 1994. Digital elevation model grid size, landscape representation, and hydrologic simulations. *Water Resources Research* 30, 1019–1028.

Yang, J., Abbaspour, K.C., Reichert, P., 2005, Interfacing SWAT with systems analysis tools: a generic platform. In: Srinivasan, R., Jacobs, J., Day, D., Abbaspour, K. (Eds.), *Third International SWAT Conference Proceedings*, July 11–15, Zurich, Switzerland. pp. 169–178.

Yang, J., Reichert, P., Abbaspour, K.C., Yang, H., 2007a. Hydrological modelling of the Chaohe Basin in China: statistical model formulation and Bayesian inference. *Journal of Hydrology* 340, 167–182.

Yang, J., Reichert, P., Abbaspour, K.C., 2007b. Bayesian uncertainty analysis in distributed hydrologic modeling: a case study in the Thur River basin (Switzerland). *Water Resources Research* 43, W10401. doi:10.1029/2006WR005497.

APPENDICES

A: Full Automatic version of SUFI 2

START Function

```
clear all,
clc

cd('C:\Hru_5_calibration_HRU4_initial');

% number of possible parameters in SWAT

count=input('simulationCount: ');
parametreAraligi=1:3;
hesapla2(parametreAraligi,count);

fid=fopen('\SUFU-2.OUT\summary_stat.txt', 'r');
bestgoal=textscan(fid, '%*s %*s %*s %*s %*s %*s %*s %*s %*s %*f');
    r2=bestgoal{1,1};
    fclose(fid);
saveas (figure(1),'ilktur.jpg')
if r2<1;
    parametreAraligi=4:10;
    hesapla2(parametreAraligi,count);
    saveas (figure(1),'ikincitur.jpg')
end
if r2<1;
    parametreAraligi=11:16;
    hesapla2(parametreAraligi,count);
    saveas (figure(1),'ucuncutur.jpg')
end
```

Main Function

```
function hesapla3(parametreAraligi,count)
```

```
npar = 17;
par(1).name='r__CN2.mgt';
par(1).min=-0.4;
par(1).max=0.2;
par(2).name='r__SOL_AWC().sol';
par(2).min=-0.3;
par(2).max=0.1;
par(3).name='r__SOL_K().sol';
par(3).min=-0.8;
par(3).max=0.8;
par(4).name='r__SOL_BD().sol';
par(4).min=-0.5;
par(4).max=0.6;
par(5).name='a__GWQMN.gw';
par(5).min=0;
par(5).max=25;
par(6).name='a__GW_REVAP.gw';
par(6).min=-0.1;
par(6).max=0;
par(7).name='v__REVAPMN.gw';
par(7).min=0;
par(7).max=500;
par(8).name='v__ALPHA_BF.gw';
par(8).min=0;
par(8).max=1;
par(9).name='v__GW_DELAY.gw';
par(9).min=30;
par(9).max=450;
par(10).name='v__ESCO.hru';
par(10).min=0.8;
par(10).max=1;
par(11).name='v__SFTMP.bsn';
par(11).min=-20;
par(11).max=20;
par(12).name='v__SMTMP.bsn';
par(12).min=-20;
par(12).max=20;
par(13).name='v__SMFMX.bsn';
par(13).min=0;
par(13).max=20;
```



```

par(14).name='v__SMFMN.bsn';
par(14).min=0;
par(14).max=20;
par(15).name='v__TIMP.bsn';
par(15).min=0;
par(15).max=1;
par(16).name='v__SURLAG.bsn';
par(16).min=0.05;
par(16).max=24;

for ix=1:npar
par(ix).opt=false;
end

minArrayElement=min(parametreAraligi);
maxArrayElement=max(parametreAraligi);

for paramIndex=minArrayElement:maxArrayElement
par(paramIndex).opt=true;
end

% run SWAT once

p = SUFI-2_func1(par, count);

% find initial NSR
fid=fopen('\SUFU-2.OUT\summary_stat.txt', 'r');
cd('C:\Calibration_HRU_8_SOL_SLP_CN');
fid=fopen('\SUFU-2.OUT\summary_stat.txt', 'r');
bestgoal=textscan(fid, '%*s %*s %*s %*s %*s %*s %*s %f');
NSR=bestgoal{1,1};
PBIAS=textscan(fid, '%*s %*s %*s %*s %*s %*s %*s %*s %f');
PBIAS1=PBIAS{1,1};
HATA=PBIAS1(2,1);
fclose(fid);

old_NSR=NSR;
new_NSR=1;

```

```

old_HATA=HATA;
new_HATA=0;

cmap = rand(20, 3);
figure(1)
clf
subplot(3, 1, 1)
hold on
subplot(3, 1, 2)
hold on
subplot(3, 1, 3)
hold on

countloop = 0;
while (new_NSR > old_NSR+ 0.001) || (countloop < 15)
    % prepare par_inf.txt
    if exist ('\SUFU-2.OUT\new_pars.txt', 'file')
        fid1=importdata('\SUFU-2.OUT\new_pars.txt');
        num_params=size(fid1.textdata,1)-2;
        fileID=fopen('SUFU-2.IN/par_inf.txt','w');
        fprintf(fileID, '%d %s \r\n', num_params, ': Number of Parameters (the program only reads the
first 4 parameters or any number indicated here)');
        fprintf(fileID, '%d %s \r\n', count, ': number of simulations');
        fprintf(fileID, '\r\n');
        minv=fid1.data(:,1);
        maxv=fid1.data(:,2);
        for param_no = 1:num_params
            fprintf(fileID, '%s %6.2f %6.2f \r\n', fid1.textdata{param_no+2}, minv(param_no),
maxv(param_no));
        end
        fclose(fileID);
        system('ayfer.bat', '-echo')
    else
        fprintf('Dosya içeriği boş');
        break
    end

figure(1)

```

```

subplot(3, 1, 1)
plot(countloop, NSR, '*');
title('NSR'), xlabel('Iteration number'), ylabel('NSR Value');
subplot(3, 1, 2)
plot(countloop, HATA, '*');
title('PBIAS'), xlabel('Iteration number'), ylabel('PBIAS Value')
subplot(3, 1, 3)
title('Parameter Range'), xlabel('Iteration number'), ylabel('Parameter Range')

for ix=1:num_params
    line([countloop+0.01*ix countloop+0.01*ix], [minv(ix) maxv(ix)], 'Color', cmap(ix, :))
end

countloop = countloop + 1;

% read r2
fid=fopen('\SUF1-2.OUT\summary_stat.txt', 'r');
bestgoal=textscan(fid, '%*s %*s %*s %*s %*s %*s %*s %f');
NSR=bestgoal{1,1};
PBIAS=textscan(fid, '%*s %*s %*s %*s %*s %*s %*s %*s %*s %f');
PBIAS1=PBIAS{1,1};
HATA=PBIAS1(2,1);
fclose(fid);

old_HATA=new_HATA;
new_HATA=HATA;

old_NSR=new_NSR;
new_NSR=NSR;

if new_NSR<old_NSR;
    continue
elseif new_NSR >old_NSR || new_NSR ==old_NSR;
    break
end

end

```

```
UpdateBackUp;
```

```
subplot(3, 1, 1)
```

```
hold off
```

```
subplot(3, 1, 2)
```

```
hold off
```

```
subplot(3, 1, 3)
```

```
hold off
```

```
end
```

SUFI-2_func1 Function

```
function p = SUFI-2_func1(prm, simulationCount)
```

```
%For each simulation, generate swat model output files
```

```
p = prm;
```

```
nprm = size(prm,2);
```

```
num_params = 0;
```

```
for ix=1:nprm
```

```
if prm(ix).opt
```

```
    num_params = num_params + 1;
```

```
    min_values(num_params) = prm(ix).min;
```

```
    max_values(num_params) = prm(ix).max;
```

```
    params{num_params} = prm(ix).name;
```

```
end
```

```
end
```

```
fileID=fopen('SUFI-2.IN/par_inf.txt', 'w');
```

```
fprintf(fileID,'%d %s \r\n', num_params, ': Number of Parameters (the program only reads the first 4  
parameters or any number indicated here');
```

```
fprintf(fileID,'%d %s \r\n', simulationCount, ': number of simulations');
```

```

fprintf(fileID, '\r\n');

for param_no = 1:num_params

    fprintf(fileID, '%s %6.2f %6.2f \r\n', char(params(param_no)), min_values(param_no),
max_values(param_no));
end

fclose(fileID);

%generate def file
DEF_ID=fopen('.\SUF2-swEdit.def', 'w');
starting=1;
fprintf(fileID, '%d %s \r\n', starting, ' : starting simulation number');
fprintf(fileID, '%d %s \r\n', simulationCount, ' : ending simulation number');
fprintf(fileID, '\r\n');
fclose(DEF_ID);

% call latin hypercube
% it uses par_inf.txt, trk.txt
fprintf('Running the latin hypercube executable SUFI-2_LH_sample.exe\r\n');
answer_fid = fopen('ayfer_1.txt', 'w');
fprintf(answer_fid, 'Y\r\n');
system('SUF2-LH-sample.exe < ayfer_1.txt', '-echo');
fclose(answer_fid);
system('del ayfer_1.txt', '-echo');
fprintf('Latin hypercube executable run completed\r\n');

%call SUFI-2_make_input
%It uses trk.txt, par_inf.txt, par_val.txt
%system('SUF2-make_input.exe');
%Output files in ECHO\echo_make_par_txt
%Output files model.in

%call SUFI-2_execute.exe
%It uses SUFI-2_extract_*.def, outout.*, SUFI-2.IN\var_file_*.txt, SUFI-2.IN\trk.txt, SUFI-
2.IN\observed*.txt
system('start /w SUFI-2_execute.exe')

```

```

system('start /w SUFI-2_extract_rch.exe')

%call SUFI-2_goal_fn.exe
system('start /w SUFI-2_goal_fn.exe')
%Output files ar Echo\echo_goal_fn.txt, SUFI-2.OUT\*.*, SUFI-2.OUT\goal.txt, SUFI-
2.OUT\best_sim.txt,
%SUFI-2.OUT\best_par.txt, SUFI-2.OUT\beh_pars.txt, SUFI-2.OUT\best_sim_nr.txt

system('start /w SUFI-2_95ppu.exe')
%It uses SUFI-2.IN\par_inf.txt, files listed in var_file_rch.txt, SUFI-2.IN\observed.txt, SUFI-
2.IN\var_file_rch.txt
%output files of its are Echo\echo_95ppu.txt, SUFI-2.OUT\95ppu.txt, SUFI-
2.OUT\summary_stat.txt,
%SUFI-2.OUT\best_sim.txt, SUFI-2.OUT\best_par.txt

%call SUFI-2_new_pars.exe
system('start /w SUFI-2_new_pars.exe')
%it uses SUFI-2.IN\observed.txt, SUFI-2.OUT\goal.txt, SUFI-2.OUT\best_par.txt
%Output files of its are Echo\new_pars_all.txt, SUFI-2.OUT\new_pars.txt
%call SUFI-2_95ppu.exe
end

```

UpdateBackUp Function

```

function UpdateBackUp

system('copy *.pnd Backup /Y');
system('copy *.rte Backup /Y');
system('copy *.sub Backup /Y');
system('copy *.swq Backup /Y');
system('copy *.wgn Backup /Y');
system('copy *.wus Backup /Y');
system('copy *.chm Backup /Y');
system('copy *.gw Backup /Y');
system('copy *.hru Backup /Y');
system('copy *.mgt Backup /Y');
system('copy *.sdr Backup /Y');

```

```
system('copy *.sep Backup /Y');
system('copy *.sol Backup /Y');
system('copy *.dat Backup /Y');
system('copy *.fig Backup /Y');
system('copy *.fin Backup /Y');
system('copy *.hmd Backup /Y');
system('copy *.pst Backup /Y');
system('copy *.out Backup /Y');
system('copy *.pcp Backup /Y');
system('copy *.qst Backup /Y');
system('copy *.rch Backup /Y');
system('copy *.rsv Backup /Y');
system('copy *.sed Backup /Y');
system('copy *.slr Backup /Y');
system('copy *.std Backup /Y');
system('copy *.swr Backup /Y');
system('copy *.Tmp Backup /Y');
system('copy *.wql Backup /Y');
system('copy *.wwq Backup /Y');
system('copy *.ini Backup /Y');
end
```


B: 4-HRU TYPES based on combinations of SOL_K, CN2 and Slope classification

AVERAGE=2.14, R2=0.15

```
if (curv_no>70) && (sol_k<=10.15) && (slope_class>0.10)
    if (curv_no<=94&&
curv_no>=80)&&(slope_class>0.20)&&
        hru_image(ii, jj) = 1;
    elseif (curv_no<80&&
curv_no>=73)&&(slope_class>0.10 && slope_class<0.20)
        hru_image(ii,jj)=2;
    end
else
    if (curv_no<70&& curv_no>=61)&&(slope_class>0.05
&& slope_class<0.10)
        hru_image(ii,jj)=3;
    else
        hru_image(ii,jj)=4;
    end
end
end
```

AVERAGE=2.06, R2=0.15

```
if (curv_no>70) && (sol_k<=10.15) &&
(slope_class>0.10)
    if (curv_no<=94 &&
curv_no>=80)&&(slope_class>0.20)&&(sol_k==3.3)
        hru_image(ii, jj) = 1;
    elseif (curv_no<80 &&
curv_no>=73)&&(slope_class>0.10 && slope_class<0.20)&&(sol_k==10.15)
        hru_image(ii,jj)=2;
    end
else
    if (curv_no<70&& curv_no>=61)&&(slope_class>0.05
&& slope_class<0.10)
        hru_image(ii,jj)=3;
    else
        hru_image(ii,jj)=4;
    end
end
end
```

AVERAGE=0.74, R2=0.31

```
if (curv_no>70) && (sol_k<=10.15) &&
(slope_class>0.10)
    if (curv_no<=94 &&
curv_no>=80)&&(slope_class>0.20)&&(sol_k==3.3)
        hru_image(ii, jj) = 1;
    elseif (curv_no<80 &&
curv_no>=73)&&(slope_class>0.10 && slope_class<0.20)&&(sol_k==10.15)
        hru_image(ii,jj)=2;
    end
else
    if (curv_no<70&& curv_no>=61)&&(slope_class>0.05
&& slope_class<0.10)&&(sol_k==33)
        hru_image(ii,jj)=3;
    end
end
```

```

else
    hru_image(ii,jj)=4;
end
end

```

AVERAGE=0.93, R2=0.28

```

if (curv_no>70) && (sol_k<=10.15) && (slope_class>0.10)
    if (curv_no<=94 && curv_no>=80)&&(sol_k==10.15)
        hru_image(ii, jj) = 1;
    elseif (curv_no<80 && curv_no>=73)
        hru_image(ii,jj)=2;
    end
else
    if (curv_no<70&& curv_no>=61)&&(sol_k==33)
        hru_image(ii,jj)=3;
    else
        hru_image(ii,jj)=4;
    end
end
end

```

AVERAGE=1.24, R2=0.28

```

if (curv_no>70) && (sol_k<=10.15) &&
(slope_class>0.10)
    if (curv_no<=94 && curv_no>=80)&&(sol_k>=3.3 &&
sol_k<=10.15)
        hru_image(ii, jj) = 1;
    elseif (curv_no<80 && curv_no>=73)
        hru_image(ii,jj)=2;
    end
else
    if (curv_no<70&& curv_no>=61)&&(sol_k==33)
        hru_image(ii,jj)=3;
    else
        hru_image(ii,jj)=4;
    end
end
end

```

AVERAGE=0.84, R2=0.32

```

if (curv_no>70) && (sol_k<=10.15) &&
(slope_class>0.10)
    if (curv_no<=94 && curv_no>=80)&&(sol_k>=3.3 &&
sol_k<=10.15)&&(slope_class>=0.13)
        hru_image(ii, jj) = 1;
    elseif (curv_no<80 && curv_no>=73)
        hru_image(ii,jj)=2;
    end
else
    if (curv_no<70&&
curv_no>=61)&&(sol_k==33)&&(slope_class>=0.5 && slope_class>=0.10)
        hru_image(ii,jj)=3;
    else
        hru_image(ii,jj)=4;
    end
end
end

```

C: 4-HRU TYPES based on combinations of SOL_K, CN2 and Slope classification

AVERAGE=1.10, R2=0.41

```

        if (curv_no>70) && (sol_k<=10.15)
            if (curv_no<=94 && curv_no>=80)&&(sol_k>=3.3 &&
sol_k<=10.15)&&(slope_class>=0.13)
                hru_image(ii, jj) = 1;
            elseif (curv_no<80 &&
curv_no>=73)&&(slope_class>=0.10 && slope_class<0.13)
                hru_image(ii,jj)=2;
            end
        else
            if (curv_no<70&&
curv_no>=61)&&(sol_k==33)&&(slope_class>=0.5 && slope_class>0.10)
                hru_image(ii,jj)=3;
            else
                hru_image(ii,jj)=4;
            end
        end
    end

```

AVERAGE=5.74, R2=0.15

```

    if (curv_no>70)&&(sol_k<=10.15)
        if (curv_no<=94 && curv_no>=80)&&(sol_k>=3.3 &&
sol_k<=10.15)&&(slope_class>=0.13);
            if (curv_no >84)
                hru_image(ii, jj) = 1;
            else
                hru_image(ii, jj) = 2;
            end
            elseif(curv_no<80 &&
curv_no>=73)&&(slope_class>=0.10 && slope_class<0.13);
                if curv_no>=79
                    hru_image(ii, jj)=3;
                elseif curv_no<79
                    hru_image(ii,jj)=4;
                end
            end
        else
            if (curv_no<70&&
curv_no>=61)&&(sol_k==33)&&(slope_class>=0.5 && slope_class>0.10);
                if (curv_no>66)
                    hru_image(ii,jj)=5;
                else
                    hru_image(ii,jj)=6;
                end
            elseif( curv_no<61 && curv_no>=39)
                if curv_no>55
                    hru_image(ii,jj)=7;
                else
                    hru_image(ii,jj)=8;
                end
            end
        end
    end
end
AVERAGE=0.26, R2=0.14

```

```

        if (curv_no>70) &&
(sol_k<=10.15)&&(slope_class>=0.15)
            if (curv_no<=94 && curv_no>=80)
                if(curv_no> 84)&&(slope_class>=0.25)
                    hru_image(ii, jj) = 1;
                else
                    hru_image(ii, jj) = 2;
                end
            elseif (curv_no<80 &&
curv_no>=73)&&(slope_class>=0.15)&&(slope_class<0.25)
                if (curv_no>=79)
                    hru_image(ii,jj)=3;
                elseif curv_no<79
                    hru_image(ii, jj)=4;
                end
            end
        else
            if (curv_no<70&&
curv_no>=61)&&(slope_class>=0.10 && slope_class<0.15)&&(sol_k>=3.3)
                if (curv_no>66)
                    hru_image(ii,jj)=5;
                else
                    hru_image(ii, jj)=6;
                end
            elseif (curv_no<61 &&
curv_no>=39)&&(slope_class<0.10)
                if curv_no>55
                    hru_image(ii,jj)=7;
                else
                    hru_image(ii,jj)=8;
                end
            end
        end
    end
end

```

AVERAGE=0.28, R2=0.16

```

if (curv_no>70) && (sol_k<=10.15)&&(slope_class>=0.15)
    if (curv_no<=94 &&
curv_no>=80)&&(slope_class>=0.25)
        if(curv_no> 84)
            hru_image(ii, jj) = 1;
        else
            hru_image(ii, jj) = 2;
        end
    elseif (curv_no<80 &&
curv_no>=73)&&(slope_class>=0.15)&&(slope_class<0.25)
        if (curv_no>=79)
            hru_image(ii,jj)=3;
        elseif curv_no<79
            hru_image(ii, jj)=4;
        end
    end
else
    if (curv_no<70&&
curv_no>=61)&&(slope_class>=0.10 && slope_class<0.15)&&(sol_k>=3.3)
        if (curv_no>66)
            hru_image(ii,jj)=5;
        else
            hru_image(ii, jj)=6;
        end
    end
end

```

```

        end
        elseif (curv_no<61 &&
curv_no>=39) && (slope_class<0.10)
            if curv_no>55
                hru_image(ii,jj)=7;
            else
                hru_image(ii,jj)=8;
            end
        end
    end
end

```

AVERAGE=0.30, R2=0.18

```

if (curv_no>70) && (sol_k<=10.15) && (slope_class>=0.15)
    if (curv_no<=94 &&
curv_no>=80) && (slope_class>=0.25) && (sol_k==10.15)
        if (curv_no> 84)
            hru_image(ii, jj) = 1;
        else
            hru_image(ii, jj) = 2;
        end
        elseif (curv_no<80 &&
curv_no>=73) && (slope_class>=0.15) && (slope_class<0.25) && (sol_k==3.3)
            if (curv_no>=79)
                hru_image(ii,jj)=3;
            elseif curv_no<79
                hru_image(ii, jj)=4;
            end
        end
    else
        if (curv_no<70 &&
curv_no>=61) && (slope_class>=0.10 && slope_class<0.15) && (sol_k>=33)
            if (curv_no>66)
                hru_image(ii,jj)=5;
            else
                hru_image(ii, jj)=6;
            end
            elseif (curv_no<61 &&
curv_no>=39) && (slope_class<0.10)
                if curv_no>55
                    hru_image(ii,jj)=7;
                else
                    hru_image(ii,jj)=8;
                end
            end
        end
    end
end

```

AVERAGE=0.30, R2=0.18

```

    if (curv_no>70) &&
(sol_k<=10.15) && (slope_class>=0.15)
        if (curv_no<=94 &&
curv_no>=80) && (slope_class>=0.25) && (sol_k==10.15)
            if (curv_no> 84)
                hru_image(ii, jj) = 1;
            else
                hru_image(ii, jj) = 2;
            end
        end
    end

```

```

elseif (curv_no<80 &&
curv_no>=73)&&(slope_class>=0.15)&&(slope_class<0.25)&&(sol_k==3.3)
    if (curv_no>=79)
        hru_image(ii,jj)=3;
    elseif curv_no<79
        hru_image(ii, jj)=4;
    end
end
else
    if (curv_no<70&&
curv_no>=61)&&(slope_class>=0.10 && slope_class<0.15)
        if (curv_no>66)
            hru_image(ii,jj)=5;
        else
            hru_image(ii, jj)=6;
        end
    elseif (curv_no<61 &&
curv_no>=39)&&(slope_class<0.10)
        if curv_no>55
            hru_image(ii,jj)=7;
        else
            hru_image(ii,jj)=8;
        end
    end
end
end

```

AVERAGE=9.36, R2=0.25

```

    if (curv_no>70) &&
(sol_k<=10.15)&&(slope_class>=0.15)
        if (curv_no<=94 &&
curv_no>=80)&&(slope_class>=0.25)&&(sol_k==3.3)
            if (curv_no> 84)
                hru_image(ii, jj) = 1;
            else
                hru_image(ii, jj) = 2;
            end
        elseif (curv_no<80 &&
curv_no>=73)&&(slope_class>=0.15)&&(slope_class<0.25)&&(sol_k==10.15
)
            if (curv_no>=79)
                hru_image(ii,jj)=3;
            elseif curv_no<79
                hru_image(ii, jj)=4;
            end
        end
    else
        if (curv_no<70&&
curv_no>=61)&&(slope_class>=0.10 && slope_class<0.15)
            if (curv_no>66)
                hru_image(ii,jj)=5;
            else
                hru_image(ii, jj)=6;
            end
        elseif (curv_no<61 &&
curv_no>=39)&&(slope_class<0.10)
            if curv_no>55
                hru_image(ii,jj)=7;
            else

```

```

        hru_image(ii,jj)=8;
    end

    end
end

AVERAGE=1.10, R2=0.23

if (curv_no>70) && (sol_k<=10.15)&&(slope_class>=0.15)
    if (curv_no<=94 &&
curv_no>=80)&&(slope_class>=0.25)&&(sol_k==3.3)
        if(curv_no> 84)
            hru_image(ii, jj) = 1;
        else
            hru_image(ii, jj) = 2;
        end
    elseif (curv_no<80 &&
curv_no>=73)&&(slope_class>=0.15)&&(slope_class<0.25)&&(sol_k==10.15
)
        if (curv_no>=79)
            hru_image(ii,jj)=3;
        elseif curv_no<79
            hru_image(ii, jj)=4;
        end
    end
else
    if (curv_no<70&&
curv_no>=61)&&(slope_class>=0.10 && slope_class<0.15)&&(sol_k>33)
        if (curv_no>66)
            hru_image(ii,jj)=5;
        else
            hru_image(ii, jj)=6;
        end
    elseif (curv_no<61 &&
curv_no>=39)&&(slope_class<0.10)
        if curv_no>55
            hru_image(ii,jj)=7;
        else
            hru_image(ii,jj)=8;
        end
    end
end
end

```


CURRICULUM VITAE

PERSONEL INFORMATION

Surname, Name: Özdemir, Ayfer
Nationality: Turkish (TC)
Date and Place of Birth: 22 April 1980, Ankara
Marital Status: Single
Phone: +90 533 443 75 93
Email: ozdemir.ayfer@gmail.com

EDUCATION

Degree	Institution	Year of Graduation
MS	Ankara University Geological Engineering	2006
BS	Ankara University Geological Engineering	2003
High School	Aydınlıkevler High School	1997

WORK EXPERIENCE

2012-...	Ministry of Forestry and Water Affairs Directorate General for Water Management Ankara, Turkey	Engineer
2011 –2012	Turkey State of Hydraulic Water Affairs, DSI 5. The Regional Directorate, Geotechnical Services and Groundwater Branch Office, Ankara, TURKEY	Engineer
2010-2011	Middle East Technical University, Graduate School of Natural and Applied Sciences, Department of Geodesy and Geographic Information Technologies, Ankara, TURKEY	Research Assistant
2010-2007	Middle East Technical University, Graduate School of Natural and Applied Sciences, Department of Geological Engineering, Ankara, TURKEY	Research Assistant
2006-2007	Aksaray University, Graduate School of Natural and Applied Sciences, Department of Geological Engineering, Aksaray, TURKEY	Research Assistant

FOREGEIN LANGUAGES

Advanced English, German (A1)

PUBLICATIONS

1. **Özdemir**, A., Reservoir quality of Upper Paleocene-Lower Eocene sandstones in Guney Formation, Eregli-Ulukisla Basin, Marine and Petroleum Geology (submitted to journal)
2. **Özdemir**, A., Leloğlu, U.M., Abbaspour, K., Hierarchical Approach to Hydrological Model Calibration, Enviromental Earth Sciences, (submitted to journal)
3. **Özdemir, A.**, Altuntaş, A., Koç, A., and Turan, G., Groundwater Recharge And Hydrogeochemical Assessment For Determining Protection Areas In Namazgah Dam Basin, Izmit, Turkey, Applied Radiation and Isotopes (submitted to journal)

ORAL PRESENTATIONS

1. A. Altuntaş, **A. Özdemir**, A. Koç, G. Turan, Determination of the relationship between surface water and groundwater, and protection areas by using natural isotopes, Namazgah Barrage Lake Basin, İzmit, Turkey, 4. National Isotope Hydrology Symposium, 2015, Istanbul, TURKEY
2. **A.Ozdemir, 2015**, Guney Formation Oil Reservoir Rock Characterization, Eregli-Ulukisla Basin. Turkey, 2015, Earth Science and Climate Change 2015, 16-18 June 2015, Alicante SPAIN
3. **A.Ozdemir**, U.Leloğlu, Climate Change Impact Assessment on River Basin: Sarisu-Eylikler River, Turkey, SUWAMA 2014,Sarıgerme Muğla, TURKEY
4. **A.Ozdemir**, U.Leloğlu, Bathymetry and Water Quality Measurement of Shallow Waters using Hyperion: Serçin Lake, SIU2014, 2014, Trabzon, TURKEY